A study on the dissolution of non-porous alumina films on aluminium

Pickup, George Kelvin

THE UNIVERSITY OF DURHAM

A STUDY OF THE DISSOLUTION OF NON-POROUS ALUMINA FILMS ON ALUMINIUM

Thesis submitted for the award

of the degree of

MASTER OF SCIENCE

by

GEORGE KELVIN PICKUP B.Sc. (London)

For Pauline and My Parents.

Acknowledgements

This work was carried out in the Materials Science Laboratories at Sunderland Polytechnic.

I am indebted to Dr. C.W. Goulding for his helpful suggestions and encouragement throughout the course of the work.

I also wish to thank:-

Dr. G. Kohnstam for acting as my University Supervisor,

Mr. E. Lewis and the technical staff of the Chemistry Department for their help throughout,

Mr. J. Hindmarch and his assistants of the Chemistry Department Workshops for their help in the construction of apparatus,

Sunderland Education Authority for the studentship which enabled me to carry out the work,

my wife for her help with the preparation of this thesis.

ABSTRACT

The dissolution behaviour in sulphate solutions of so-called non-porous anodic alumina films and films formed in dry oxygen and in a moist oxygen atmosphere on chemically polished aluminium has been investigated.

Evidence is presented which indicates that the non-porous anodic films, formed at 7-30 volts, consisted of two regions, a thin, less soluble region adjacent to the metal and a thicker, more soluble outer region into which hydroxyl ions were incorporated. The structure might be related to the initial method of surface preparation adopted.

It is suggested that films formed in dry oxygen at 500°C consist of crystalline γ-alumina, whilst those formed in the moist oxygen atmosphere at 500°C possibly consist of amorphous alumina with some adsorbed water and are less faulted than the crystalline oxide. Again, there is some indication that the structure of these films is strongly influenced by the initial method of surface preparation used.

The dissolution behaviour of the anodic films and films formed in dry oxygen at 500°C can be understood in terms of the extent of sulphate ion adsorption, apparently greater under the same conditions for the former type, and its effect on rate of tranfer of protons, hydroxyl ions and water across the oxide/solution interface. A ...

reaction scheme, proposed earlier to account for the behaviour during dissolution of the barrier layer of porous films formed anodically in sulphuric acid, appears adequate to explain the dissolution behaviour observed in the present studies. However, the type of behaviour, although rather similar for both anodic non-porous and films formed in dry oxygen at 500°C, was quite different from the barrier layer of porous films formed anodically in sulphuric acid.

CONTENTS

CHAPTER I

The Present Investigation.

CHAPTER II

The Oxidation of Aluminium in Dry and Moist Oxygen and Air.

CHAPTER III

Anodically-Formed Oxide Films.

CHAPTER 1

The Present Investigation.

1.1. Introduction.

It is well known that the resistance of aluminium metal to oxidation and corrosion arises from the protective natural oxide film present on the surface. It is the presence of this film which renders the metal useful as a structural material, and agents which tend to remove or disrupt it lessen the usefulness of the metal. The oxide is also of interest from the point of view of its electrical properties. Thus, films of the barrier type (see later) are widely used in capacitors, and are known to have semiconducting properties. These latter properties have been discussed in terms of the non-stoichiometric structure of the oxide [1,2,3], and also in terms of the presence of structural faults in the film[4]. Such factors as non-stoichiometry and the presence of flaws are also of concern in consideration of the processes of film formation and dissolution as will be discussed later.

1.2. Types of Oxide Films on Aluminium.

The oxide film found naturally on aluminium metal, or that resulting from such processes as electropolishing or chemical polishing, is only a few angstrom units in thickness[5]. It may be thickened for specific purposes by either oxidation in a gaseous atmosphere or by anodic oxidation. The formation of a thickened film by either

process depends on ion movement through the oxide under the influence of the field, provided either by the applied anodising voltage or by adsorbed ions at the outer surface.

The details of these processes are discussed in the next chapters, but the extent of film thickening which is possible may be illustrated by the fact that the thickness of non-porous anodic films is limited by the breakdown voltage of 500-700 volts[6], which corresponds to film thicknesses of 7 000 - 10 000 Å. Porous anodic films may be grown to many times this thickness under appropriate conditions.

The anodisation of aluminium is commercially important, and films of two kinds may be produced by variations of the process. These are (i) non-porous barrier films, and (ii) those of the porous type in which an outer layer containing discrete pores [7,8] overlies an inner layer of the barrier type. The type of electrolyte, its concentration and temperature, decide the type of film produced and its porosity. Generally speaking, porous films are produced in electrolytes which are solvents for alumina; 15% w/v sulphuric acid solution is a typical example of such an electrolyte. Both porous and non-porous films have good corrosion and mechanical resistance, and additionally the porous types provide a good base for dyeing treatments.

The question of the amorphous or crystalline structure of oxide

films of all types is considered in the next two chapters.

1.3. Behaviour of the Naturally Occurring Oxide Film on Aluminium in Aqueous Solutions.

Aspects of the behaviour of the naturally occurring oxide film on aluminium when immersed in solutions have been widely studied in relation to the corrosion of the underlying metal. Thus, corrosion inhibition of aluminium has been discussed in terms of film dissolution and repair processes in solutions containing different types of ions [9]. The liability of the metal to attack in solutions containing halide ions has been related to the polarisabilities of these ions and their ease of entry into the electrical double layer at the solution interface[10] as well as to their capacity to form soluble compounds. In solutions of other types the hydroxyl ion has been regarded as the most polarisable, and the possibility of film repair processes discussed in terms of its presence in the double layer[9,10,11].

Methods of investigation which have been used have included much work on the anodic and cathodic processes which occur on the oxide-coated metal[12-15]. Rather similar electrode kinetics to those observed for the metal iron have been reported[16-19]; differences in the cathodic polarisation results for iron and aluminium have been interpreted in terms of a much lower cathode to anode area ratio for the latter metal[20-23]. Very little attention has

been paid to the chemical processes associated with dissolution of the oxide film, although such work would of course be difficult in view of the extremely thin layer present in the natural state. A few investigations of these aspects of dissolution have been made for thickened films, as is reported in the next section. It must be borne in mind that it may be difficult to form conclusions concerning the behaviour of the natural film by considering the processes which occur in artificially thickened films, because of the internal structure of the latter type.

1.4. Dissolution of Anodic Films on Aluminium.

Until quite recently there has been little investigation of the chemical and kinetic features of dissolution processes which occur when anodically formed films on aluminium are immersed in solutions, other than determinations of overall thinning rates[24]. This is in spite of the fact that immersion of prepared films in solvents has been used to enlarge the pore structure[25].

General discussion of the solubility of anodic films on aluminium has taken place, for example, to account for the observed low coating ratios in the process of anodising. The coating ratio is the ratio of the weight of oxide formed to the weight of aluminium consumed, and should have the value 1.89 if the current efficiency is 100%[26]. The ratio should in fact be higher than this if anion incorporation of the type discussed in Chapter III is taken into

consideration. The low value has been discussed in terms of dissolution of the outermost oxide occurring simultaneously with its formation.[27,28]

In only a few cases have detailed studies of the mechanism and kinetics of dissolution been reported. For example, the dissolution in citrate solutions containing fluoride ion of sealed porous anodic alumina films has been investigated and found to proceed via fluoride complex formation[29,30]. This is, however, a special effect; fluoride ions are known to enter the oxide lattice, and second solid phases have been reported to separate[31]. Other types of complex have been noted in the course of dissolution of barrier type films on aluminium immersed in ethylene glycol-ammonium pentaborate electrolytes[4]. This is of interest, since this process may be one mode of failure of electrolytic capacitors. The proposed mechanism included attack by the solution at weak spots in the oxide film, and acceleration of the attack produced by addition of water to the electrolyte was noted. Such an effect may again be a pointer to the significance of the hydrogen and hydroxyl ions in dissolution processes.

1.5. Dissolution of Porous Anodic Oxide.

Although detailed studies of the mechanism and kinetics of oxide film dissolution should be of technological interest, and could aid in deciding on the structure of anodic films, only recently has

a detailed study of porous film dissolution been made by Nagayama and Tamura[32]. Films were formed on aluminium by anodising the metal in aqueous sulphuric acid, and were then permitted to dissolve on open circuit in the same solution, while the potential-time behaviour and the loss of aluminium from film to solution were studied. The variation of specimen potential with time was rather similar to decay curves observed elsewhere for nickel oxide electrodes[33], and for passivated iron electrodes[34], and was related by Nagayama and Tamura to the loss of the porous layer. The rate of dissolution increased slightly with time to a critical time t_R, which corresponded to a large shift in specimen potential in the base direction. t_R was found to be independent of the porous layer thickness, and the process was regarded[32] as indicative of dissolution proceeding by pore widening. A rate of increase of pore diameter and of decrease of porous layer thickness of 0.75 Å min^{-1} was reported, which is comparable with the value noted by Hunter and Fowle[24]. The whole process was discussed in terms of the Keller model of pore structure[7].

Differences between the influence of chloride and sulphate ions on the dissolution rate of oxide films formed on aluminium by sulphuric acid anodising have been reported by Diggle, Downie and Goulding[23,28,35,36]. These workers investigated the dissolution rates of the porous and barrier parts of these films by a com-

bination of methods.

Provided that the solution pH was less than a critical value of about 2, an increase in capacitance with time was always noted when the films were immersed. At the frequencies used, this increase was associated with the behaviour of the barrier layer[36], and the state of aeration or de-aeration of the solution had little effect on the results. On the assumption that capacitance changes reflected changes in film thickness, there was surprisingly little difference between the rates of thinning in chloride and sulphate solutions[23,36]. Graphs of reciprocal capacitance (1/C) versus time (t) were usually almost linear in acid solutions of high ionic strength (I = 1), which is consistent with an oxide thinning process of zeroth order with respect to the film thickness. Deviations from linearity increased however, as the solution pH increased and/or ionic strength decreased, and it was here that differences between the behaviour in the presence of the two types of ion became apparent, since the deviations from linearity were in opposite directions. In dilute chloride solutions capacitance increases were greater than expected on the basis of zeroth order kinetics, while in sulphate solutions they were less.

The situation was complicated by the simultaneous dissolution of both barrier and porous parts of the film. It was deemed possible to identify the time of removal of the porous layer since, in sulphate

solutions, similar types of potential-time curves to those reported by Nagayama and Tamura were noted. The large base shift in potential coincided with the greatest rate of change of capacitance, and also coincided with the time t_b after which the film would no longer take up dye. t_b was found to be independent of porous layer thickness, but was proportional to the pore wall thickness, and this observation led to the proposal of a model of concurrent pore widening and shortening for the dissolution of the porous layer. When the anodised metal was immersed in either chloride or sulphate solutions of pH greater than the critical value, the barrier layer capacitance at first increased and then decreased with time. In sulphate solutions both dyeing experiments and the occasional isolation of corrosion product were taken to indicate the possibility of pore sealing processes resulting in an increase of dielectric thickness which would produce a capacitance decrease[37].

The initial increase in capacitance in these high pH sulphate solutions could imply an initial stage of thinning. It was noted that during this stage a linear relationship existed between $1/C$ and $(t)^{\frac{1}{2}}$, which could be indicative of a diffusion controlled process. The indications were that the diffusing species was the hydroxyl ion; the ion could either be diffusing into the oxide, or through a zone close to the oxide surface [21,38,39].

The first stage of capacitance increase in high pH chloride

solutions showed similar time dependence to that noted in the last paragraph, but the magnitude of the slope $d.1/C\ /d.(t)^{\frac{1}{2}}$ was considerably greater. From the dependence of this slope on the ionic strength of the solution and pH, it was tentatively suggested[23,36] that chloride ion diffusion was responsible for this effect. Since it is known that these ions may enter an alumina lattice[10], it is possible that part of the initial capacitance change could be due to a change in film dielectric constant produced by chloride ion entry.

From their observations of the concentration and pH dependence of the rates of capacitance change, Diggle, Downie and Goulding[36] suggested possible sequences of reactions to account for the dissolution of the alumina films in low pH solutions and for the production of pore blocking material in solutions of higher pH. These reactions are discussed in relation to the present investigation in Chapter V (5.7), but it may be noted here that in solutions of pH greater than the critical value, some degree of competitive adsorption of hydroxyl and sulphate ions was postulated.

1.6. Present Investigation.

1.6.1 Relationship to the Previous Work.

In the work discussed in the last two sections of this chapter, a chemical mechanism and physical models of the dissolution process have been tentatively presented for porous anodic films on aluminium. The process is complex, since in porous films, both layers of the

oxide must be dissolving simultaneously. The conclusions of Diggle and his coworkers[23] rest upon the measurement of rates of capacitance change, and on the assumption that such changes are indicative of thickness. This is probably true to a first approximation, but may not be an accurate measure of thickness in the complex systems considered. The appropriate form of specimen area to use in capacitance calculations has been discussed by Dekker and Urquhart[40] and Hoar and Wood [42]. Lorking has concluded[5] that when the film is coherent and impermeable the capacitance may be used as a measure of thickness; under suitable conditions the accuracy may be within 1% of the true value. However, when the film had been rendered porous by corrosive solutions, Lorking concluded that capacitance values could not be used to obtain accurate estimates of film thickness.

Diggle, Downie and Goulding were aware of these difficulties of interpretation of capacitance results, and, using the proposed pore widening model which must result in exposure of increasing area of barrier layer to the solution, obtained an expression for the change in barrier layer capacitance with time. The expression is discussed in Chapter V (5.7); it did not take into account possible changes in dielectric constant of the oxide in the course of dissolution, nor were sufficient results available to test it conclusively.

These complexities are due to the presence of two oxide layers

of very different structure in the porous films. Possibly more precise information could be obtained for this type of system in the absence of the porous layer. The difficulty of preparation would be considerable in view of the very short period of time required for the barrier layer to be completed[22,42,43].

1.6.2. Types of Oxide Film Used in the Present Work.

The present work was intended as an investigation of the dissolution characteristics of non-porous films in one type of solution to compare the features of the process with those for porous films. No previous work of this kind has been reported for anodic films formed on aluminium in tartrate solutions, or for films formed on the metal by gaseous oxidation; the dissolution of both kinds of film in sulphate solutions was studied.

Although both of these film types are compact, they are reported to have internal structure, and to differ in crystalline content. To further investigation of this last point, a few investigations were also made using oxide films which had been grown in moist oxygen.

1.6.3. Experimental Work.

The points felt to be of particular interest in the present work were:-

(a) the structures of these compact films,

(b) the reaction steps involved in dissolution and the kinetic features of the process,

(c) examination to see if the change in behaviour reported for porous films at pH > 2 were repeated, or if this type of behaviour is characteristic of the presence of pores,

(d) correlation of potential-time and capacitance-time behaviour during dissolution, and comparison with the reported behaviour of porous films.

In the attempt to elucidate the dissolution characteristics of these non-porous oxide films, capacitance-time changes were determined when they were immersed in sulphate solutions. Sulphate solutions were chosen to avoid possible complications due to the suggested entry of chloride ions into the oxide. Experiments were carried out in solutions of selected pH and ionic strength values both under aerated and de-aerated conditions. A few direct determinations of the concentration of aluminium ions in solution as a function of time were also made. The behaviour was correlated with changes in specimen potential during immersion.

In order to obtain an indication of the complexity of structure of the films, electrical analogues [37] were constructed to have the same frequency response to input signals as the films themselves, and barrier voltage determinations [44,45] were also used to assess the crystallinity of the films formed by gaseous oxidation.

1.7. Arrangement of the Thesis.

The thesis is arranged in seven chapters. Before details of

the experimental work carried out are given, a discussion of the oxide films formed on aluminium by gaseous and anodic oxidation is presented in Chapters II and III. Chapter III also includes a brief review of methods which have been used elsewhere for the determination of film thickness.

Details of specific items of apparatus which were used in the present investigations have been kept to a minimum in the body of the thesis. A list of the more important instruments is contained in Appendix I. All references are listed at the end of the thesis.

It will be noted that diagrams and graphs are listed both as plates and as figures in the text. Diagrams and graphs which present the results of the present work are labelled as figures; all others are labelled as plates.

CHAPTER II

Oxidation of Aluminium in Dry and Moist Oxygen and Air.

2.1 Dry Oxidation of Aluminium.

Both anodic and air-formed oxide films on aluminium have been considered by many investigators to have structures related to that of γ-alumina. The term 'γ-alumina' is in general use in the literature, and is used to describe both highly crystalline oxide and other forms which may be amorphous.

2.1.1 Structure of γ-Alumina.

Several workers[46,47,48] have invoked the concept of an anion lattice for amorphous γ-alumina in interpreting their results. Long range order cannot exist in such a structure, but presumably elements of short range order may do so.

The structure of γ-alumina in all its modifications has been considered to differ from the normal spinel structure only in the sense that eight cations must be distributed among sites occupied by nine cations in the spinel lattice [49]. Dignam [46] has pointed out that since ionic conduction in the amorphous oxide takes place by movement of aluminium ions, fresh amorphous oxide being deposited at the oxide oxidising atmosphere interface [48], a true γ-alumina structure is unlikely since one would expect conduction to be via cations vacancies in this structure, there being one vacancy per

nine cation sites. Indeed, it was found that annealed anodic and amorphous films formed in dry oxygen could not be distinguished, which is consistent with Wilsdorf's model[50] for amorphous alumina consisting of 'randomly oriented molecular groups of γ- alumina'.

2.1.2 Crystallinity of γ-Alumina.

Although there seems to be agreement between different investigators that, below a certain temperature of oxidation of aluminium, the oxide formed is amorphous, the published values of this limiting temperature have varied widely. Thus Dignam[46] has reported that only amorphous oxide is formed when electropolished aluminium is oxidised in dry oxygen below 450°C. de Broukere[51] oxidised abraded aluminium in air and found the limiting temperature to be 600°C, a value which has also been reported[52] for electropolished aluminium when oxidised in air. Hass[53] found that stripped amorphous oxide films crystallised at 680°C, whereas metal-adherent films crystallised at 500°C.

2.1.3 Mechanism of Crystallisation and Growth.

Although there is disagreement as to the minimum temperature for crystallisation, several workers agree on the nature of the nucleation process. Above about 450°C crystals of γ-alumina nucleate beneath the amorphous oxide formed originally[46-48,51] on the metal. At 500°C in the absence of oxygen, there is apparently no conversion of the initially-formed amorphous oxide

to the crystalline form [54], this process occurring only at higher temperatures near to the melting point of aluminium for stripped oxide films. It has been reported [54,55] that at temperatures in excess of 550°C, amorphous oxide is converted to the crystalline form at the metal-oxide interface during oxidation in both wet and dry oxygen and air. Dignam and Fawcett[47], although regarding the position as uncertain, have suggested that conversion of amorphous to crystalline γ-alumina is possible during the growth of crystallites. They proposed the edges of the growing crystal to be separated from the metal by a very thin layer of amorphous oxide, and further suggested that the presence of a very large electrochemical potential gradient across this thin film would render possible the atomic reorganisation necessary for the conversion.

Some evidence for the necessity of the presence of oxygen during crystallisation was provided by Beck and his co-workers [48], who, however, used anodically-formed films. A barrier type film was prepared on aluminium by anodising in neutral tartrate solution. After the specimen had been heated for 24 hours in a vacuum of 5×10^{-7} torr, no crystals were detected by electron-optical study. The process was repeated, but oxygen was admitted to the system after the initial vacuum treatment; immediate crystal nucleation was observed; when the system was re-evacuated growth of the crystals ceased.

The concentration of nuclei has been reported to be about 10^9 cm^{-2} [47,48] and to be almost independent of temperature. The nucleation process occurs very quickly. Crystallites reach a terminal thickness almost immediately, and then grow radially until they impinge on each other. Dignam and Fawcett [47] found the thickness of the crystals to decrease with increasing temperature but Beck [48] found little variation of thickness with temperature.

2.1.4 Growth of Amorphous Oxide.

The kinetic features of the process of oxidation of aluminium under dry conditions may be described in terms of weight gain (Δw), as a function of time (t), and appear to be temperature dependent. From low temperatures to about 300°C the growth law is inverse logarithmic in type [46,56,57] ($\Delta w = K/\log t$), which implies that the rate of oxidation is controlled by the rate of migration of aluminium ions through the oxide under the influence of the electric field created by oxygen ions at the outer surface [56]. In the temperature range 350-450°C the oxidation is best described in terms of a parabolic law [48,58,59] ($\Delta w = k(t)^{\frac{1}{2}}$), which is interpreted in terms of diffusion of aluminium ions through the oxide being the rate-controlling step of the process. Beck and his coworkers [48] found that the amorphous oxide formed according to a parabolic law at 450-575°C, even after discrete crystals of γ -alumina had appeared, and that this amorphous growth continued

indefinitely. The result was that the total oxide thickness slowly increased even after completion of the underlying crystalline layer. That the rate at which the amorphous oxide thickened was unaffected by the appearance of crystalline γ-alumina indicates that the diffusion rate of aluminium ions remained sensibly constant. In this connection it has been reported that the electronic resistivities of amorphous and crystalline γ-alumina are very similar [60], although Beck and his co-workers [48] have found the crystalline oxide to have the much lower ionic resistivity of the two forms. As will be discussed later, Beck and his co-workers reported that their crystalline films were highly faulted.

Dignam and his co-workers [46,61] found that when only amorphous oxide grew, the weight gain data were better described in terms of an inverse logarithmic law rather than a parabolic law at temperatures at which the latter would be expected to hold. They also report, in contradiction to the findings of Beck and his co-workers, that limiting weight gain is achieved in the temperature range 478-501°C.

Above about 450°C during the initial period of oxidation, only amorphous γ-alumina forms. This initial period decreases with increasing temperature [48,62]. A discontinuous reduction in the parabolic rate constant after a short period at 525°C has been reported [48], the activation energy for the formation of amorphous

oxide remaining the same. This was interpreted in terms of a change in the 'defect structure' of the amorphous oxide at this temperature.

Reasons for the formation of both crystalline and non-crystalline oxide have been suggested [48]. The rate of growth of the amorphous form was suggested to be controlled by the rate at which aluminium ions reach the oxide-gas interface, while transport of oxygen ions through the amorphous layer was suggested to control the rate of growth of crystalline oxide.

2.1.5 Effect of the Initial Surface Preparation.

It is interesting to compare some of the data evaluated by Beck and his co-workers[48] with the results reported by Dignam and Fawcett [47] for a similar process of oxidation of aluminium in producing amorphous film. The discrepancies in results can be seen in Table 1.

TABLE 1

Comparison of Reported Data for the Formation of Amorphous Oxide Films on Aluminium.

Reference	Δw ($\mu g\ cm^{-2}$) at 500°C	Energy of Activation ($kcal\ mole^{-1}$)
47	6.1 (a)	25.3 (b)
48	12.5 (c)	54

(a) Interpolated value from results at other temperatures.

(b) From data before crystallite appearance.

(c) Oxidation time of 40 hr to correspond with (a).

Beck and his co-workers prepared their specimens by etching the surface with caustic soda. They stated that this treatment had no effect on the ionic resistance of the oxide and that the surface produced was reasonably smooth. Dignam and Fawcett electropolished their specimens before oxidation. The former workers suggested that the initial surface preparation may be important, and that incorporation of anions resulting, for example, from electropolishing could result in reduced ionic resistance of the oxide film. It should be noted that the proposed growth laws for the oxide were different in the two cases.

Another aspect of the importance of initial surface preparation has been pointed out[46] in casting doubt on the theoretical value of studies concerned with the elucidation of the basic reaction mechanisms for the oxidation of aluminium in dry oxygen from 400-650°C [62]. The initial surface preparation was by abrasion with emery, and this is suggested to result in cracking and buckling of the oxide film during oxidation, exposing fresh metal and giving, as a result, excessively high weight gains.

2.1.6 Dimensional effects and Oxidation Rate.

Above about 450°C, when crystal formation occurs, much higher

weight gains are found than would be expected from an extension of the low temperature growth laws [47,48,55,62,63]. A typical plot of weight gain versus time is shown in Plate I. The sigmoidal shape of the curve has been interpreted [48] in terms of the radial growth of crystallites, the final reduced rate of increase in weight resulting from the impingement of the oxide crystals.

However, it has been reported [64] that for aluminium initially bearing a natural oxide film, during the epitaxial formation of the crystalline oxide, because of small differences in the dimensions of the aluminium and crystalline γ-alumina lattices, fractures between crystalline film located on metal of different crystal orientations take place. This cracking exposes bare metal and increased weight gains are therefore observed. This may be an important factor in the accelerated rate of film formation found during crystalline growth.

2.1.7 Conclusions.

Perhaps many of the differences found between the work of Dignam and his co-workers and Beck and his co-workers may be ascribed to the different initial surface preparations used. The difference between laws reported by these workers for the growth of amorphous oxide appears to be significant. The composition of the oxidising atmosphere may have some influence on the minimum temperature for crystallite nucleation (425-600°C) reported by the workers already

Relationship of weight of γ- alumina to time of oxidation in 76 torr dry oxygen at 500°C.[48]

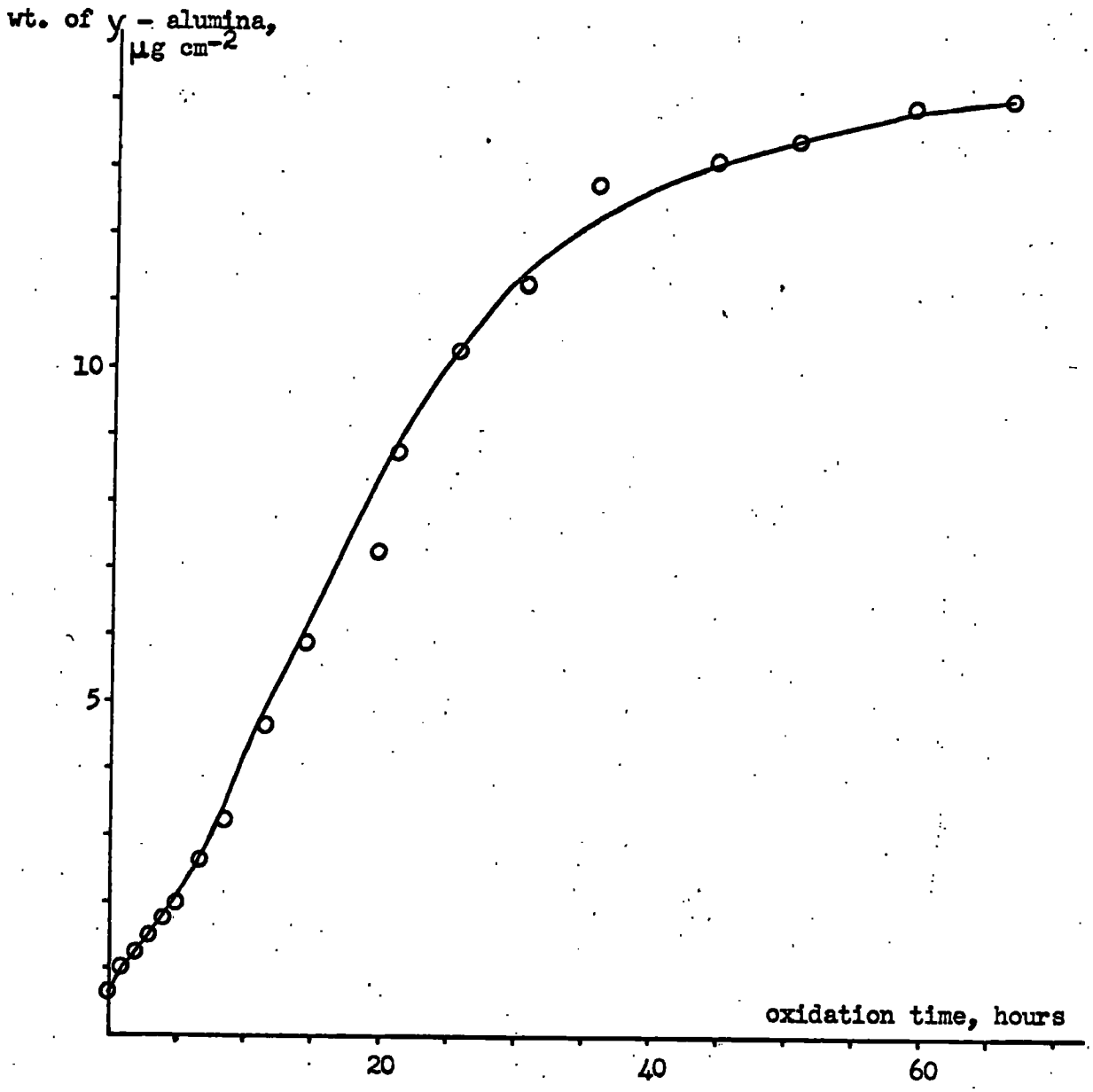

Plate I.

mentioned. For metal-adherent films the possibility of the conversion of amorphous to crystalline γ-alumina exists in the temperature range 450-600°C in the presence of oxygen. This conversion mechanism has not apparently been distinguished experimentally from crystallite nucleation involving the metal itself.

2.2. Oxidation of Aluminium in Moist Atmospheres.

There is considerable evidence that alumina films will adsorb water, and at high temperatures will react with water vapour, resulting in gas evolution. The influence of moist atmospheres used in oxidation on the structure and properties of the resulting oxide are considered in this section.

2.2.1 Adsorption of Water by Alumina.

Spannheimer and Knoezinger[65] have studied the adsorption of water at temperatures up to 453°C from the gas phase on to crystalline γ-alumina initially dehydrated at 800°C. At a given temperature part of the water was irreversibly adsorbed. These workers found adsorption enthalpies to be high, and concluded that even for reversible adsorption, the forces of interaction with the surface were largely of a chemical nature. The enthalpy of adsorption increased from 21.7 to 32.2 kcal $mole^{-1}$ as the temperature was increased from 98-412°C, and had increased only to 24.0 kcal $mole^{-1}$ at 328°C. The extent of adsorption fell from 16.0 to 3.2 mg of water per g of alumina at 10 torr gaseous water pressure at 98°C

and 412°C respectively. The amount of adsorbed water at a given temperature increased with increased gaseous water pressure for all temperatures.

Lippens and de Boer[66] found that the hydrated form of alumina, boehmite (AlOOH), was converted to γ-alumina at about 450°C. Well-crystallised boehmite underwent conversion only slightly at 400°C whilst poorly-crystallised boehmite was transformed to γ-alumina at less than 350°C, indicating that the temperature of the transition increased with increasing crystallinity.

Other workers[67] have studied the oxidation of aluminium powders with a 7% or 15% alumina content. After water removal in air, powders were compacted either immediately or after exposure to a humid atmosphere, to preserve the gas content. On exposure to a normal atmosphere, (80% relative humidity), at 400°C, a layer of boehmite was formed. At 600° and 700°C, little adsorption of water took place, the oxide being in the γ- form. In a humid atmosphere, (100% relative humidity), however, considerably more adsorption of water took place at 600°C, but there was still very little adsorption at 700°C; this was ascribed to a decrease in the surface area of the oxide and to a complex water/ γ-alumina interaction. It is suggested by the present author that the conversion of amorphous to crystalline γ-alumina might be involved here.

Based on degassing-kinetic curves at 20-700°C, Litvintsev and

Arbuzova[67] have proposed that the following conversions take place:-

$$Al_2O_3.3H_2O \xrightarrow{150^oC} Al_2O_3.2.5H_2O \xrightarrow{175\text{-}310^oC} Al_2O_3.H_2O \xrightarrow{530\text{-}550^oC} \gamma\text{-}Al_2O_3$$

hydrargillite unstable boehmite

When the aluminium powders were dried in argon, readsorption of water was negligible even in a very humid atmosphere, and argon was found to be adsorbed on the oxide surface. This was stated to be the probable cause of the loss of activity of the oxide surface.

2.2.2 Hydrogen Evolution.

In studies of hydrogen production at elevated temperatures by the reaction of aluminium powders with gaseous water, the following reactions have been proposed by Litvintsev and Arbuzova[67]:-

(a) $2Al+3H_2O \longrightarrow Al_2O_3+3H_2$

(b) $2Al+6H_2O \longrightarrow Al_2O_3.3H_2O+3H_2$

The probable initiation reaction at temperatures less than 210°C was proposed to be:-

$$2Al+4H_2O \longrightarrow Al_2O_3.H_2O + 3H_2$$

boehmite

These workers have reported that hydrogen evolution took place at temperatures as low as 90°C, probably by reaction (b). At temperatures greater than 210°C, (a) was suggested to be the initiating reaction since hydrogen production was much increased. At 490-500°C the rate of hydrogen production again increased and was found to

coincide with boehmite decomposition. The water produced was proposed to result in more hydrogen evolution by reaction (a).

It has also been reported[54] that for the oxidation of aluminium, bearing a natural oxide film, temperatures in excess of 550°C in the presence of wet oxygen or air, epitaxial growth of the crystalline γ-oxide was speeded up by diffusion of hydrogen atoms from the metal to the metal-oxide interface and into the oxide, Hydrogen was said to act as a stabilising impurity in the crystalline lattice of the oxide making possible the formation of a defect-type spinel lattice, assumed to be γ-AlOHAl$_2$O$_3$

2.2.3 Conclusions.

Summarising, one might expect that the oxidation of aluminium in moist air or oxygen would lead to some hydrargillite formation at temperatures less than about 150°C.[67] From 175°C to about 500°C, some boehmite might be formed[66,67]. At temperatures in excess of about 500°C, some crystalline γ-alumina might be formed[54] with a little water adsorbed[65] and the growth of crystallites would be expected to be faster than under dry conditions[54]. For oxidation at temperatures in excess of about 90°C, hydrogen evolution might occur[67], and at all temperatures the amount of water adsorbed should increase with increasing water content of the oxidising atmosphere[65].

CHAPTER III

Anodically-Formed Oxide Films.

3.1 Introduction.

Anodic oxide films are prepared by making aluminium the anode in an electrolytic cell using a suitable electrolyte depending on the type of oxide film required. Two types of oxide film can be produced by anodic oxidation, namely porous and non-porous or barrier-type films. The electrolyte used determines the type of oxide formed.

Barrier-type films are formed in electrolytes having low solvent power for alumina, including neutral boric acid solution, aqueous solutions of ammonium borate or tartrate, ammonium tetraborate in ethylene glycol, and some organic compounds including citric, malic and glycollic acids.

Porous films are produced in electrolytes in which the oxide film is more soluble. The commercially important pore-forming electrolytes are sulphuric, phosphoric, chromic and oxalic acids, all of which have been used over a wide range of concentrations.

The thickness of barrier-type films depends on the electrolyte temperature and anodising voltage, but is independent of the electrolyte chosen. For porous-type films thickness depends on the electrolyte temperature, the current density, the anodising time and the electrolyte itself. The maximum thickness of barrier-type films

is restricted by the oxide breakdown voltage[6], 500-700 volts. This limitation is absent for porous-type films. At low temperatures of 0-5°C, porous films are thick, compact and hard, and the production process is called hard-anodising. At higher temperatures (60°-75°C), the porous film is soft, thin and non-protective; the process is approaching the condition for electropolishing, the oxide film being dissolved almost as soon as it is formed.

Porous films consist of a thick, porous outer layer overlying a thin, compact inner layer. The thickness of this inner layer is, as for barrier-type films, dependent on formation voltage, and the inner layer of porous films is normally referred to as barrier layer.

3.2 Anodising Ratio.

Barrier-type films conduct electrons at low field strengths. At high field strengths, ions are also conducted, and for a given metal, a minimum field strength exists below which ionic conductance is negligible. Above this minimum value ionic current leads to the growth of the oxide film upon the metal, and, if the oxide is completely non-porous, growth continues as long as the ionic current persists. The reciprocal of the minimum field strength required to cause ionic conduction is called the anodising ratio, which, for non-porous films on aluminium, is close to 14 Å volt^{-1} [68,69].

During anodisation in pore-forming electrolytes, the field strength does not fall to the minimum for ionic conduction, so the

anodising ratio for the barrier layer is less for porous-type than for barrier-type films. Table II lists anodising ratios reported for the barrier layer[7,31,43] of porous-type films in various electrolytes, all for alumina films on aluminium.

TABLE II

Anodising Ratios for Porous Oxide Films.

Electrolyte Acid	Temperature °C	Anodising Ratio, Å volt^{-1}
15% Sulphuric	10	10.0
2% Oxalic	24	11.8
4% Phosphoric	24	11.9
3% Chromic	38	12.5

3.3 Barrier Layer Growth in Porous-type Films.

Plate II(a) shows the behaviour of the barrier layer thickness[24,41,43] during the first 30 seconds of anodising in 15% w/v sulphuric acid. The barrier layer appears to be completed within a few seconds[23,43]. Plate II(b) shows the corresponding current density behaviour[43]. The dotted portion corresponds to the behaviour for barrier-type films, that is, the behaviour for both types of film is identical initially. The final current densities differ markedly, the current being mainly ionic for porous films and having a much larger electronic contribution for non-porous films. The current density be-

haviour at A, in Plate II(b), has been interpreted in terms of pore initiation. This necessitates the thinning of the barrier layer formed in this time leading to increased current density. Hoar and Yahalom[42] have, however, suggested that the barrier layer current decreases exponentially, the increase in current density arising from a pore current. It has been pointed out that these workers have not specified the origin or driving force for this pore current.[70]

The minimum current density at A, that is at the point of pore initiation, occurs earlier the higher the applied voltage and the more acidic the electrolyte. The thinning of the barrier layer ceases after a few seconds. This may be understood in terms of increasing field strength across the barrier layer as it thins until the rate of barrier layer production equals and then exceeds its rate of loss in the formation of porous layer[43]. Ultimately, these two processes must be balanced.

3.4 Structural Features of Anodised Films.

Verwey[71-74] has reported that barrier-type films consist of crystalline γ'-alumina. The difference between γ'-and crystalline γ-alumina lies in the cation arrangement; both have the same anion lattice. Harrington and Nelson[75] reported that both porous and non-porous films formed in a wide variety of electrolytes consisted of alumina of random structure, the structure tending to be less random

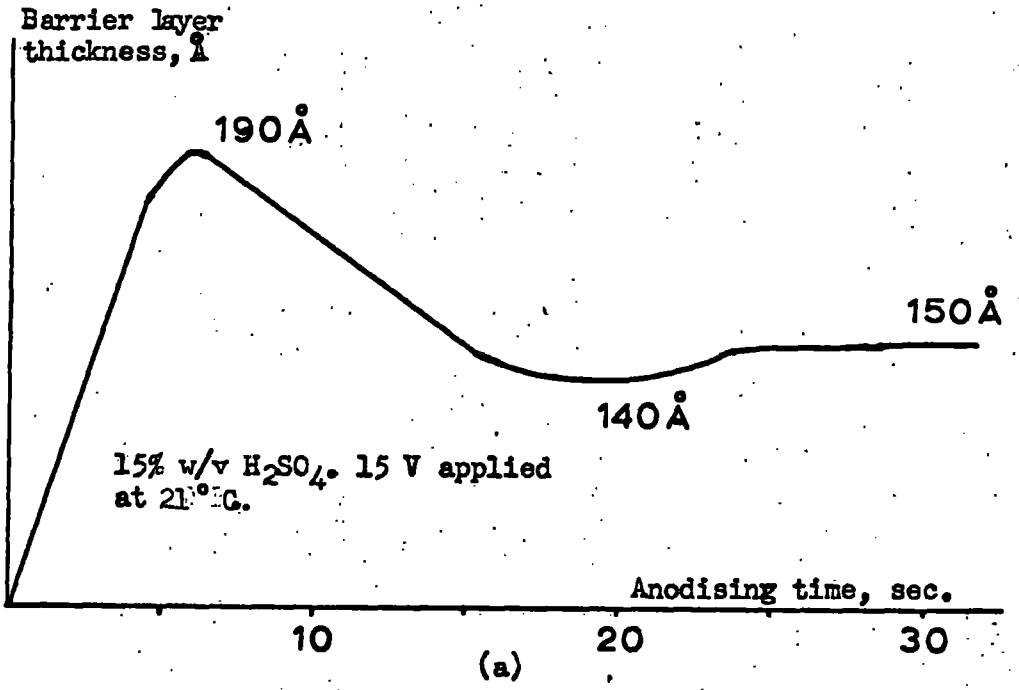

(a)

Changes observed, during the initial 30 seconds, in the formation of porous alumina films [24,41,43]

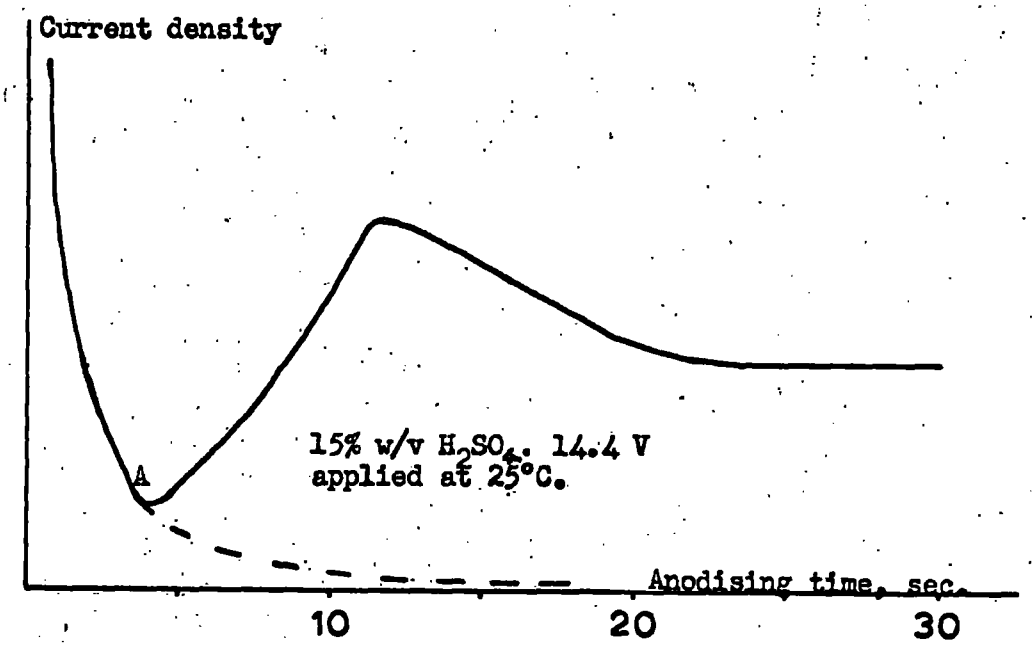

(b)

Plate II

for high temperatures of film formation. This has been interpreted[76,77] as being due to an increase in the crystalline proportion of the film at higher temperature, which is also favoured by increasing film thickness, high formation voltages, the use of dilute electrolytes and the use of alternating current. Below 100 volts formation voltage, barrier-type films were found[77] to be amorphous, but some crystalline γ-alumina was also detected above 100 volts.

Altenpohl[78] reported that barrier-type films consist of an outer soluble layer and an inner insoluble layer. The inner layer was assumed to be crystalline γ-alumina, the proportion of which increased with increasing temperature and formation voltage. However, Stirland and Bicknell[77] did not consider that the crystalline and amorphous oxide existed in a layer-type structure.

Franklin[79] has investigated barrier-type films prepared in boric acid-borax electrolyte and reported at least three types of oxide to be present, (a) hydrated oxide at the oxide-electrolyte interface, (b) irregular patches of crystalline γ-alumina, and (c) amorphous oxide which is the main constituent. The complexity of these films increased as the formation voltage increased, probably as a result of increased crystallinity. Trillat and Tertain[80] found a similar structure for porous films formed in 20% w/v sulphuric acid. An outer layer was reported to consist of a mixture of boehmite and crystalline γ-alumina and an inner layer of amorphous alumina.

An infra-red reflectance technique used by Dorsey[81-83] has

indicated that the barrier layers formed in all electrolytes are alumina trihydrates which undergo structural changes when porous films are formed. The absorption band of the barrier layer was reported to be between 900 and 1000 cm^{-1} wave numbers. The position of this absorption band for films formed in boric acid was found to be unchanged by the length of the anodising or formation time, implying that the barrier-type film is truly non-porous. In pore-forming electrolytes, the band shifted to higher frequencies as porous oxide growth proceeded. Dorsey has proposed that in order to form pores, a cyclic alumina trihydrate existing in the barrier layer decyclises, there is an effective lowering of polymer weight and hence the absorption band moves to higher frequencies. Kormany[84] has reported the presence of alumina trihydrate in barrier layers, along with γ-alumina, aluminium hydroxide and boehmite.

Diggle, Downie and Goulding[70] have pointed out that since no indication is given by Dorsey as to the sensitivity of the absorption band to decyclisation, there is some doubt as to whether boric acid films can be said to be truly non-porous. Porous layer was detected by Dorsey by this method for supposedly non-porous films formed in ammonium tartrate and tartaric acid solution. The absorption band for porous layer was found for films formed in typical pore-forming electrolytes such as sulphuric and phosphoric acids.

Some of this work is apparently contradictory but it can be

said that, in general, non-porous films are regarded as amorphous and porous films as crystalline, both being anhydrous[85-87]. The work of Dorsey indicates that the oxide films are not anhydrous. The presence of water is regarded by some workers[88,89] as necessary to stabilise the spinel-type structure of alumina, possibly by replacement of oxygen ions in the alumina lattice by hydroxyl ions.

3.5 Anion Incorporation.

The extent of the incorporation of anions of the anodising electrolyte into the oxide structure appears to be greatest for pore-forming electrolytes and least for those electrolytes giving rise to barrier-type films. A 1% incorporation of boron into films formed in ethylene glycol-ammonium pentaborate and boric acid-borax electrolyte has been found[79,90] while porous films formed in sulphuric acid have been reported to contain up to 17% of sulphate ion[91-93]. Mason[93] has reported sulphate ion incorporation to be higher the lower the anodising temperature and the higher the current density during film formation. Hoar[94] has suggested that this is due to the increasing importance of the following reaction as the temperature is increased:-

$$\underset{\text{FILM SURFACE}}{SO_4^{2-}} \longrightarrow SO_3(aq) \qquad + \underset{\text{FILM}}{O^{2-}}$$

In porous-type films, anions of the electrolyte can be incorporated into the porous layer in two ways, in a "bound" form result-

ing from conversion of barrier to porous layer and in a "free" form resulting from the accumulation of anions in the pores[95]. For sulphuric acid formed films, Ginsberg[95] has reported a total sulphur content corresponding to 13% sulphur trioxide which fell to 8% after prolonged washing, so that 5% of the total anion incorporation was "free". Thach Lan and his co-workers[86] have reported that sulphur is present as the anion, whereas other workers[96-98] have reported that it is present as a basic sulphate.

It has been suggested[99] that the porous layer is formed by conversion of the outermost portion of the barrier layer, that is, that formed by cation transport. The result of this should be a uniform incorporation of anions from the electrolyte in the porous layer. This has been confirmed[27] using an electron probe microanalysis technique.

3.6 Water Content of Oxide Films.

Although non-porous films are generally regarded as anhydrous, some workers regard water as necessary to stabilise the spinel-type structure. Lichtenberger[85] has indicated that 2.5% water, present as boehmite, is necessary.

15% w/w water content in porous films formed in sulphuric and oxalic acid has been reported by Pullen[91]. Edwards and Keller[100] found 1-6% in sulphuric acid formed films and Philips[92] found sufficient water in films formed in oxalic acid to produce $2Al_2O_3.H_2O$

within the film.

The extent to which water is incorporated depends on the conditions and treatment during formation[70]. It is probably never in the "free" form but occurs either as hydroxide or hydrated oxide or both.

3.7 Properties of Barrier-type Films.

Thus far in this chapter, matters relevant to both barrier-type films on aluminium and to porous parts of oxide films have been discussed. The two types of film differ in characteristics; this section is largely concerned with studies of the barrier layer.

3.7.1 A.C. Resistance of Barrier-type Films.

In an investigation of the mobilities of protons and hydroxyl ions during the anodic oxidation of aluminium in tartrate solutions, Brock and Wood[38] showed that the a.c. resistance of the outer part of the film decreased as current was allowed to decay at constant formation voltage. These workers related the decrease in resistance to the formation of pores at the low current densities which obtained during current decay, and to increased hydration of the film as a result of an increase in the hydroxyl ion content of the electrical double layer under the same conditions. At pH 5 and 7 in aqueous tartrate solution under current decay conditions discrete pores were observed, and it was suggested[38] that the presence of minute invisible pores under steady current conditions could account

for the observed low ionic resistance of alumina formed in this manner. No pores were observed during anodisation of aluminium in non-aqueous borate solutions, and the a.c. resistance of films formed in this medium was independent of the formation current density; it was suggested that hydration played a part in pore formation.

Brock and Wood[39] have also discussed the ease of entry of hydroxyl ions into tartrate formed films, and concluded that, under conditions in which the activity of protons or hydroxyl ion is high in solution, the extent of entry is little affected by the rate of film formation. The conclusionsof this work are interesting since tartrate formed films are conventionally regarded as non-porous.

Earlier, Heine and Pryor[21] studied the a.c. electronic and ionic resistance of films formed in 3% w/v ammonium tartrate solution at pH7. The initial surface treatment consisted of an etch in sodium hydroxide solution, and current surges during anodising were restricted to 5 mA cm^{-2} in order to avoid film damage due to local heating. The current was allowed to decay to 15-20μA cm^{-2} at a predetermined voltage. Films were thinned uniformly in passivating sodium chromate solution of pH 7-9. Heine and Pryor found that this technique left the metal passive and the inherent specific resistance of the oxide was unaffected by the dissolution process. Brock and Wood[38,39] have also used this technique.

Heine and Pryor[21] found four regions in the oxide produced by anodising to 20 volts in 3% w/v, pH7, ammonium tartrate solution.

a) A region of low electronic resistivity extending to 60-80 Å from the metal-oxide interface, the ionic resistivity increasing from about 4×10^{9} ohm cm 25Å from the metal-oxide interface to about 2×10^{10} ohm cm 80Å from the interface. Apparently, in this region there is a departure from stoichiometry. This was considered[21] to be due to the proximity of the metal-oxide interface and to represent an n-type region of excess aluminium ions.

b) From about 60-160 Å, the electronic and ionic resistivities were constant, that is, the metal substrate no longer exerted any influence.

c) Beyond lay a region about 60 Å thick having a low ionic resistivity. This region was diffuse, and was believed[21] to contain hydroxyl ions from the anodising electrolyte, a view shared by Brock and Wood[38,39].

d) The outermost region, about 20 Å thick had a high ionic resistivity. Heine and Pryor have suggested that strong oxidising conditions could be present at the surface, resulting in a complete anion lattice and bound positive holes giving a p-type defect structure.

For films formed under the same conditions but anodised to 15

volts, region (b) was absent.

Brock and Wood[39] have found similar behaviour to the above following formation with maximum current surges restricted to 10 ma cm^{-2}. For 100 μA cm^{-2} maximum current surges, the outermost region (d) was absent and this too was in support of the findings of Heine and Pryor.

3.7.2 Ionic Charge Transport in Barrier-type Films.

Considering a cation mobile system in which movement of cations depends upon the electric field strength across the oxide film, two types of ionic charge transport are possible.

a) High field conduction, where it is assumed that the field strength prevents movement of cations against the field.

b) Low field conduction, where cation movement against the field can no longer be assumed to be negligible.

Theories of ionic conduction assume that high field ionic conduction takes place during anodising since electric field strengths are 10^6-10^7 volts cm^{-1}, which is regarded as sufficient to prevent movement of cations against the field.

Guntherchultze and Betz[101-105] have shown that under high field conditions, the ionic current density (i_+) and the electric field strength(E) are related by the exponential law.

$$i_+ = A_+ \exp B_+E \qquad (1)$$

where A_+ and B_+ are temperature-dependent constants involving ionic

transport parameters. Several attempts have been made to justify this equation theoretically in terms of the possible rate determining step being ion transport across the metal-oxide interface[56,106], ion transfer through the bulk of the oxide[107] or a combination of these two processes[108,109].

Difficulties in interpretation arise since these theories consider the transport of ions through a crystalline lattice whereas the filmsare known to have a high degree of amorphous nature. It is also difficult to explain the existence of current transient phenomena by means of this treatment.

Dignam[110-112] has proposed a theory of ionic conduction leading to oxide growth based on an amorphous structure. This theory is claimed to account for steady state and transient phenomena for oxide growth on aluminium, tantalum, niobium and bismuth, and also accounts for anion migration, neglected in the previously-mentioned theories.

3.7.3 Determination of Thickness.

Any method for determining the thickness of barrier-type films should preferably be rapid and non-destructive and ideally be an "in-situ" measurement. Some of the methods which fulfil some of these requirements are now considered, but not all in detail.

3.7.3.1 Application of Faraday's Laws.

The volume, V, of oxide laid down by passage of a quantity Q of electricity, assuming 100% current efficiency is given by

$$V = \frac{QM}{2yF\rho} \qquad (2)$$

where M is the molecular weight of the oxide A_xO_y of density ρ, and F is the Faraday. The thickness can be evaluated if the apparent area of specimen surface covered is known. The effective molecular weight depends on the purity of the oxide and the current efficiency must be known. The density can usually be found by the method reported by Jepson[113].

Because of these difficulties, this method is seldom used, although Bray, Jacobs and Young[114] applied it to study the anodic oxidation kinetics of tantalum and found the results to be consistent with the Dewald dual barrier theory[108,109] of ionic conduction. Bernard and Cook[115] found that for barrier-type films formed on aluminium in ethylene glycol/ammonium pentaborate solution, the agreement between the film thickness determined by this method and by optical methods was satisfactory.

3.7.3.2 Optical Methods.

Spectrophotometric[116-120] and ellipsometric[69,121-123] methods are the most widely used methods of thickness measurement. The data obtained are usually the most accurate, provided that satisfactory values of the optical constants for the oxide and the underlying metal are known. Measurements can be made "in-situ" provided that the optical constants of the film-forming electrolyte differ apprec-

iably from those of the film substance.

3.7.3.3 Capacitance Method.

For an oxide of uniform thickness, the system metal-metal/oxide interface-oxide-oxide/electrolyte interface-electrolyte which is present is analagous to the system present in a parallel plate condenser. The capacitance C is given by

$$C = \varepsilon A/4\pi d \qquad (3)$$

where ε is the dielectric constant of the oxide, A the surface area and d the oxide thickness.

Several precautions must be borne in mind in interpreting capacitance measurements in terms of the oxide thickness. The electrical double layer makes a contribution C_{edl} to the measured value C_m[124]. Since C_{edl} is in series with the capacitance C_{ox} due to the oxide film, equation (4) must give the relationship between these quantities, viz:-

$$1/C_m = 1/C_{ox} + 1/C_{edl} \qquad (4)$$

When $C_{edl} \gg C_{ox}$ the measured capacitance C_m approximates closely to that due to the oxide.

The type of oxide present also affects the validity of the interpretation. Lorking[5] has shown that if the film is coherent and impermeable C_{ox} may be used to estimate film thickness. However, when the film has been rendered porous by corrosive solutions,

incorrect values are obtained.

If accurate thickness values are required, an accurate value of dielectric constant must be found, possibly by calibration using films of known thickness. Since dielectric constant is often a function of the frequency, capacitance measurements are usually made at constant signal frequency. Again, extreme care must be used to ensure that the input signal does not affect the specimen potential in cases in which C_{ox} does not differ greatly from C_{edl}, since the electrode potential will influence the double layer present and hence influence C_{edl}[124].

Many methods have been used to measure the capacitance of specimens, including the d.c. transient method[125-127] which has been applied to the determination of surface roughness factors[127]. Bridge techniques have also been used[128]; Wood, Cole and Hoar[129] developed a bridge containing the experimental cell as unknown impedance and a balancing impedance. An amplifier and oscilloscope were used to detect balance, and an accuracy of better than $\pm$ 5% was attained for input voltages of 1-100 mV at 10-500 Hz. The type of signal used determines the extent of balance. If sine waves are used, any combination of resistance and capacitance can be exactly balanced by one resistance and one capacitance in series. In the case of square waves, however, components of all frequencies are present, and every element of a complex impedance must be balan-

ced individually.

A third method of capacitance measurement involves the use of analogue circuits, of which many have been designed. The two simplest are the series and parallel circuits illustrated in Plate III (a). R_s, R_p and R represent non-inductive resistance boxes and C_p and C_s decade condensers. The use of the simple parallel analogue has been demonstrated by McMullen and Hackerman[124] who applied the same square wave input signal to the test electrode and analogue. The response voltage time curve from the test electrode was displayed on an oscilloscope, compared with that from the analogue, and the two curves matched by selecting values of R_s, R_p and C_p. When $R_s = 0$ then ohmic drop exists through the electrolyte and/or the external circuit. Types of response curves to square wave inputs are shown in Plate III. Analogue or comparison circuits have been used by Leach and Isaacs[130-133] in studies of the capacitances of metals as functions of the electrode potential, and complex analogues have been used by Hoar and Wood[42] in studies of the sealing of porous anodic oxide films on aluminium.

3.7.3.4 Direct weighing techniques.

Direct weighing of specimens has been used by several workers[124,125,134] For example, the amount of oxide formed anodically can be found by weighing the specimen before and after oxide dissolution in a reagent such as phosphoric-chromic acid mixture, which dissolves the

(a) Simple analogue circuits.

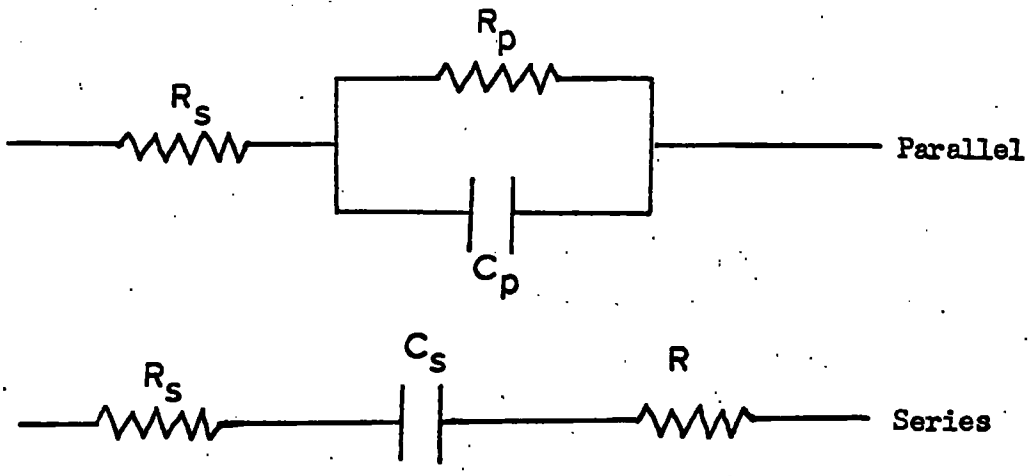

(b) Four types of V-time trace obtainable from a simple analogue circuit.[124]

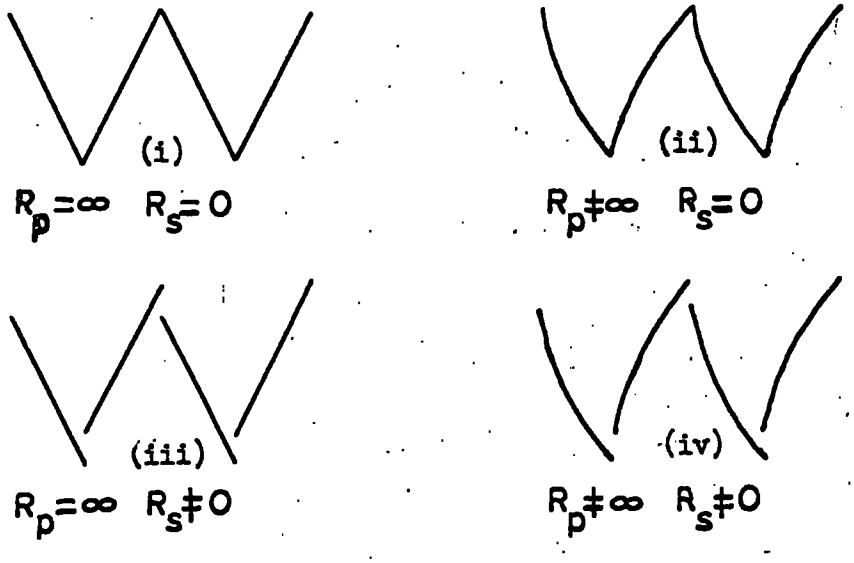

Plate III

oxide and leaves the metal unattacked. Knowledge of the oxide density and apparent surface area of specimen covered by oxide gives the oxide thickness.

3.7.3.5 Miscellaneous methods.

Hunter and Fowle[24] have determined the barrier layer thickness in porous anodic oxide by a method in which the minimum voltage required to cause further growth was used to estimate the film thickness. It was assumed that a minimum electric field strength is required to promote ionic conduction across a presumably fixed barrier thickness. The barrier film was immersed in an electrolyte having a negligible solvent power for the oxide. A slowly increasing voltage was applied across the film and the applied voltage, V, at which the current suddenly increased, indicating the flow of ionic current, was noted. If E is the minimum field strength required for ionic conduction and d is the film thickness, from the relationship $V/d = E$, d can be calculated if E is known. Using 3% w/v ammonium tartrate electrolyte at pH 7, Hunter and Fowle observed the type of behaviour illustrated in Plate IV(b) for sulphuric acid formed films; Diggle[23] reported the type of behaviour shown in Plate IV(a) for the same system.

Hunter and Fowle assumed the anodising ratio for barrier layer on aluminium to be 14 Å volt^{-1}. This value is somewhat suspect, since the ammonium tartrate solution has, apparently, a slight solvent

power for the film. The evidence for this solvent power will be discussed later in Section 8.1. To assume, however, that all of the applied voltage appears across the barrier layer involves greater error.

Considering the parallel plate condenser eq.(3) and assuming that the expression $V = Ed$ is valid, it follows that

$$V = E. \frac{\varepsilon A}{4\pi C} \qquad (6).$$

A plot of V versus $1/C$ should be linear and pass through the origin if all of the applied voltage appears across the barrier layer. It has been reported[135] that this plot is linear for aluminium anodised in neutral 3% ammonium tartrate solution, but that the intercept on the voltage axis is at about -2 volts. Vermilyea[136] has proposed that the true voltage across the barrier layer (V_t) is related to the applied voltage (V_a) by equation 7:-

$$V_t = V_a - (\eta_c + aiR) + V_r. \qquad (7).$$

η_c is the cathode overpotential, a the surface area, i the current density and R the total resistance of the solution and any external series resistance. V_r is the e.m.f. corresponding to the reaction

$$2\ Al + 3\ H_2O = Al_2O_3 + 3\ H_2$$

which, from thermodynamic data,[137] may be calculated to be 1.5 volt. Using equation (6)

$$V_a = E. \frac{\varepsilon A}{4\pi C} + (\eta_c + aiR) - V_r \qquad (8)$$

It is clear that this equation predicts that a graph of V_a versus 1/C should not pass through the origin.

Hunter and Fowle[24], however, have reported an accuracy of approximately 3Å in their determination of barrier layer thickness if a correction is applied to allow for the expected electronic leakage level of 100 μA cm^{-2}. The required voltage value is taken to be that required to increase the current density to a value in excess of 100 μA cm^{-2} as is illustrated in Plate IV (b).

Among other methods, the scattering of α-particles has been used[138] to determine the thickness of oxide films on anodised aluminium. Measurements were based on determinations of the difference between the energies of α-particles scattered from the oxide surface and the underlying metal. Films from 10 to 130 μgcm^{-2} were reported to have been analysed non-destructively with a relative standard deviation of 3.5%. The average time of analysis was 30 minutes with an incident beam current of up to about 1 μA.

3.8 Porous Anodic Oxide Films on Aluminium.

3.8.1 Solvent Action in Pore Formation.

The formation of porous alumina and concurrent dissolution processes can be understood in terms of the following:-

a) Ionic migration, forming an initial barrier layer which will remain as a barrier layer if the electrolyte has no solvent power for the oxide.

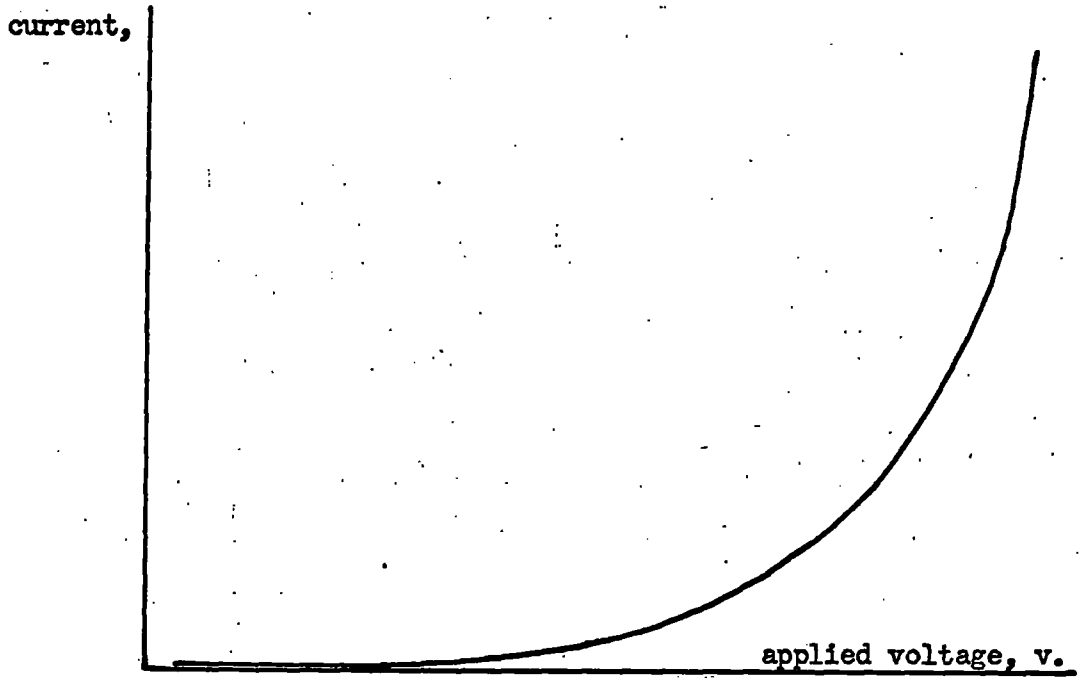

(a) The type of behaviour observed[23] for a porous alumina film immersed in 3% w/v ammonium tartrate solution during the application of a steadily increasing voltage.

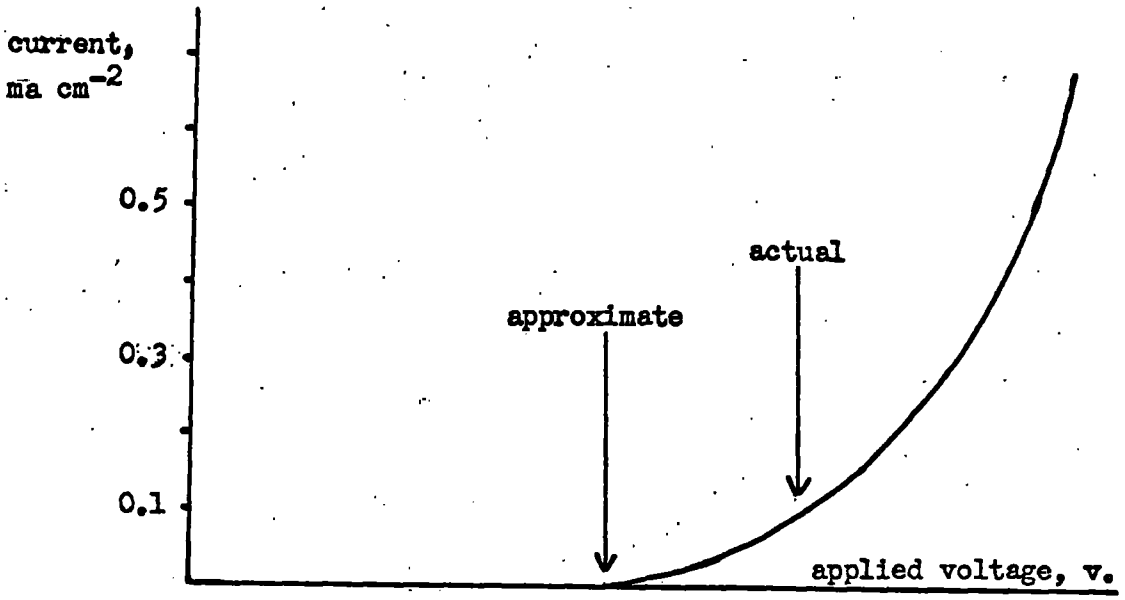

(b) The determination of the barrier thickness of a porous alumina film by the method of Hunter and Fowle[24]. The approximate and actual barrier voltages are as indicated, assuming an electronic leakage current value of 100μa cm^{-2}.

Plate IV

b) In electrolytes with solvent power, conversion of barrier to porous layer takes place when the barrier layer has reached a certain thickness[24,41,43]. This conversion is believed to be a field-assisted electrochemical process[23,41,139]. Pore formation begins earlier in 15% sulphuric acid films than in 4% phosphoric acid films[140], indicating that in the former case, the conversion process is more rapid. This is borne out by the lower anodising ratio found for the barrier layer of sulphuric acid-formed films (Table II). Murphy[141] suggested that both protons and anions are involved in pore formation and found that the pore density decreased linearly with decreasing pK_a for the series of electrolytes 15% sulphuric acid, 2% oxalic acid, 3% chromic acid and 4% phosphoric acid. If aluminium is anodised in ammonium tartrate solutions for long periods in excess of 60 minutes, the current density-time behaviour is similar to that observed during sulphuric acid anodising[142], but the final current density is much lower. As in the case of anodising in pore-forming electrolytes[41], the current minimum is observed earlier the lower the pH of the electrolyte and this could indicate that pore formation is occurring. Hoar and Yehalom[41] found that in pore-forming electrolytes the minimum current density occurred earlier the higher the applied voltage, which is evidence for field-assisted dissolution.

c) The porous layer thickness is a function of current density, time, electrolyte temperature and, to a small extent, the electrolyte concentration.

d) Because of external surface dissolution of the oxide by the electrolyte, porous films are found to be thinner than would be expected by consideration of the amount of charge passed in formation[27,28]. The process is strongly temperature-dependent and is slightly affected by the electrolyte concentration.

e) There is considerable evidence that so-called non-porous barrier type films do possess some porosity. The resemblance of current transient phenomena during anodising for long periods of time in ammonium tartrate solutions to those in formally pore-forming electrolytes[142] has already been mentioned. Dunn[143,144] has found that anodising in 1% ammonium pentaborate at high film formation rates (high current densities) produces non-porous films but at low formation rates porous layer is formed. This is reminiscent of the findings of Brock and Wood[39], that for anodising in aqueous tartrate solution, pH 6-8, the a.c. resistance of the outer part of the film was much less for low than for high current densities and presumably the extent of hydration, probably by hydroxyl ion diffusion, was much greater in the former case[39]. Hunter and Towner[118] have reported that anodising in 3%, pH 5.6 ammonium tartrate solutions produces a non-

porous oxide film if the voltage is held constant and the current is allowed to decay only until it reaches a minimum, that is, the barrier film is completed. If anodising is continued beyond this point, porous layer begins to form and has been detected by electron microscopy after long periods of anodising[118]. These workers have reported that 50% of the leakage current is involved in porous layer formation at a small constant rate. Dorsey[81-83] has detected porous layer produced by anodising aluminium in ammonium tartrate and tartaric acid by the presence of the porous layer infra-red absorption band. The work of Dorsey was discussed earlier. Barber[145], however, found pores in oxide produced anodically in aqueous ammonium citrate and citric acid but that pore formation was reduced by ultrasonic vibration of the anodising cell. He concluded that the pores probably arose from bubbles in the anodising cell.

3.8.2 Structure of Porous-type Alumina Films.

From many electronoptical investigations[7,134,146-148], both by the replicating and the direct transmission technique and from some gas adsorption studies[25,149], the structure of the porous anodic oxide film would appear to be essentially that reported by Keller, Hunter and Robinson[7].

In essence, the structure is as follows. Each pore lies in the centre of a hexagonal-shaped oxide cell, width c. The pore diameter

is reported to be independent of both the anodising voltage and the time of film formation, and to depend only on the electrolyte used. Some indication of the pore diameters is shown in Table III.

Table III

Pore Diameters in Different Electrolytes.

Electrolyte concentration and temperature		Pore Diameter Å
4% phosphoric acid	24°C	330
3% chromic acid	38°C	240
2% oxalic acid	24°C	170
15% sulphuric acid	10°C	120

The oxide cell width depends on the anodising voltage, and the pore wall thickness has a certain anodising ratio as has the barrier layer thickness.

Table IV

Anodising Ratios for the Barrier Layer and Pore Wall Thickness.

Electrolyte concentration and temperature		Barrier layer Å volt^{-1}	Pore wall thickness Å volt^{-1}
4% phosphoric acid	24°C	11.9	11.0
3% chromic acid	38°C	12.5	10.9
2% oxalic acid	24°C	11.8	9.7
15% sulphuric acid	10°C	10.0	8.0

As the anodising voltage increases, the width, c, of the oxide cell increases and so the pore density decreases. This is illustrated in Table V for 15% sulphuric acid at 10°C [7].

Table V

Pore Densities of Films Formed by Anodising in 15% Sulphuric Acid at 10°C.

Anodising voltage	Pore density, x $10^9 cm^{-2}$
15	83
20	56
30	30

The pore volume is the fractional volume of the porous layer occupied by pores. If these are considered to be perfect cylinders[7], the pore volume should be independent of porous layer thickness, current density, electrolyte concentration and anodising temperature. However, there is evidence that the pore volume is a function of all of these parameters[25,99,150]. The true pore shape has been proposed[25] to be that of a truncated cone with the basal diameter that reported by Keller, Hunter and Robinson[7], and with a pore mouth diameter dependent on the current density and the anodising time, that is, the film thickness. This is illustrated in Table VI for the anodisation of aluminium in 20% sulphuric acid.

Table VI

Pore Base and Mouth Diameters Reported for Oxide Films Formed in 20% Sulphuric Acid[25].

Current density mA cm^{-2}	Anodising time min.	Pore bases diameter Å	Pore mouth diameter Å
10	30	120	159
15	30	120	182
15	60	120	246
25	30	120	208

The slope of the pore wall is very slight, since, for example, in the case of pore base diameter 120Å, pore mouth diameter 159Å, the porous layer thickness is 9μm. A possible limitation on porous layer thickness might be expected, since if anodising were continued sufficiently long and/or at increased current density, the pore mouth diameter might equal the oxide cell width. Indeed any further anodising beyond this point might result in reduced thickness by surface chemical dissolution by the electrolyte. Some evidence for a limiting maximum oxide thickness has been reported by Diggle, Downie and Goulding[70] based on the work of Liechti and Treadwell[96] and Sacchi[151]. Golubev and Ignatov[152] have also found evidence for this type of behaviour.

3.8.3 Frequency Dependence of the Impedance of Porous-type Films.

Jason and Wood[153] have proposed an electrical analogue to represent the impedance of porous anodic films on aluminium. This is illustrated in Plate V(b) and is clearly in keeping with the cylindrical pore model (Plate V(a)). Hoar and Wood[42] found that this analogue adequately represented the frequency dependence of the impedance of films formed in 15% w/v sulphuric acid. They found, in common with Jason and Wood, that for unsealed films, the measured series capacitance and resistance decreased as the a.c. measuring frequency increased. Above 10^3Hz the resistance remained approximately constant at 25 ohm cm^{-2}; this was identified with R_1, since at these frequencies, R_2 was completely by-passed by the low impedance of C_2.

Below 10^3Hz, the measured resistance increased as the impedance of C_2 increased. It was also observed that below 10^4Hz, the measured capacitance was the barrier layer capacitance C_2 since C_o has a high impedance at such frequencies due to its low capacitance. R_o is so large that it makes an insignificant contribution to the impedance at all frequencies. Therefore, below 10^3Hz the barrier layer capacitance and resistance are measured after balancing out the ohmic drop across the solution plus that in the external circuit using square waves and this requires the simple analogue represented by R_2 and C_2 in parallel and both in series with R_1.

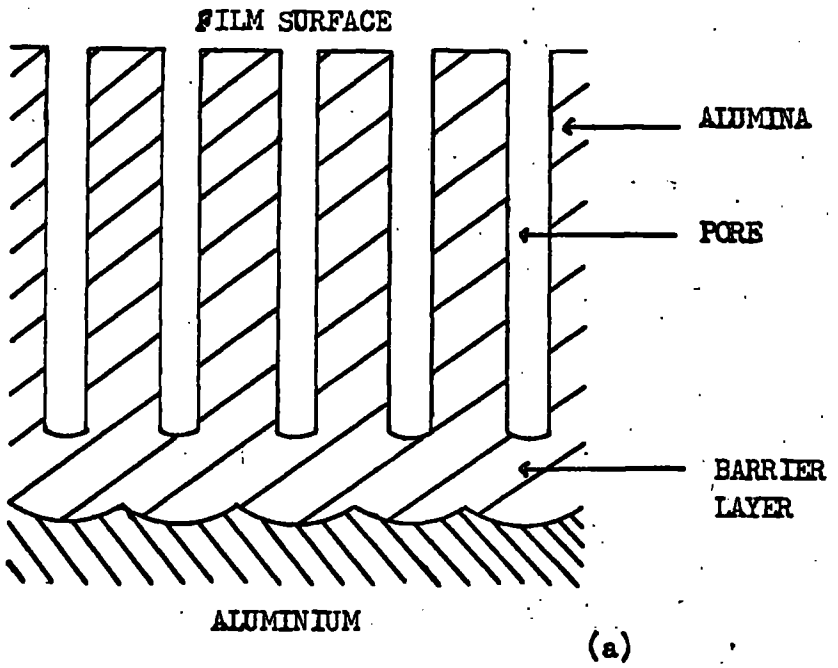

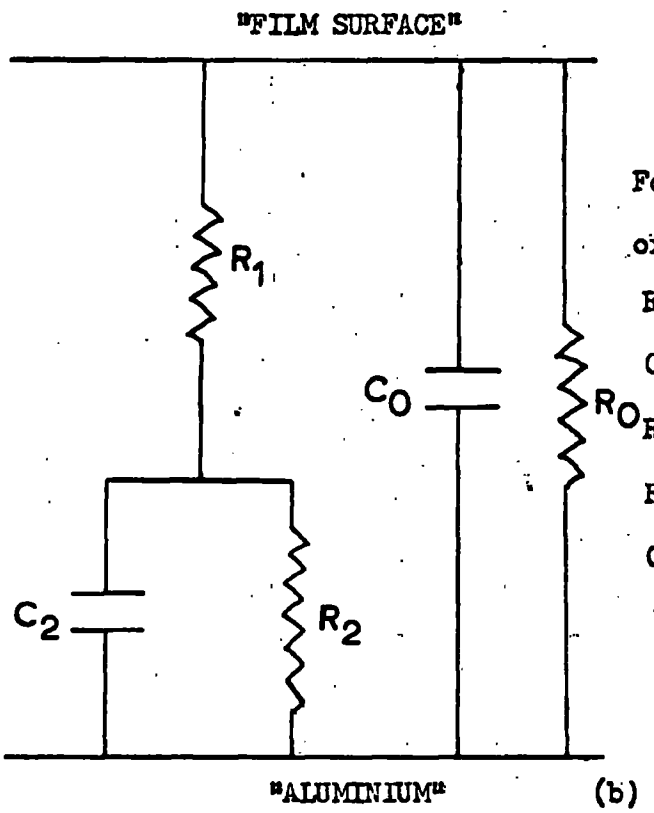

For total film thickness of 1.5×10^{-3} cm.

R_0 ca 5 MΩcm^2

C_0 ca 1×10^{-3} μF cm^{-2}

R_1 a few Ωcm^2

R_2 ca 700kΩcm^2 for 20 v film

C_2 ca 0.39μF cm^{-2} for 20 v film

Plate V. (a) Structure of porous film

(b) Electrical analogue for porous film after Jason and Wood[153]

CHAPTER IV

Experimental

4.1 Preliminary Preparation of Specimens.

The aluminium used was the British Aluminium Company's super-purity (99.99% Al.) grade, which was melted in alumina crucibles and cast into ingots in a copper chill mould.

In a few cases, specimens were in the form of wire of about 1.7 mm. diameter and 20 cm long, but the majority were cylinders about 1.5 cm long, having a cross-sectional area of about 0.6 cm^2. In the case of wire formation, ingots were rolled to size and drawn through dies to form wires of known diameter. The cylindrical specimens were produced by sectioning ingots and tapping a few turns of thread at one end so that good electrical and mechanical contact was made with a threaded aluminium wire suspension. The untapped end of the cylinder was the surface for oxide film formation; this end was polished with emery paper using light liquid paraffin as a lubricant, working through the grades 0/0 to 4/0.

Wires, to a chosen length, and cylinders at the polished surfaces, were degreased with acetone and then chemically polished at about 95°C for three minutes in a solution made up from 125 ml concentrated sulphuric acid, 350 ml. ortho-phosphoric acid and 25 ml. concentrated nitric acid[5,13-15,28]. Specimens were then washed in running distilled water for one minute, rinsed with acetone and air-dried.

Lorking[5] has suggested that at 80°C, the oxide film produced by this method is about 10Å thick and the reproducibility of film characteristics is good. Capacitance measurements made by Diggle[23] indicated a thickness a little less than this at the temperature used in the present case.

4.2 Oxide Film Preparation.

Three methods of film preparation were adopted. These were anodic oxidation to form films of the so-called non-porous barrier type, and films produced by the oxidation of aluminium in dry oxygen and in oxygen having a known gaseous water content.

4.2.1 Anodisation to Form Barrier-type Films.

Where not given in the text, details regarding instruments used are given in Appendix I.

The anodising electrolyte used was 3% w/v ammonium tartrate, buffered with ammonia to pH 7, which produces barrier-type films on aluminium. The cathode was of super-purity aluminium in the form of a cylinder surrounding the anode. Anodising was performed at 25.0 ± 0.1°C in a thermostatted water bath. A valve voltmeter was used to measure the potential difference between specimen and cathode, and the voltage applied across these was tapped from a stabilised supply. Ionic current surge was limited to 200 μA cm^{-2}, a value considerably less than those used by other workers[21,39] whose films were apparently coherent, to avoid film damage from local heating.

When the desired potential drop from anode to cathode was achieved, this value was maintained by reducing the current density to the electronic leakage level of 25-40 $\mu A\ cm^{-2}$. Heine and Pryor[21] found electronic leakage levels to be 15-20 $\mu A\ cm^{-2}$ where the initial surface preparation was an etch with sodium hydroxide solution. In the present work, anodising was regarded as completed when a low steady current density was maintained for about five minutes. The circuit was broken by removing the applied voltage, the specimen was removed and washed with distilled water.

Wire specimens were anodised to the length required. Before anodising, cylindrical specimens had their degreased sides covered with Bostik. This was applied after dilution with acetone. The electrical insulation was tested by completely covering a specimen, except at the tapped end, with diluted Bostik. After drying, the specimen was attached to a supporting wire and partially immersed in a mixture of N sulphuric acid and N sodium sulphate having a pH value of 1.0. This solution was one of the most aggresive to the oxide film used in these investigations. Over a period of twenty-four hours, no potential was recorded for the specimen with respect to a saturated calomel electrode and this demonstrated that the insulation was satisfactory for the times normally used in the present work.

Since wire specimens had such a small diameter compared with the

length immersed, errors in, for example, capacitance studies, due to creep of electrolyte and edge effects should be negligible. However, this is not the case for cylindrical specimens and measurements were therefore performed with the sides coated with Bostik and with the anodised surface just touching the appropriate electrolyte. In the case of cylindrical specimens this treatment with Bostik was used after the other types of oxide film studied had been prepared.

4.2.2 Films Formed in Dry and Moist Oxygen at 500°C.

4.2.2.1 Apparatus.

The line used for oxidation in the presence of gaseous water is shown in Plate VI. Taps and joints were greased with Apiezon M grease whose vapour pressure is negligible up to 200°C. Distilled water in tube A was thermostatted at the chosen temperature and the temperature control was, at worst $\pm$ 0.1°C, leading to variations in water vapour pressure of not more than 1%. The gases in the furnace tube, during oxidation, were in contact with the section of line isolated by taps 1 and 2. Heating tape, heating electrically to about 100°C, between the water vapour source and the furnace tube, ensured that the partial pressures of gases throughout the section were the same, since the water vapour source was always at a temperature considerably less than 100°C. Also, water from the thermostat was passed through the jacket surrounding the top of the furnace tube before entering the jacket for the tube A. The pressure in the

furnace tube, always close to 1 atmosphere, was measured with the U-manometer containing Apiezon B oil, whose vapour pressure is negligible at room temperature. The furnace was nichrome-wound, asbestos-lagged and the temperature was controlled by a Transitrol Type 990 Temperature Controller in conjunction with a chromel/alumel thermocouple and by-pass resistance. The source of power was a constant voltage transformer which supplied the primary of a variable transformer and the controller itself. Thus, temperature changes due to mains voltage fluctuations were avoided. A second calibrated chromel/alumel thermocouple was positioned in an inlet from the bottom of the tube reaching to the height of the specimens and was used to monitor their temperatures.

4.2.2.2 Oxidation in moist oxygen.

Specimens were suspended by aluminium wires in the furnace tube, taking care that the prepared surfaces were not in contact with the glass (Pyrex) to avoid silica contamination at elevated temperatures. Specimens were oxidised at 500 $\pm$ (2°C. The choice of the period of oxidation, 49 hours, will be discussed in the following section on oxidation in dry oxygen. In order to reproduce specimen treatment as nearly as possible, a routine procedure was adopted. The section of the line isolated by taps 1 and 2 was evacuated, flushed out twice with oxygen from a cylinder and was finally filled with oxygen to about atmospheric pressure. Tap 3 was closed, power to the heating

tape switched on and the thermostatted water was circulated. The N.P.L. standard thermometer, positioned near to the tube A containing water, was read to check that the temperature was at the desired value. At thermal equilibrium, the furnace tube was introduced into the furnace whose temperature was already 500°C, by raising the jack supporting the furnace. The top of the gap between furnace and tube was packed with asbestos wool to reduce heat loss and the system was adjusted so that specimens were positioned near to the centre of the furnace. When thermal equilibrium was again attained, after about ten minutes, tap 3 was opened and then tap 1 was quickly opened and closed to release excess pressure into the line beyond which contained oxygen at a little less than one atmosphere pressure. The pressure in the section of the line isolated by taps 1 and 2 was monitored from time to time by means of the oil-filled manometer. When oxidation was completed, the power source to the furnace was switched off and, when the specimen temperature had fallen to about 50°C, tap 3 was closed to avoid water condensation in the furnace tube. After about $1\frac{3}{4}$ hours, the furnace had cooled to room temperature and the tape and water circulation were switched off. With this slow cooling, differential thermal contraction of the oxide and underlying metal should not result in cracking of the oxide film. Tap 4 was opened to relieve the partial vacuum and the specimens were removed. It was considered unwise to store these specimens and all

were used immediately after oxidation.

4.2.2.3 Oxidation in dry oxygen.

The thermostatted tube was replaced by a simple tube, the heating tape removed, the furnace-tube cooled with tap water and a little anhydrous copper sulphate covered with a piece of filter paper introduced into the specimen store B and the trap C to detect moisture. The line to the left of tap 2 was flushed out and filled with oxygen, first dried in trap D by means of liquid air, to near atmospheric pressure as before. The procedure during heating and cooling of specimens was similar to that used before. Since the furnace tube was in connection with two 2 litre globes, little increase in pressure occurred during the heating of the furnace tube.

Dignam, Fawcett and Bohni[61] have determined limiting weight gains for the oxidation of electropolished superpurity aluminium in dry oxygen between 478° and 601°C. The data are summarised in Plate VII and indicate that a period of 49 hours oxidation should be more than sufficient to achieve limiting weight gain at 500°C. This period was used in the present work since this behaviour is possibly nearer that obtaining in the present work than the behaviour determined by Beck and his co-workers[48]. The electropolishing pre-preparation used by Dignam and his co-workers probably produces initial surface oxide film properties more like those in the present work than the etch in sodium hydroxide solution used by Beck and his co-workers.

Oxidation line.

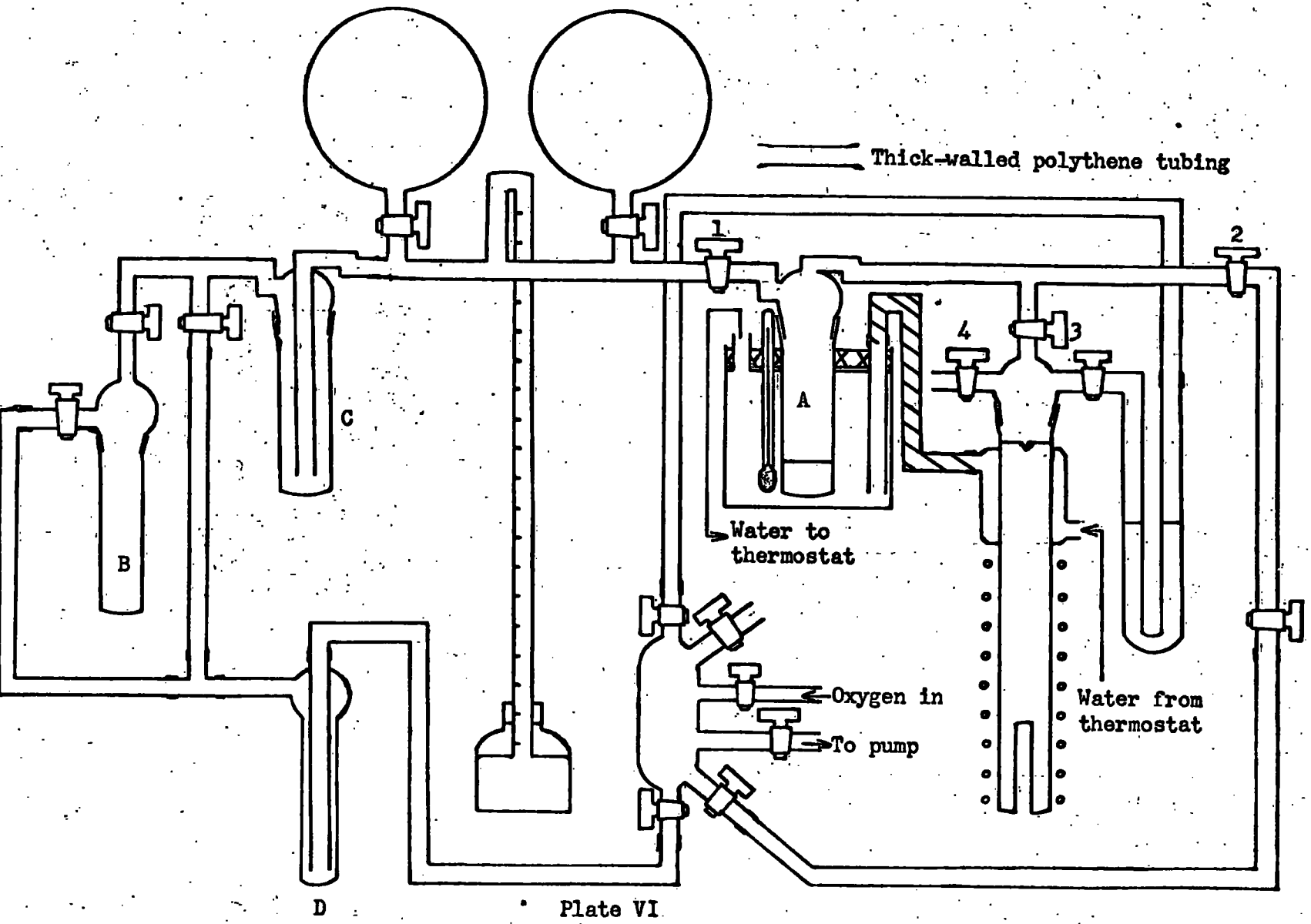

Plate VI

Limiting weight gains and times to attain them as a function of the temperature of oxidation of aluminium in dry oxygen.

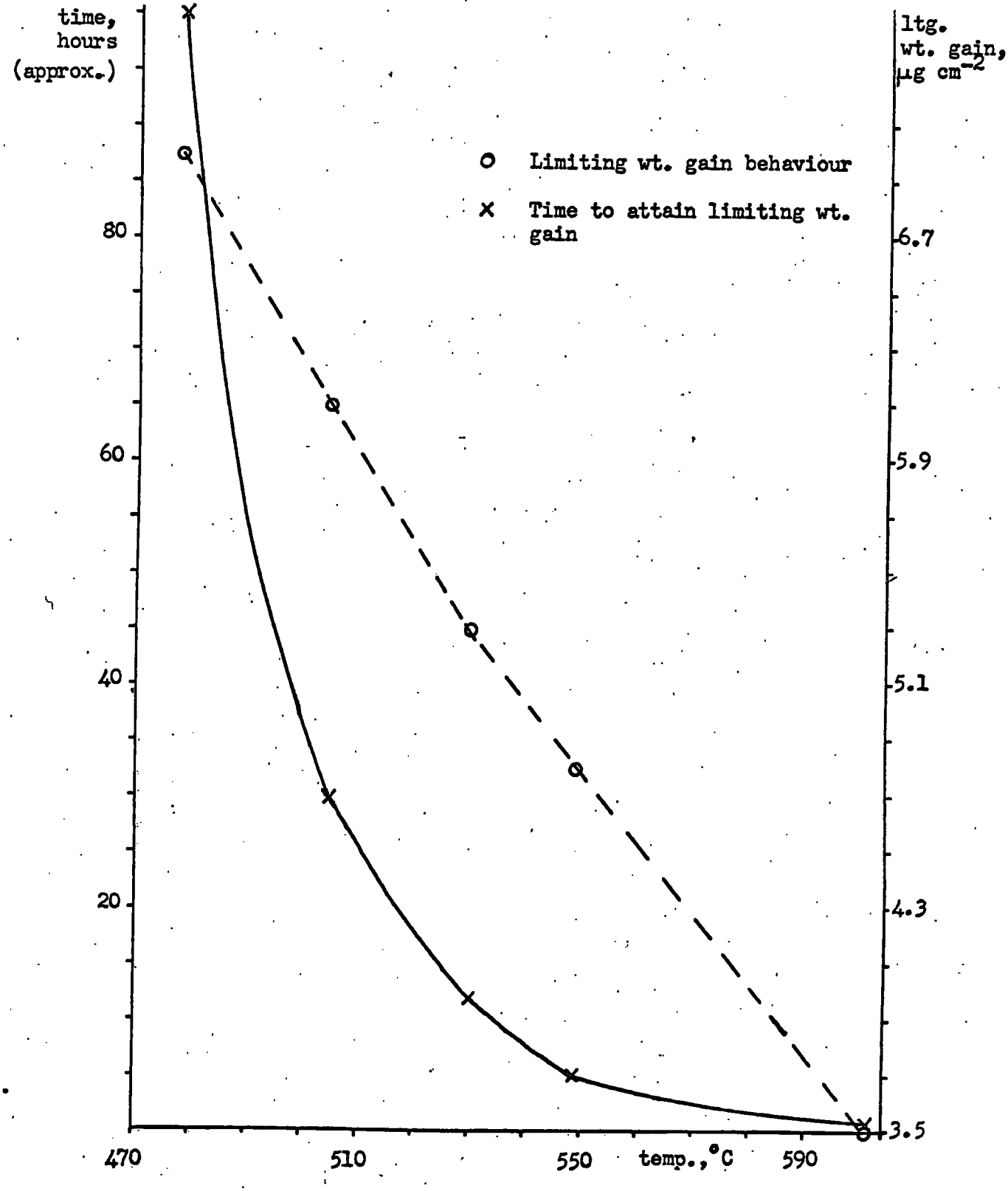

Plate VII

Also the expected thickness of films is about 165 Å based on the limiting weight gain at 500°C inferred from the work of Dignam and his co-workers. Specimens anodised to 14 volts in barrier-type film-forming electrolytes have oxide films of about this thickness. For comparison, the same period was chosen for oxidation in oxygen with a gaseous water content.

4.3 Types of Measurement.

In order to compare the behaviour of these oxide films with the porous-type examined previously[4,23,28,32] the following types of measurement were made on all types of oxide film produced:-

a) Construction of full electrical analogues.

b) Impedance changes during film dissolution.

c) Specimen potential/time behaviour during film dissolution.

In addition the following measurements were made:-

d) Barrier voltage determinations (films formed in oxygen at 500°C).

e) Determination of aluminium ion concentrations during film dissolution (anodically-formed films).

Dissolution in aerated and solutions deaerated with hydrogen was studied in mixtures of aqueous sodium sulphate and sulphuric acid of known ionic strength and the pH was adjusted to that required.

4.3.1 Construction of Full Electrical Analogues.

A full electrical analogue has the same frequency response as the oxide film itself. The method used here is that previously used

by Hoar and Wood[42] in their study of the construction of full electrical analogues for porous films formed by anodisation in sulphuric acid, both in the unsealed condition and during the process of sealing.

Using the same apparatus as in the impedance studies during oxide dissolution, with a sine wave signal, the impedance of films in the almost non-solvent, 3% w/v ammonium tartrate buffered to pH 7, was studied as a function of frequency at 25°C using a simple series capacitance-resistance analogue. The latter was then used to arrive at the full electrical analogue. The ohmic drop across the solution was measured at high frequency[42] with a copper specimen whose immersed area was that of the aluminium specimen. All types of oxide films were studied in this way; anodised films were studied for several anodising voltages and in the case of 14 volt anodised films, as a function of the time of anodisation at the lowest current density.

4.3.2. Impedance Changes During Film Dissolution.

4.3.2.1 Method.

It was anticipated that the rate of thinning of the oxide films would be not too dissimilar from that observed for porous films[23,36]. Accordingly the process was followed using a similar method, a modification of that due to McMullen and Hackerman[124]. Synchronised sine or square wave signals were fed simultaneously to the cell containing the specimen under test, and to a simple analogue circuit, and the response curves displayed on a double beam oscilloscope. Using low

amplitude signals the resistance and capacitance of the analogue were adjusted until the response curves matched. The circuit diagram is shown in Plate VIII and the dissolution cell in Plate IX.

4.3.2.2 Apparatus.

The components of the analogue were screened resistance and capacitance decade boxes and these were calibrated by means of a Wayne Kerr Bridge. Attentuators were also screened resistance boxes which were also calibrated. All external leads were screened, the cell was enclosed in an aluminium box as were the switching gear and coaxial sockets and their leads to complete the circuit. All screens were interconnected and earthed to minimise a.c. pick-up. The aluminium cell enclosure was lagged externally with expanded polystyrene and the front, made from perspex covered with aluminium foil with windows left for observation, was attached by four screws in contact with the foil so that the screening was complete. Both heating and cooling devices were necessary; cold tap water was circulated through glass tubes in the enclosure. An electrically screened 100 watt bulb was fitted on the rear inside surface of the aluminium enclosure, and the temperature was controlled by a bimetallic strip thermostat in conjunction with a relay. Temperature control was $\pm$ 0.5°C or better at 25°C; an ambient temperature of 29°C, which was never reached in normal practice, was necessary to make it impossible to maintain a temperature of 25°C in the box.

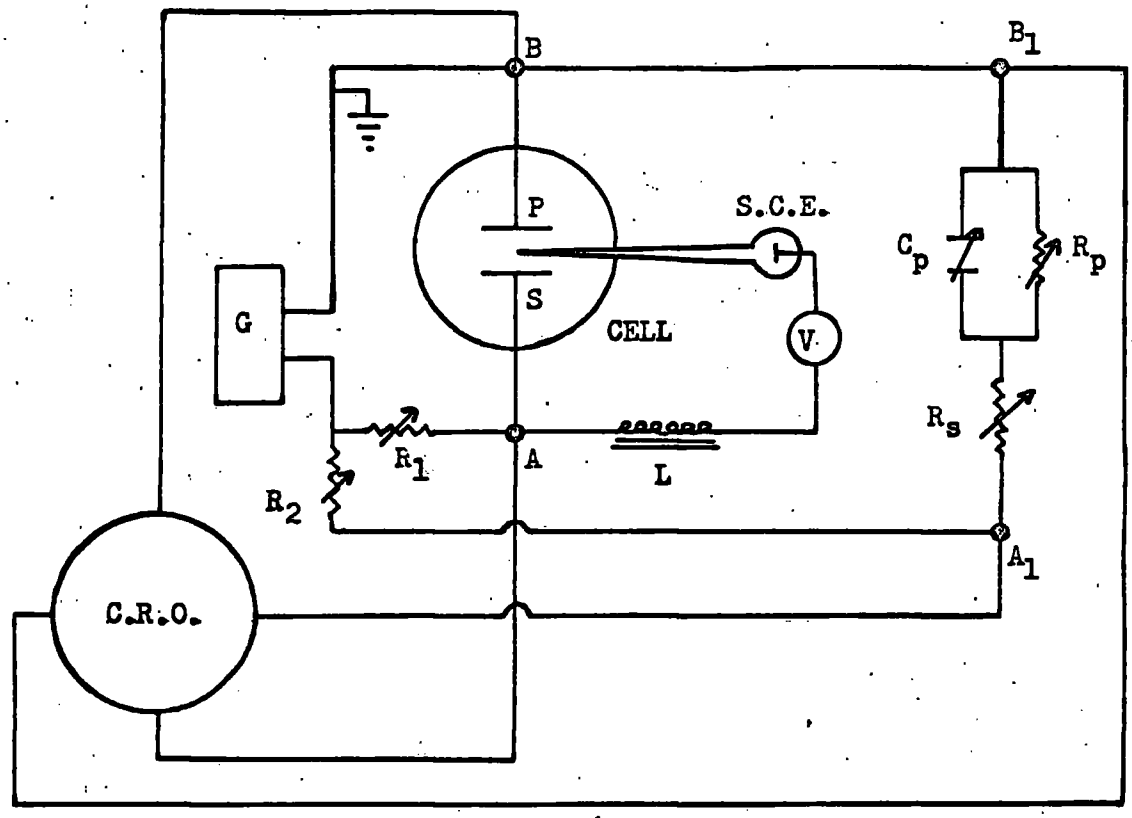

Circuit used in Section 3.2.[23,36]

C.R.O.	Cathode Ray Oscilloscope
G	Sine and Square Wave Oscillator, the signal of which was applied across AB and A_1B_1 simultaneously
V	Voltmeter
S.C.E.	Saturated Calomel Electrode in a salt bridge
R_1 and R_2	Decade Resistance Boxes attenuating Generator Signal. Range 0-100 kΩ in 1Ω intervals, matched within 1%
L	Inductance to prevent A.C. stray into D.C. circuit
S	Aluminium Specimen
P	Subsidiary Platinum Gauze Electrode of 30 cm^2 area
R_s and R_p	Decade Resistance Boxes. Ranges 0-10 kΩ in 0.1Ω intervals and 0-100 kΩ in 1Ω intervals respectively
C_p	Capacitance Decade Boxes. Range 0-30 μF in 0.001 μF intervals.

Plate VIII

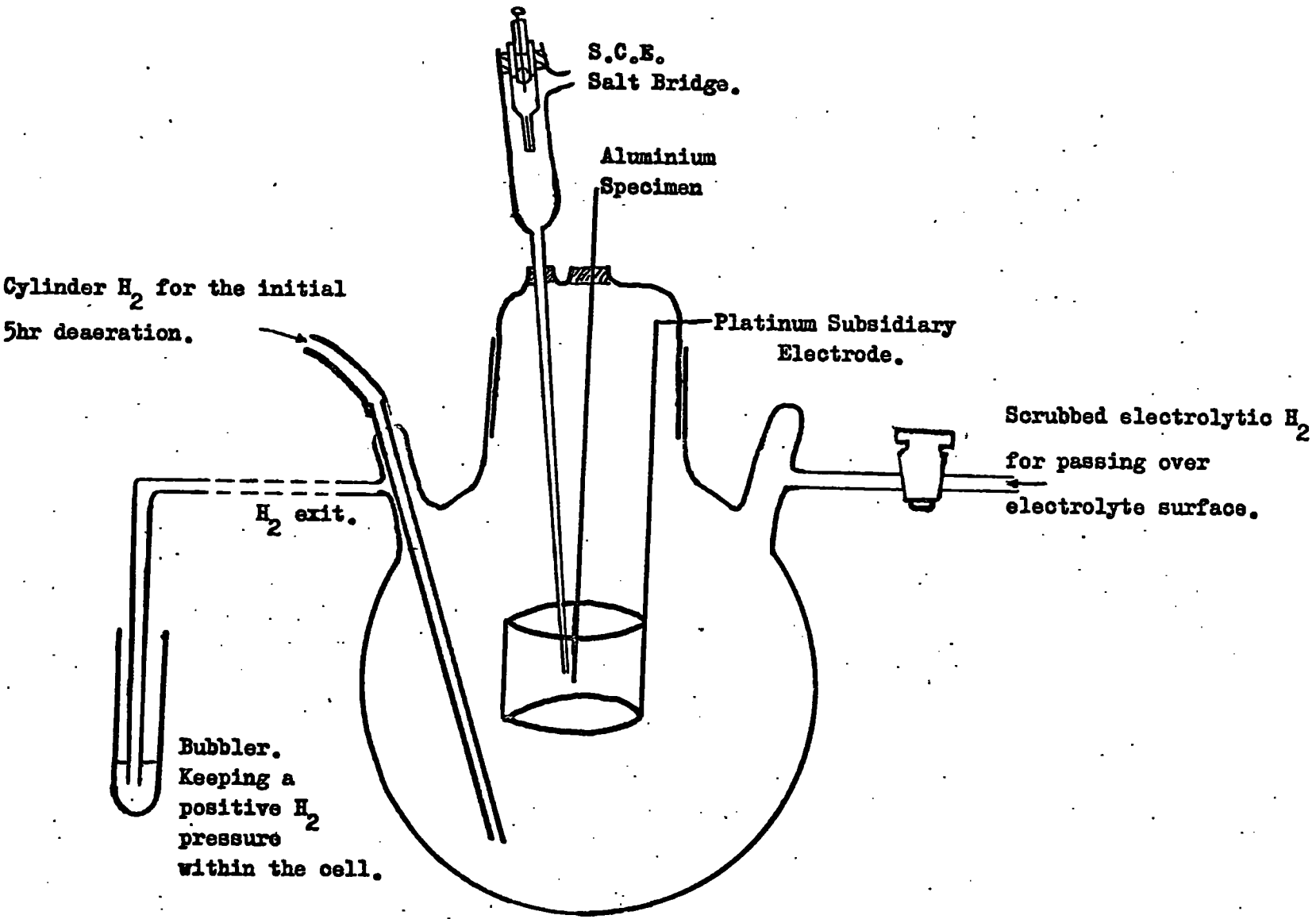

Plate IX Cell used for impedance studies during oxide dissolution.[23,36]

A horizontal steel bar passed through the centre of the box with clamps to support two cells so that two runs could be done simultaneously.

The cell was of about 500 ml capacity, and contained a platinum gauze subsidiary electrode of area large in comparison with the specimens. The specimen potential could be monitored with respect to a saturated calomel electrode which was isolated from the bulk of the solution by a tube containing the test electrolyte. Arrangements were also made to permit tests to be carried out in deaerated solutions; in these experiments a slight positive pressure of hydrogen gas was maintained above the solution.

4.3.2.3 Experimental.

In dissolution in deaerated solution, cylinder hydrogen was bubbled through the solution with the tap open (see Plate IX) for at least five hours before an experiment was begun. Diggle, Downie and Goulding[36] found that a period of deaeration of five hours was required to obtain reproducible behaviour for potential/time studies on porous alumina films on aluminium during dissolution. Before the gas entered the flask, it was passed through a bubbler containing the electrolyte under examination, and the gas outlet was connected to a tube dipping under about 1 cm of electrolyte so that there was always a small positive pressure of hydrogen in the cell. Prior to specimen introduction into the solution, the tap was closed

so that hydrogen passed over the surface of the electrolyte.

Wire specimens were immersed to a known depth in the cell with the bottom of the specimen level with the bottom of the platinum gauze counter electrode and the top of the latter level with the solution surface. For cylindrical specimens, the prepared surface just touched the electrolyte surface, so that in each case the relevant apparent specimen area was known.

Most studies were made at constant ionic strength but varying pH, or at constant pH with varying ionic strength, in aerated sulphate solutions, although for comparison purposes some work was carried out in deaerated solutions. Specimen preparation was anodisation to 7, 14 and 21 volts with the most exhaustive studies at 14 volts. Similar studies to those made using 14 volt anodised films were carried out on films formed in dry oxygen at 500°C. Again for comparison, a few studies were made of specimens for which oxygen containing gaseous water at one partial pressure only was used for oxidation.

4.3.3 Potential-Time Behaviour During Film Dissolution.

The potential-time behaviour of specimens was also examined. The cell used was as for impedance measurements (Plate IX) but the platinum gauze counter electrode was omitted. Specimen potential was measured, using a sensitive electrometer, with respect to a saturated calomel electrode and was continuously recorded on a chart recorder. A suitable backing-off potential was sometimes applied from a standard

cell to keep values within a desired range.

4.3.4 Barrier Voltage Determinations.

Some experiments were performed on films produced in oxygen at 500°C using the technique of Hunter and Fowle[24] discussed earlier in Chapter III (3.7.3.5) Specimens were immersed in 3% w/v ammonium tartrate solution buffered with ammonia to pH 7, at 25°C. By means of a motor-driven potentiometer a steadily increasing voltage was applied, across the specimen and an aluminium cathode of surface area large with respect to that of the specimen, and the current was recorded continuously. The minimum voltage drop across the film to give ionic conduction is proportional to the film thickness. As a result of using a cathode of very large surface area with respect to the specimen, the ohmic drop across the solution and the cathode over-potential at any of the required minimum voltages for ionic conduction were both negligible (See Chapter III (3.7.3.5)) with respect to the applied voltage. Also, Vr was zero since anode and cathode were of the same material. Thus, nearly all the applied voltage was across the oxide film. The effect of varying the rate of voltage increase was examined.

The method of Hart[45] was also used, in which the voltage across the film is increased in equal steps with constant intervals on open circuit. Current surges were of short duration until the field strength required for ionic conduction was achieved, when the current

transient took place over a longer period and was completed when the film had ceased to thicken. Again, precautions were taken to ensure that nearly all the applied voltage was across the oxide film. The current transients were plotted on a chart recorder and the effect of varying the time on open circuit was examined.

4.3.5 Aluminium Ion Concentration in Solution.

In an attempt to correlate the capacitance changes which were observed in the present work with film thinning, the rate of passage of aluminium ions into solution was determined. Aluminium foil specimens, either in the polished condition or after having been anodised in tartrate solutions at 7,14, or 21 volts, were immersed in sulphate solutions of pH 1.0, ionic strength 1.5.

To ensure that the initial concentration of aluminium in solution should be detectable, the foil specimens had A/V ratios (A is the apparent surface area, V the volume of solution used) of about 1 000 times greater than did the specimens used in impedance measurements. The results of tests made using 14 volt tartrate films at different A/V ratios indicated that, in the present experiments, saturation of the solution with respect to anhydrous alumina did not affect the result. This point has been discussed by Lorking and Mayne[9].

The analytical method used was developed by Gentry and Sherington[154], and has been used by Nagayama and Tamura[32]. The former

workers found that complete extraction of aluminium ions was possible over pH ranges 4.5-6.5 and 8.0-11.5 by complexing with a 1% solution of 8-hydroxy quinoline in acid-free chloroform. The complex in chloroform was found to have a peak absorption at 3900 $\mathring{A}$, and to obey the Beer-Lambert law at up to 3 μg complex ml^{-1} sample extract.

A calibration curve, shown in Fig. 1, was established by the procedure given in Appendix II to this thesis. During the dissolution experiments at 25°C, in about 500 ml. of solution, vigorous stirring took place and the containing beaker was covered with a watch glass. 2 ml. samples were taken at known times and extracted as in the calibration procedure. Concentrations of aluminium ion were determined using the same cells as for calibration, retaining the same cell for the blank throughout. Hence, the total weight of aluminium ion in the dissolution medium was determined.

Optical density versus weight of aluminium/10 ml of chloroform extract for the complex of aluminium with 8-hydroxy quinoline.

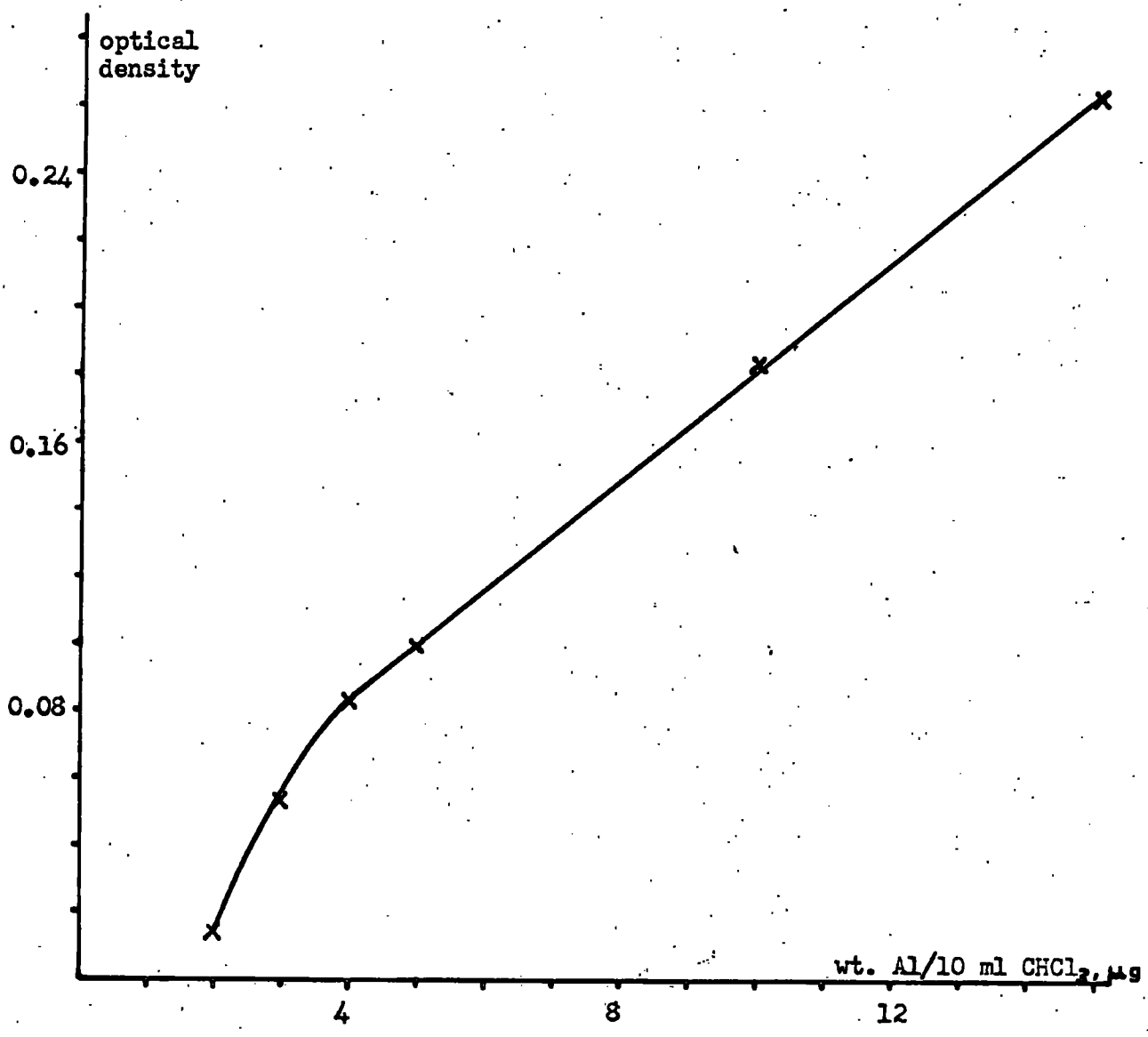

Fig. 1

CHAPTER V

Experimental Results for Anodically formed Films.

5.1 Construction of Full Electrical Analogues for Non-porous Films.

In all cases, the best correspondence with the frequency response of the oxide film was obtained with the analogue shown in Fig. 2 (a). The charging curves displayed on the oscilloscope were identical in amplitude but there was a small, sensibly frequency independent phase difference, the voltage across the simple series resistance-capacitance analogue leading that across the full analogue. No improvement in matching was obtained by modifying the analogue to represent a pore contribution[153]. Values of R_1 (see Fig. 2(a)) were identified with the measured ohmic drop, about 40 ohm cm^{-2}, across the ammonium tartrate solution.

The frequency responses of the components of the simple resistance-capacitance analogue for 14 volt anodised films, where anodising was continued at the lowest current density after current decay at 14 volts for 2, about 5, 30 and 172 minutes and at 7 volts for about 5 and for 30 minutes are shown in Figs. 3, 4 and 5 and Tables VII - XII contain a summary of the results obtained.

(a) Anodically-formed non-porous alumina films on aluminium.

(b) Alumina films formed on aluminium oxidised in dry oxygen or in the moist oxygen atmosphere at 500°C.

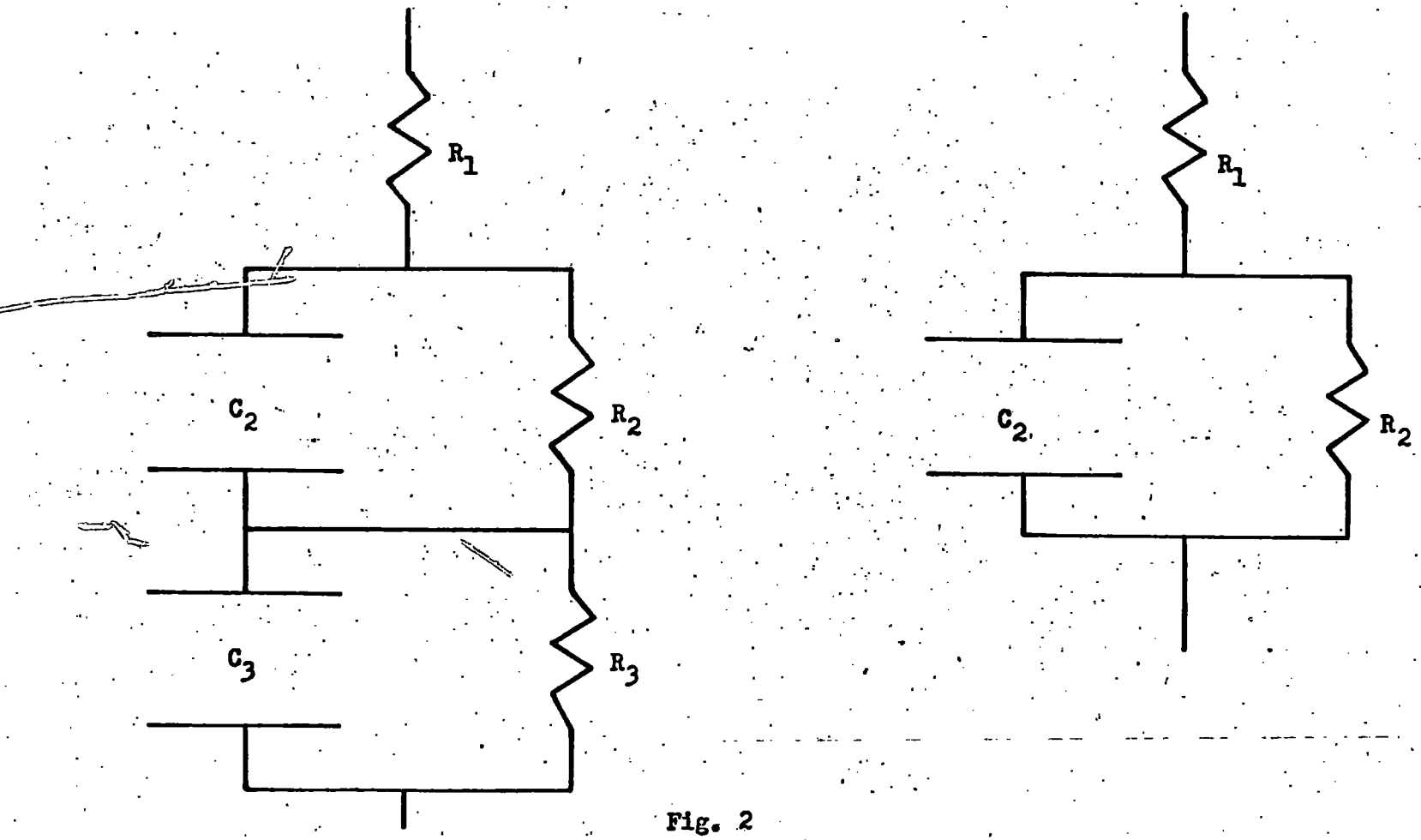

Fig. 2

Frequency dependence of balancing series capacitance for 14 volt anodised non-porous alumina films as a function of the time of anodising at the lowest current density.

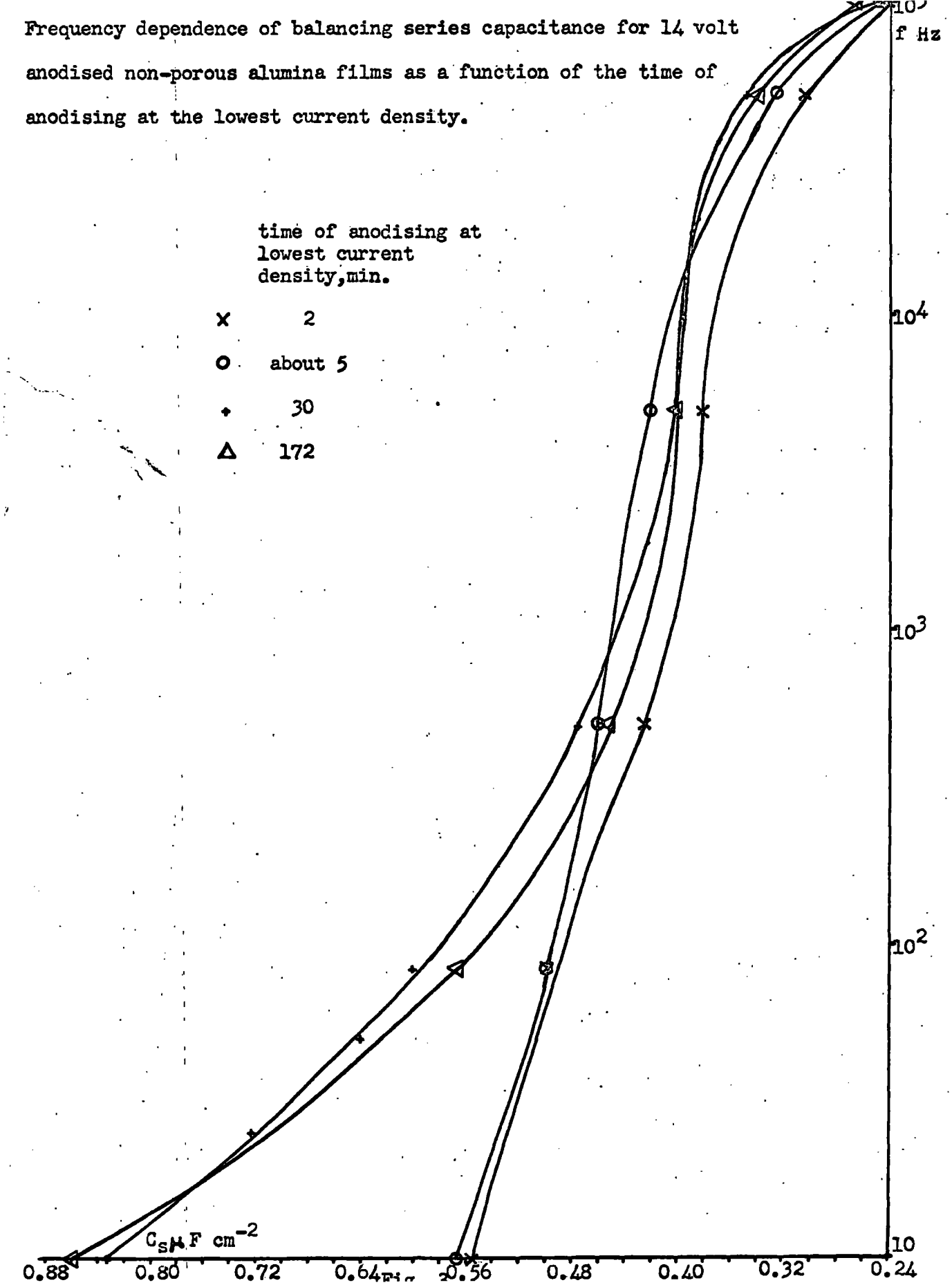

Frequency dependence of balancing series resistance for 14 volt anodised non-porous alumina films as a function of the time of anodising at the lowest current density.

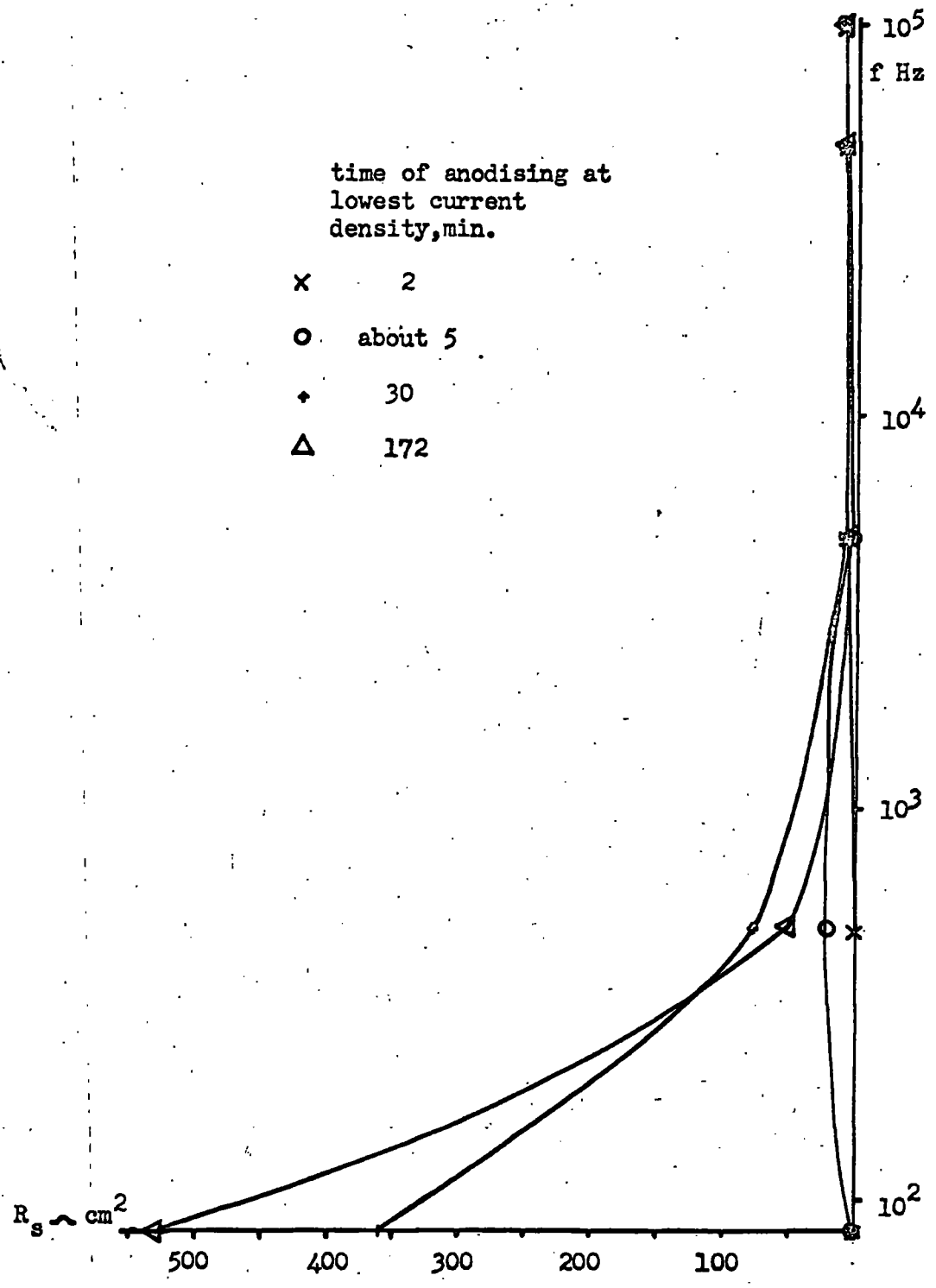

Fig. 4

Frequency dependence of balancing series resistance and capacitance for 7 volt anodised non-porous alumina films as a function of the time of anodising at the lowest current density.

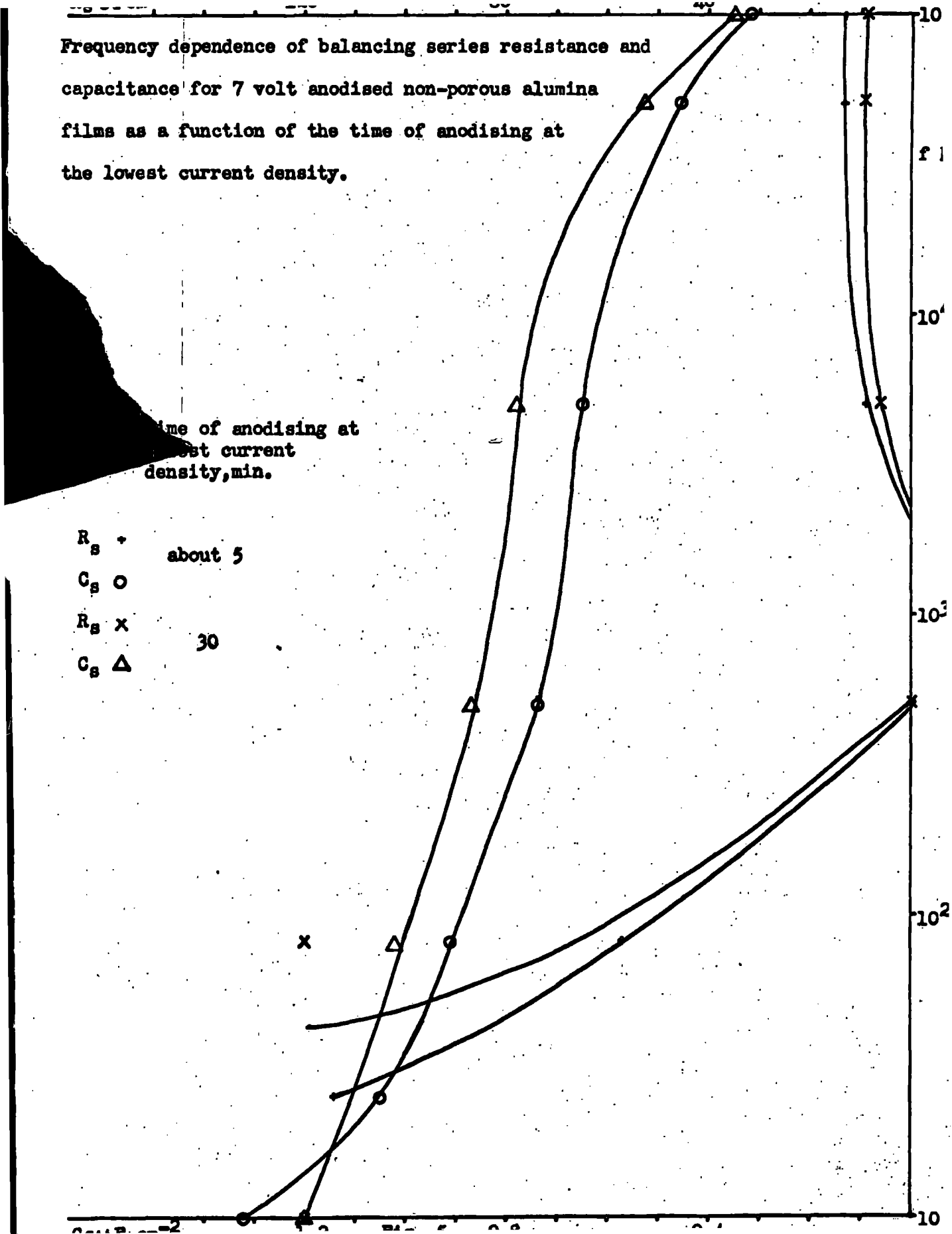

TABLE VII

Behaviour of Components of Full Analogue as a function of Anodising Voltage at 25°C for Anodising at Lowest Current Density for about 5 minutes and for 30 minutes (in parentheses).

	7v	14v	21v	30v
R_2 ohm cm^2	160 000 (42 000)	260 000 (120 000)	170 000 (125 000)	350 000 (270 000)
$C_2 \mu Fcm^{-2}$	0.93 (1.02)	0.51 (0.57)	0.43 (0.43)	0.264 (0.278)
R_3 ohm cm^2	170 (120)	160 (240)	350 (200)	290 (220)
$C_3 \mu Fcm^{-2}$	2.46 (3.30)	2.45 (1.32)	0.81 (1.28)	1.10 (1.07)

TABLE VIII

Behaviour of Components of Full Analogue as a Function at 25°C of Time of Anodisation at 14 volts at Lowest Current Density.

Time of anodisation at lowest c.d.	2 min	30 min	172 min
R_2 ohm cm^2	>320 000	120 000	35 000
$C_2 \mu Fcm^{-2}$	0.47	0.57	0.56
R_3 ohm cm^2	270	240	260
$C_3 \mu Fcm^{-2}$	2.22	1.32	1.51

At 83 Hz, the capacitative component, C_s, of the simple series analogue always contributed much more than the resistive component, R_s, to the overall impedance. In all cases, the value of the capacitative component increased by about 5% during a frequency run, the other component changing little. A little dissolution of alumina was probably taking place and changes in dielectric constant resulting from film hydration may be involved[21,38,39]. The solvent power of ammonium tartrate for alumina has previously been discussed in Chapter III (3.8.1).

The dependence of impedance on temperature in the range 20° - 45°C was shown to be negligible for the decade boxes which formed the analogue circuits.

5.1.1 Discussion.

In Chapter III (3.7.1), work of Heine and Pryor[21] and Brock and Wood[39] was discussed. These workers have reported that, for oxide films formed anodically on aluminium at 15 volts under current decay conditions with maximum permitted current surges of 100μA cm^{-2}, two regions were present in the oxide film. These were firstly a region of low electronic resistivity extending 60-80 Å from the metal-oxide interface considered by Heine and Pryor to be due to the proximity of the metal-oxide interface and to represent an n-type region containing excess aluminium ions; the outermost region was found to be about 60 Å thick and had a low ionic resistivity. This latter region was

TABLE IX

Frequency Response of Series Resistance, R_s, and Capacitance, C_s, for Non-porous 7V Anodic Films as a Function of Time of Anodising at Lowest Current Density.

Anodising Time, min	about 5		30	
Frequency Hz	R_s ohm cm^2	C_s μF cm^{-2}	R_s ohm cm^2	C_s μF cm^{-2}
10	91	1.32	120	1.20
25	114	1.05		
83	57.0	0.91	120	1.02
500	0.0	0.74	0.0	0.87
5 000	8.6	0.65	6.0	0.78
50 000	13.1	0.46	9.6	0.53
100 000	13.1	0.32	9.0	0.35

TABLE X

Frequency Response of Series Resistance, R_s, and Capacitance, C_s, for 14V Non-Porous Anodic Films as a Function of Anodising Time at Lowest Current Density.

(a).

Anodising Time, min	2		about 5	
Frequency Hz	R_s ohm cm^2	C_s μF cm^{-2}	R_s ohm cm^2	C_s μF cm^{-2}
10	1 080	0.56	0.0	0.57
83	0.0	0.50	0.0	0.52
500	0.0	0.43	21.2	0.46
5000	8.1	0.38	5.8	0.42
50 000	10.5	0.32	9.5	0.33
100 000	10.7	0.24	10.1	0.25

Table X continued

(b)

Anodising Time, min	30		172	
Frequency Hz	R_s ohm cm^2	C_s μF cm^{-2}	R_s ohm cm^2	C_s μF cm^{-2}
10	2 700	0.83	4 770	0.86
25	1 260	0.72		
50	720	0.64		
83	360	0.60	530	0.57
500	78	0.48	53.0	0.45
5 000	9.6	0.40	6.4	0.40
50 000	10.8	0.35	9.5	0.34
100 000	10.8	0.25	9.2	0.26

Table XI

Frequency Response of Series Resistance, R_s, and Capacitance, C_s, for 21V Non-porous Anodic Films as a Function of Anodising Time at Lowest Current Density.

Anodising Time, min	about 5		30	
Frequency Hz	R_s ohm cm^2	C_s μF cm^{-2}	R_s ohm cm^2	C_s μF cm^{-2}
10	580	0.48	1 590	0.56
25	580	0.45		
50	232	0.43		
83	116	0.36	159	0.45
250	139	0.37		
500	93	0.34	26.5	0.40
1 000	53.3	0.32		
5 000	12.8	0.27	6.9	0.34
10 000	11.0	0.26		
50 000	13.3	0.24	8.5	0.27
100 000	13.3	0.22	7.7	0.25

Table XII

Frequency Response of Series Resistance, R_s, and Capacitance, C_s, for 30V Non-porous Anodic Films as a Function of Anodising Time at Lowest Current Density.

Anodising Time, min	about 5		30	
Frequency Hz	R_s ohm cm^2	C_s μF cm^{-2}	R_s ohm cm^2	C_s μF cm^{-2}
10	4 640	0.35	3 300	0.35
25	750	0.32		
50	0.0	0.30		
83	0.0	0.28	165	0.29
250	11.6	0.27		
500	11.6	0.26	66.0	0.26
1 000	0.0	0.25		
5 000	9.3	0.25	10.4	0.23
10 000	8.1	0.21		
50 000	16.2	0.19	7.1	0.21
100 000	16.2	0.18	6.1	0.16

found to be diffuse and was considered[21,39] to contain hydroxyl ions from the anodising electrolyte.

The anodising conditions used in the present work were identical with the above, and the existence of a two layer structure is also indicated here. There appears to be no trend with respect to time of anodising at the lowest current density for the values of either R_3 or C_3, the region of low impedance, which could indicate, according to the treatment of Heine and Pryor, little diffusion of hydroxyl ions into this layer. Capacitance studies during dissolution, reported later, indicate that this layer is the one adjacent to the metal. The mean resistivity of the inner layer was about 5×10^8 ohm cm in all cases. Heine and Pryor[21] have reported that the resistivity of the innermost layer for 15 volt films increased from about 4×10^9 ohm cm 25 Å from the metal/oxide interface to about 2×10^{10} ohm cm 80 Å from the interface. Beck and his co-workers[48] have suggested that during the initial surface preparation of the specimen, the ionic resistance of the oxide film formed can be reduced by the incorporation of ions. Heine and Pryor[21] prepared their specimens by etching in sodium hydroxide solution, a procedure which, it has been reported[48], does not affect the ionic resistance of the oxide film produced. In the present work, specimens were initially chemically polished and the considerably lower ionic resistivity found in the present work for the inner layer could result from incorporation of ions from the

chemical polishing solution. The present results indicate a thickness of the inner layer of about 30 Å for the 7 and 14 volt films and about 80 Å for 21 and 30 volt films assuming a film dielectric constant of 10.[70]. Heine and Pryor[21] have reported this value to be about 80 Å for 15 and 20 volt anodised films.

In the present work, the time of anodising at the lowest current density did not appear to affect greatly the capacitance of the high impedance layer but the resistance of this layer fell considerably as this time increased. The resistivity was, in all cases, about 10^{11} ohm cm a few minutes after current decay had ceased and fell to about half this value after 30 minutes. In the case of 14 volt films, after 172 minutes, the resistivity of the high impedance layer was about 10^{10} ohm cm. This behaviour could be due to diffusion of hydroxyl ions into the outer region of the film,[21,39] if it is assumed that the layer forms the outer region of the film[21]. The proposed[21] diffuse nature of this region may account for the fact that identical matching of the charging curves across the full analogue and across the simple series analogue could not be obtained.

Heine and Pryor[21] found that for 20 volt films formed under conditions identical with those used in the present work, a third region was present between the two already mentioned, about 100 Å thick and having a constant resistivity of about 2×10^{10} ohm cm. In the present work, for 21 and 30 volt films, modification of the full analogue to

account for this additional layer did not lead to any improvement in the matching of the charging curves. This could be understood in terms of films, in the present case, having a reduced ionic resistance in comparison with those films prepared by Heine and Pryor, so that in the present case the rate of diffusion of hydroxyl ions into the film would be expected to be enhanced, resulting in the two layer structure which was apparently present.

5.2 Impedance Measurements during Film Dissolution.

7, 14 and 21 volt films were studied during immersion in aerated sulphate solution of pH 1.0, ionic strength 1.5. Typical plots of reciprocal capacitance (1/C) versus the square root of time $(t)^{\frac{1}{2}}$ are shown in Fig. 6. That this plot, over about the first 25 minutes, is more linear than a plot of 1/C versus t is demonstrated for 14 and 21 volt films in Fig. 7. Linearity in the first type of plot is consistent with a diffusion-controlled process whereas linearity in the second type of plot is, as will be demonstrated shortly, consistent with a zeroth order thinning process. The final, sensibly constant values of 1/C and the times to reach these values are shown in the graphs. In many cases, the final capacitance value was about 10 $\mu F\ cm^{-2}$ in close agreement with that found by Diggle, Downie and Goulding[36] for their studies of the erosion of porous-type films in sulphate and chloride solutions below the critical pH.

By way of comparison, 14 volt films were studied in deaerated sulphate solution, pH 1.0, ionic strength 1.5.(Fig. 8). Where the state of the dissolution medium, that is aerated or deaerated, is unspecified, it should be assumed that the solution was aerated.

The effect of varying the pH in the range 0.3-2.0 at ionic strength 1.5 was studied for 14 volt films and the results are shown in Fig. 9. Figs. 10 and 11 show the effect on the capacitance-time behaviour of varying the ionic strength at pH values close to 2; Fig. 12 shows the results of similar studies at a solution pH of 3.5. The behaviour in a solution of pH 5.0 and ionic strength 1.5 is shown in Fig. 13.

In every case, the slopes of the linear parts of the graphs were determined by the method of least mean squares. Since

$$C = \varepsilon A/4\pi d \qquad (3)$$

$$d = \varepsilon A/4\pi C$$

$$d(d)/dt = (\varepsilon A/4\pi)d(1/C)/dt$$

$$d(1/C)/dt = (4\pi/\varepsilon A)d(d)/dt \qquad (9)$$

The rate at which $1/C$ varies with time during dissolution is therefore inversely proportional to the true surface area of the film as one factor.(Equation (9)). Therefore, in comparing these rates, all surface areas should be corrected to a standard value, assuming that the area itself is not affected by film dissolution. The true surface areas were not known, however, but for films formed under the

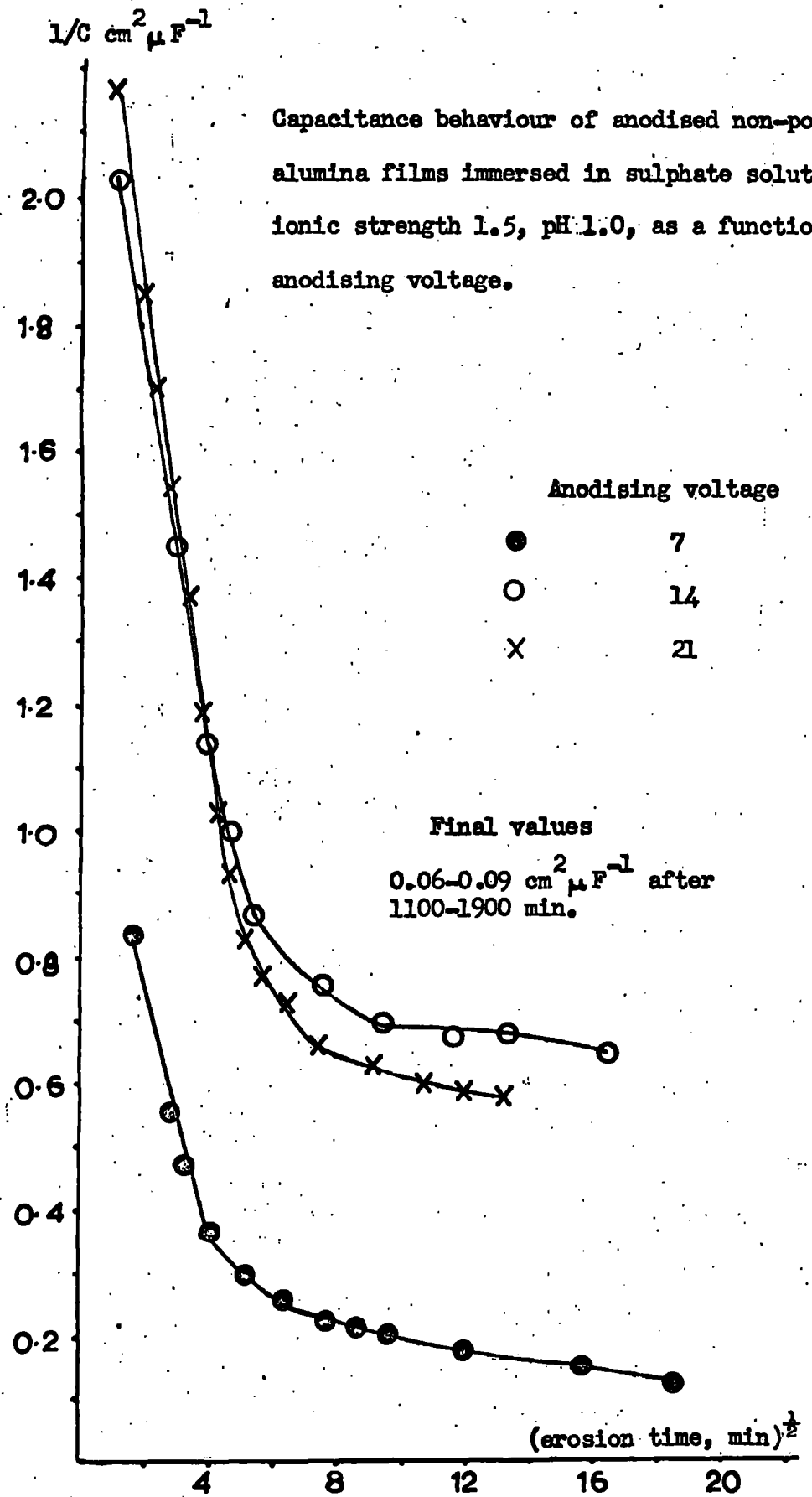

Capacitance behaviour of anodised non-porous alumina films immersed in sulphate solution, ionic strength 1.5, pH 1.0, as a function of anodising voltage.

Fig. 6

Capacitance behaviour of 14 and 21 volt anodised non-porous alumina films immersed in sulphate solution, pH 1.0, ionic strength 1.5, versus time of erosion and the square root of this time.

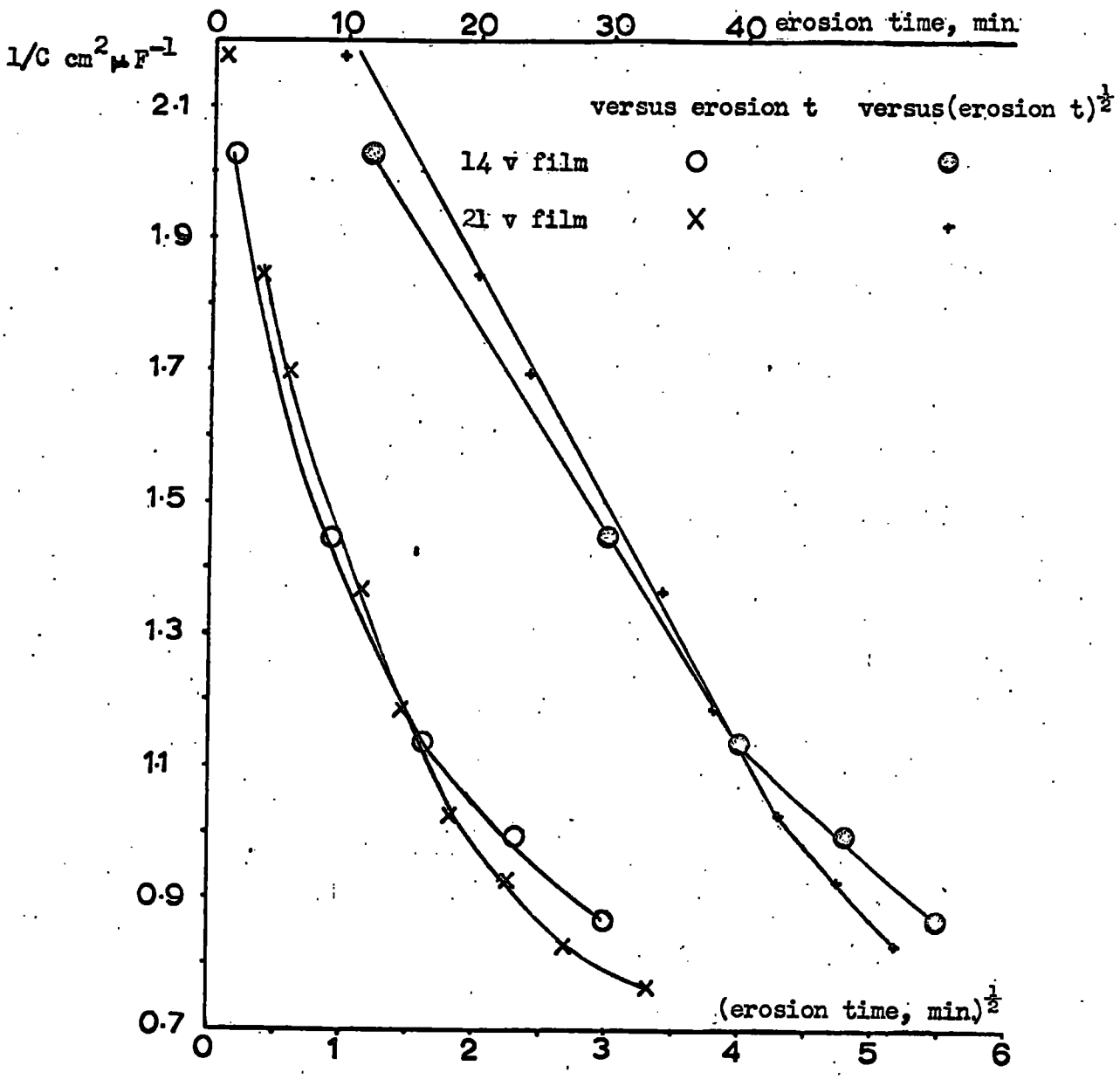

Fig. 7.

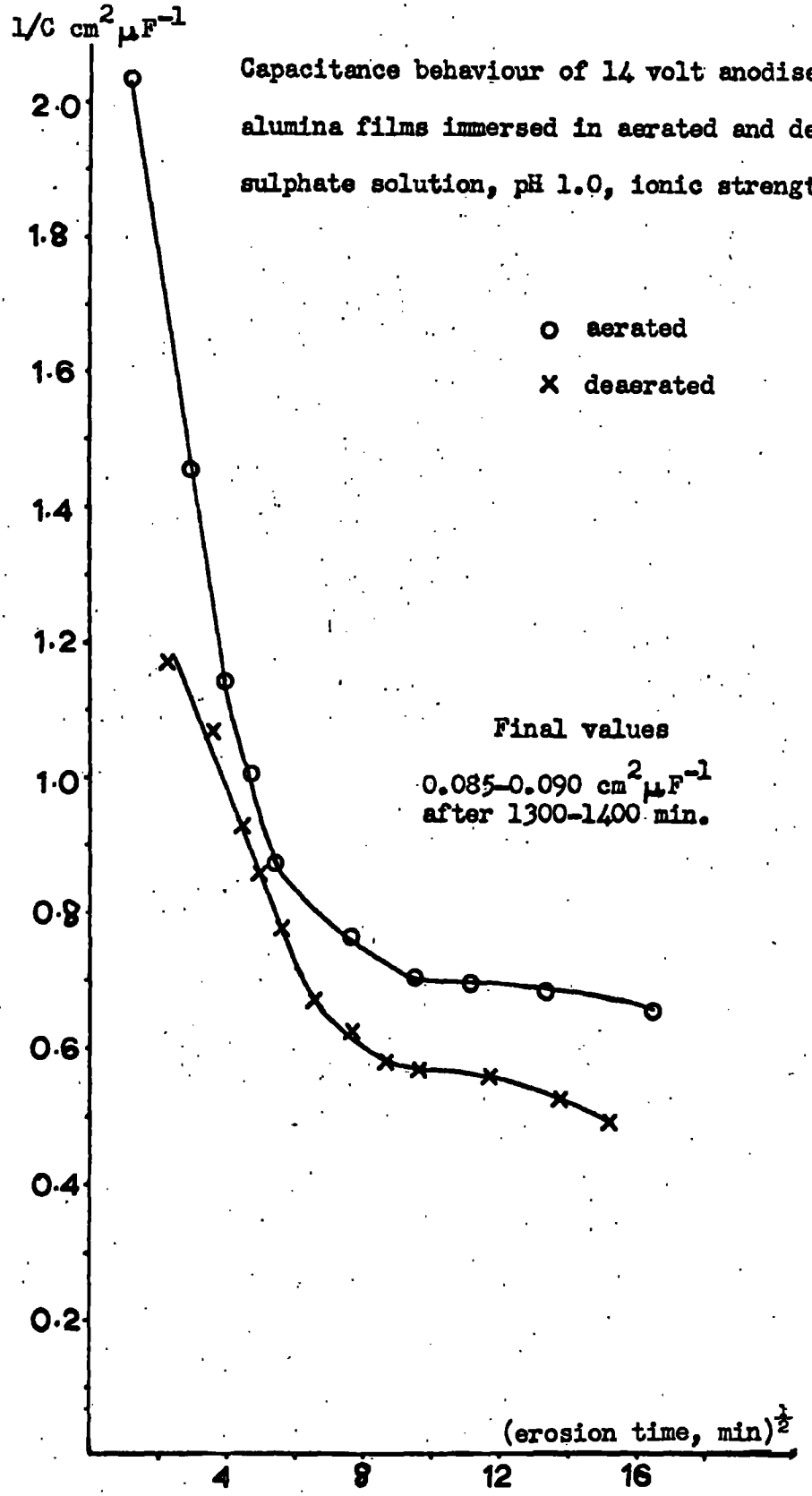
1/C cm^2 μF^{-1}
2·0
1·8
1·6
1·4
1·2
1·0
0·8
0·6
0·4
0·2
Capacitance behaviour of 14 volt anodised non- porous alumina films immersed in aerated and deaerated sulphate solution, pH 1.0, ionic strength 1.5.
o aerated
× deaerated
Final values
0.085–0.090 cm^2 μF^{-1}
after 1300–1400 min.
(erosion time, min)$^{\frac{1}{2}}$
4
8
12
16

Fig. 8.

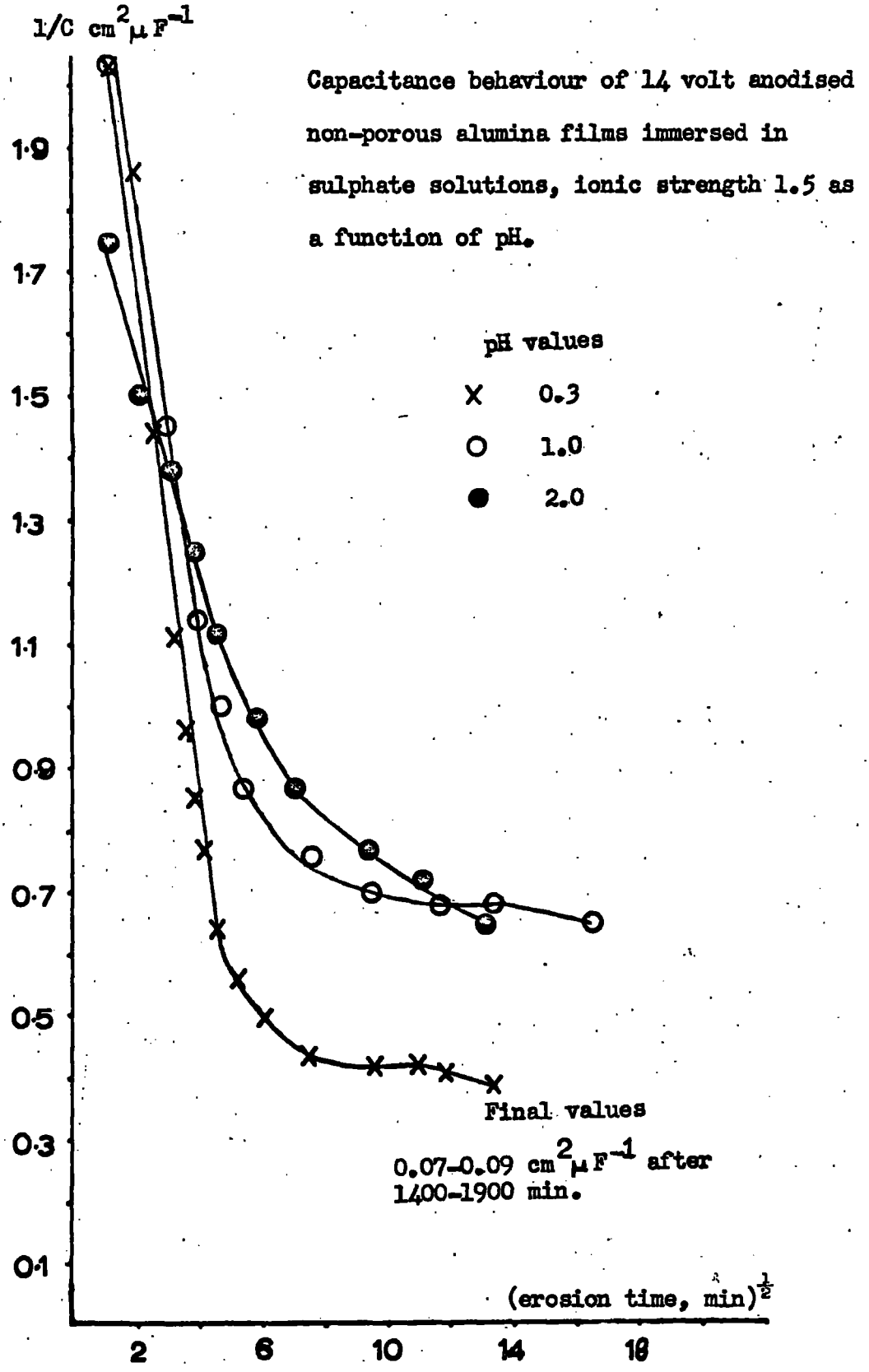
1/C cm^2 μF^{-1}
1·9
1·7
1·5
1·3
1·1
0·9
0·7
0·5
0·3
0·1
2
6
10
14
18
(erosion time, min)$^{\frac{1}{2}}$
Capacitance behaviour of 14 volt anodised non-porous alumina films immersed in sulphate solutions, ionic strength 1.5 as a function of pH.
pH values
X 0.3
O 1.0
● 2.0
Final values
0.07-0.09 cm^2 μF^{-1} after 1400-1900 min.

Fig. 9

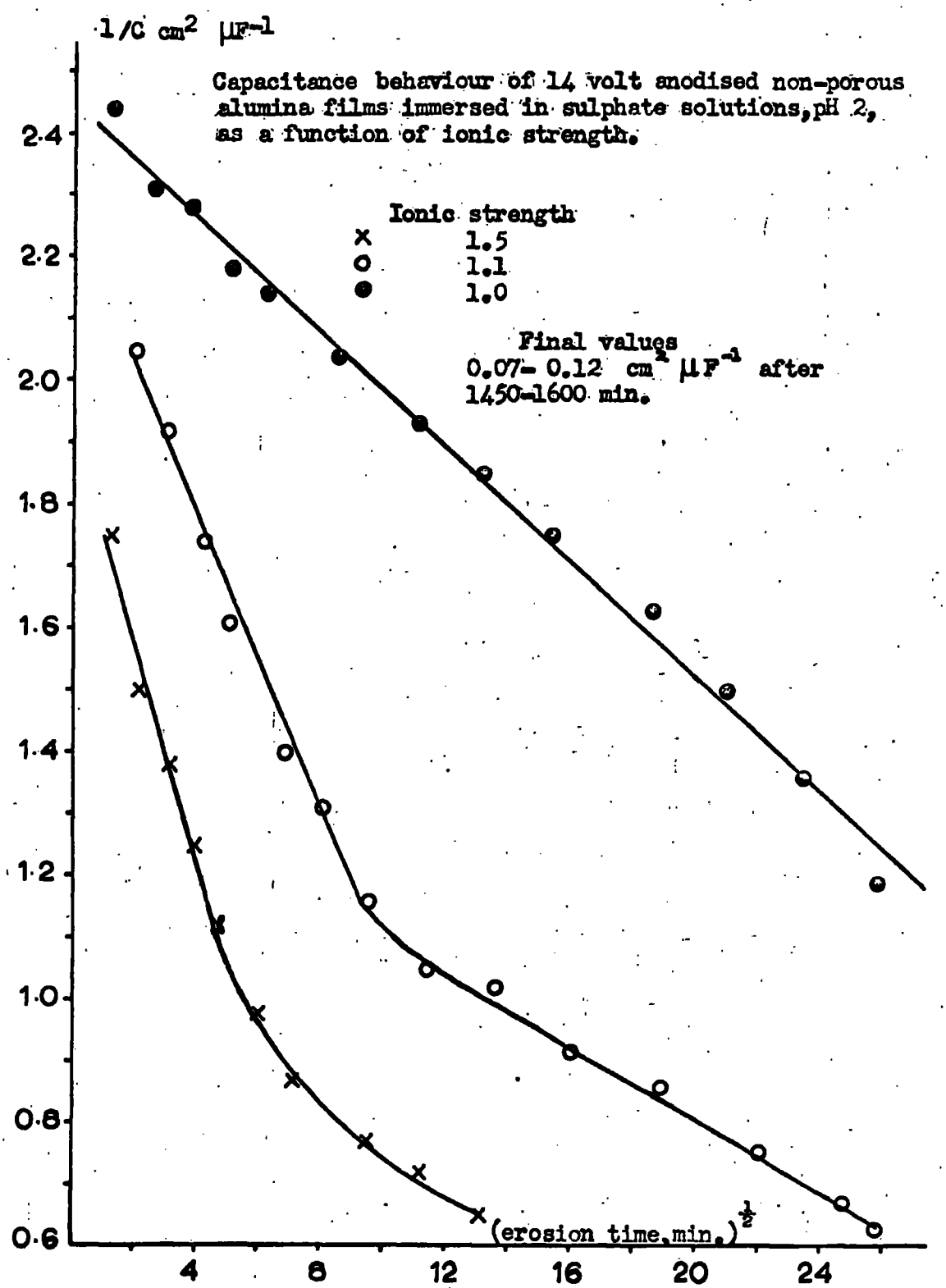
1/C cm² μF⁻¹
Capacitance behaviour of 14 volt anodised non-porous alumina films immersed in sulphate solutions, pH 2, as a function of ionic strength.
Ionic strength
1.5
1.1
1.0
Final values
0.07- 0.12 cm² μF⁻¹ after
1450-1600 min.
2.4
2.2
2.0
1.8
1.6
1.4
1.2
1.0
0.8
0.6
4
8
12
16
20
24
(erosion time, min.)½

Fig. 10

Capacitance behaviour of 14 volt anodised non-porous alumina films immersed in sulphate solutions, pH2, as a function of ionic strength.

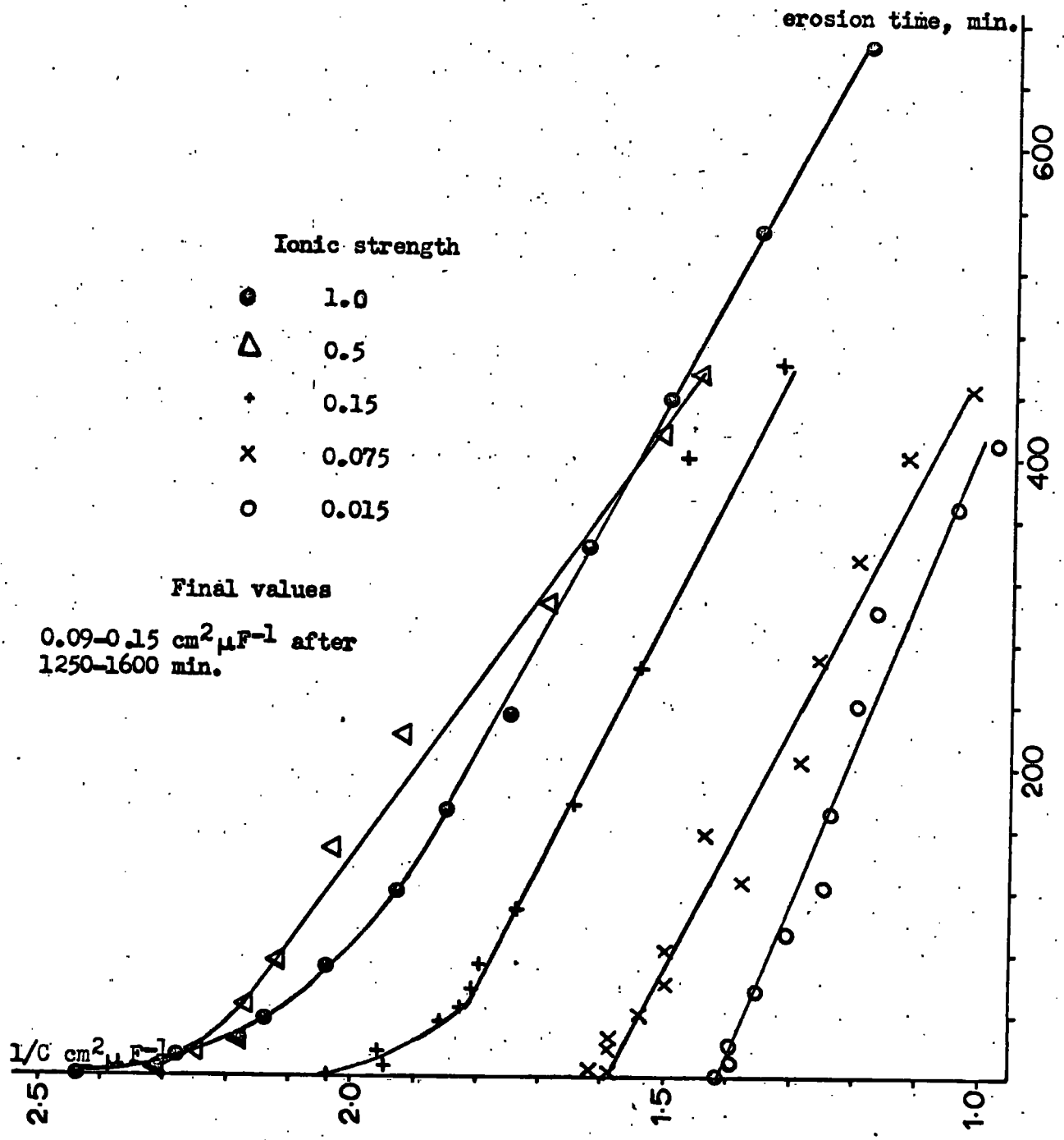

Fig. 11

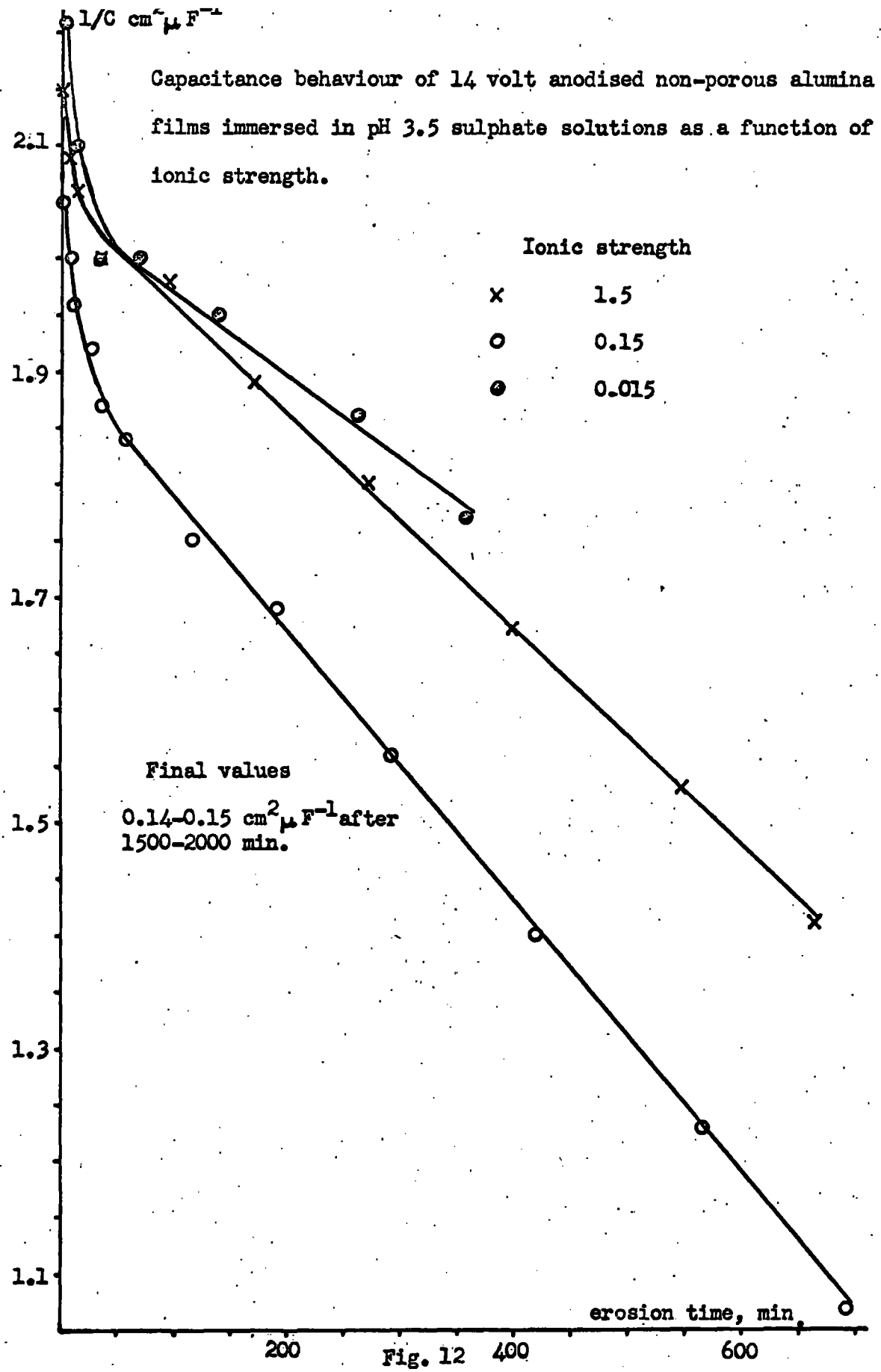
1/C cm²μF⁻¹
2.1
1.9
1.7
1.5
1.3
1.1
Capacitance behaviour of 14 volt anodised non-porous alumina films immersed in pH 3.5 sulphate solutions as a function of ionic strength.
Ionic strength
1.5
0.15
0.015
Final values
0.14-0.15 cm²μF⁻¹ after 1500-2000 min.
erosion time, min
200
400
600

Fig. 12

Capacitance behaviour of 14 volt anodised non-porous alumina films immersed in pH 5.0, ionic strength 1.5 sulphate solution.

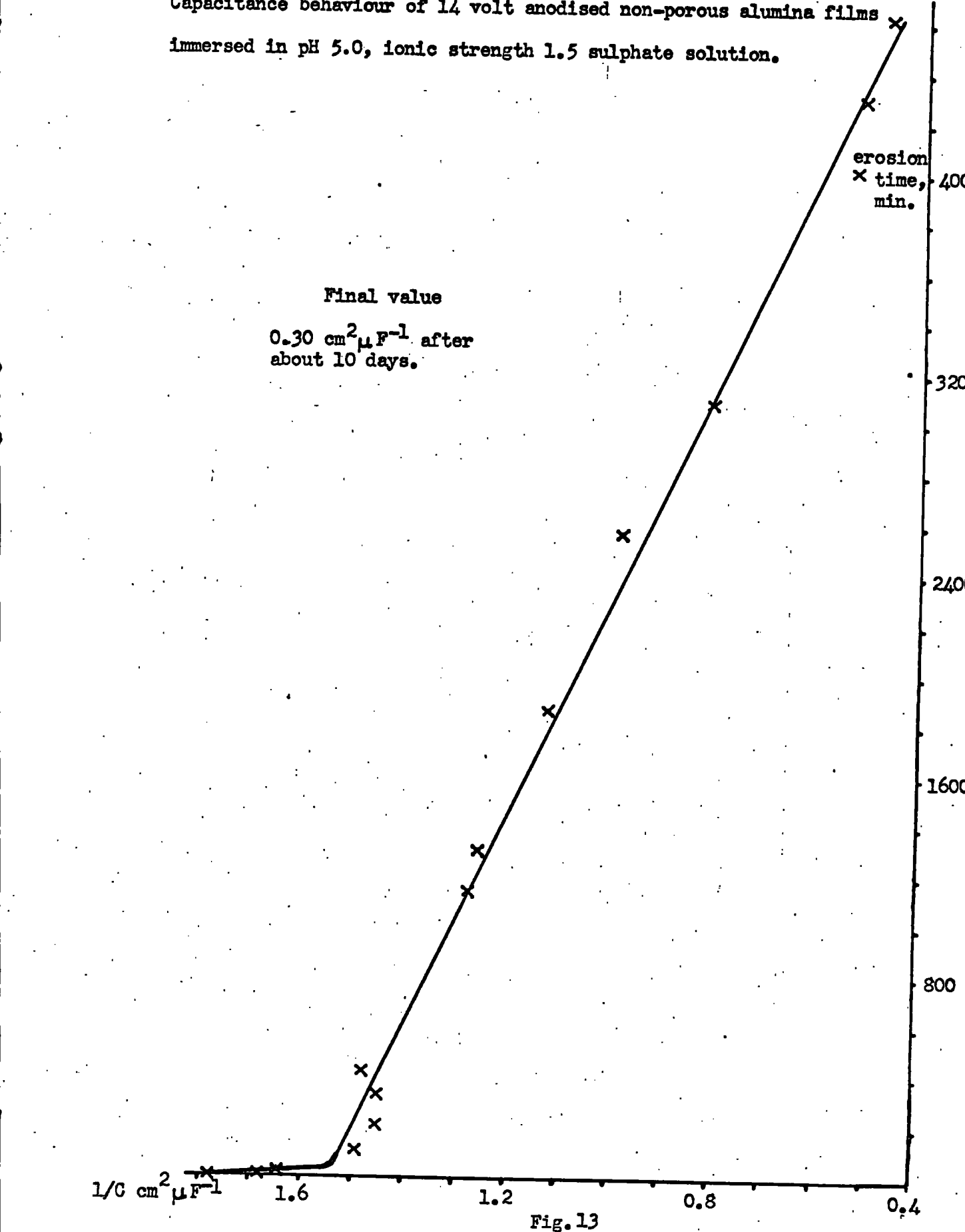

Fig. 13

same conditions, in all dissolution media used, the interpolated initial capacitance should be proportional to the true surface area (Equation (3)) since the initial film thickness and dielectric constant would be expected to be the same. Thus, all slopes were corrected in terms of standard initial capacitance values. These standard values have been taken as the overall capacitances evaluated from full analogues for 7, 14 and 21 volt films after about 5 minutes anodising at the lowest current density. This period was chosen since specimens anodised for dissolution studies were treated similarly.

Equation (9) reduces to $d(1/C)/dt$ = constant for zeroth order thinning where ϵ and A remain unchanged during dissolution. For a diffusion-controlled process in which ϵ is changing with time, mathematical analysis is more complex, but in general, for such processes a plot of 1/C versus $(t)^{\frac{1}{2}}$ should be linear.

For the simple analogue used at a fixed frequency (83 Hz) during dissolution, Rs (see Plate III (a)) was negligible at the lowest pH values, and increased only to a few tens of ohms at a solution pH of 5.0

For dissolution in solutions of high pH and/or low ionic strength R_s (see Plate III (a)) was always very large just after specimen immersion and interpolated values were about the same as those reported for the resistance of the outer high impedance layer of the corresponding full analogue. Also R_s decreased much more rapidly where the 1/C - t relationship was linear than in those cases where diffusion control was

indicated; values of R_p determined at the earliest times were much greater for suggested zeroth order thinning than for diffusion control. In either case, the greater the slope, $d(1/C)/dt$ or $d(1/C)/d(t)^{\frac{1}{2}}$, the greater was the rate of fall of R_p .

The following tables summarise the results obtained.

Table XIII

Kinetic data for

Dissolution in Sulphate Solution, pH 1.0, I = 1.5.

Anodising voltage	Slope as per graphs	Reciprocal of interpolated initial capacitance	Corrected slope	Comments
	$k_1 cm^2 \mu F^{-1} min^{-\frac{1}{2}}$	$1/C_o cm^2 \mu F^{-1}$	$k_2 cm^2 \mu F^{-1} min^{-\frac{1}{2}}$	
7	-0.20 - 0.12	1.15 0.91	- 0.26 - 0.19	Linear during about first 25 mins.
21	- 0.64 - 0.36	3.36 2.56	- 0.68 - 0.50	Ditto
14	- 0.32 - 0.36	2.41 1.85	- 0.32 - 0.46	Ditto
14	- 0.12 - 0.25	1.47 2.56	- 0.19 - 0.23	Deaerated sulphate solution. Linear during about first 40 mins.

Table XIV

Kinetic data for Dissolution of 14 volt Anodised Films in Sulphate Solutions I = 1.5.

pH value	Slope as per graphs	Reciprocal of interpolated initial capacitance	Corrected slope	Comments
	$k_1 cm^2 \mu F^{-1} min^{-\frac{1}{2}}$	$1/C_o cm^2 \mu F^{-1}$	$k_2 cm^2 \mu F^{-1} min^{-\frac{1}{2}}$	
0.3	- 0.41 - 0.62	2.54 2.70	- 0.38 - 0.55	Linear during about first 25 mins.
1.0	- 0.32 - 0.36	2.41 1.85	- 0.32 - 0.46	Ditto
2.0	- 0.18 - 0.27	1.92 2.44	- 0.22 - 0.26	Ditto

Table XV

Kinetic data for Dissolution of 14 volt Anodised Films in pH 2.0 Sulphate Solutions of High Ionic Strength.

Ionic strength	Slope as per graphs	Reciprocal of interpolated initial capacitance	Corrected slope	Comments
	$k_1 cm^2 \mu F^{-1} min^{-\frac{1}{2}}$	$1/C_o cm^2 \mu F^{-1}$	$k_2 cm^2 \mu F^{-1} min^{-\frac{1}{2}}$	
1.5	- 0.18 - 0.28	1.92 2.44	- 0.22 - 0.26	Linear during about first 25 mins.
1.1	- 0.18 - 0.12	2.33 2.26	- 0.18 - 0.13	Linear during about first 100 mins.
1.0	- 0.046 - 0.047	2.14 2.45	- 0.051 - 0.046	Possibly zeroth order after 350 mins.

Table XVI

Kinetic Data for Dissolution of 14 volt Anodised Films in Sulphate Solutions, pH Values Close to 2.0 at Low Ionic Strengths.

Ionic strength	Slope as per graphs	Reciprocal of interpolated initial capacitance	Corrected slope	Comments
	$k_1 cm^2 \mu F^{-1} min^{-1}$	$1/C_o cm^2 \mu F^{-1}$	$k_2 cm^2 \mu F^{-1} min^{-\frac{1}{2}}$	
0.5	- 0.0016 - 0.0018	2.50 2.42	- 0.12 - 0.14	Possibly diffusion controlled during first 40 mins. Zeroth order indicated up to at least 400 mins.
0.15	-0.0008 - 0.0012	1.70 2.10	- 0.09 - 0.11	Ditto
0.075	- 0.0016 - 0.0013	2.04 1.60	- 0.146 - 0.151	Zeroth order indicated up to at least 400 mins.
0.015	- 0.0010 - 0.0011	1.41 2.65	- 0.13 - 0.08	Ditto

Table XVII

Kinetic Data for Dissolution of 14 volt Anodised Films in pH 3.5 Sulphate Solutions.

Ionic strength	Slope as per graphs	Reciprocal interpolated initial capacitance	Corrected slope converted to Å min^{-1}	Comments
	$k_1 cm^2 \mu F^{-1} min^{-1}$	$1/C_o cm^2 \mu F^{-1}$		
1.5	- 0.0010	2.20	- 0.08	Indication of diffusion control during first 40 mins. Zeroth order indicated up to at least 400 mins.
0.15	- 0.0012	2.10	- 0.11	
0.015	- 0.00074	2.30	- 0.06	

Additionally when a specimen having a 14V anodised film was immersed in sulphate solution (pH 5.0, I = 1.5), the dissolution process apparently followed zeroth order kinetics for about 5 000 minutes. There was some indication that during the first 40 minutes of dissolution diffusion control may have been operating. The apparent slope of the zeroth order 1/C - t curve was - 0.00023 $cm^2 \mu F^{-1} min^{-1}$; the reciprocal of the interpolated initial capacitance was 1.90 $cm^2 \mu F^{-1}$, and the corrected zeroth order slope was - 0.022 Å min^{-1}.

5.3 Potential-Time Studies.

The results of studies of the change of specimen potential with time for 7, 14 and 21 volt films immersed in aerated sulphate solution,

pH 1.0, ionic strength 1.5, are shown in Fig. 14. 14 volt films were also studied in the same medium which was deaerated; the results are indicated in Fig. 15. For 14 volt films, the potential increased initially to a maximum after about 20 minutes, followed by a minimum after about 100 minutes. A second maximum occurred after about 800 minutes, followed by the establishing of a final steady minimum value after about 1 500 minutes. Fig. 15 indicates that the first maximum in potential for 14 volt films was absent under deaerated conditions although the behaviour was otherwise very similar to that in aerated solution. For 7 and 21 volt films (Fig. 14), only the second maximum and the final minimum found for 14 volt films were present. An approximate correspondence for the time of occurrence of these features is evident.

5.4 Weight Loss Measurements.

The weight of aluminium ions lost to solution during the immersion of 7, 14 and 21 volt films in pH1.0, ionic strength 1.5 sulphate solution as a function of the time of immersion is shown in Fig. 16. The behaviour for 14 volt films did not differ much with respect to the rate of increase with time in the weight of aluminium ions in solution for two determinations in which the apparent specimen A/V ratios (Chapter IV (4.3.5)) were about the same and for one determination where this ratio was twice that in the former case. As this

The specimen potential - time study of the erosion of non - porous anodically - formed alumina films in sulphate solution, ionic strength 1.5, pH 1.0, as a function of anodising voltage.

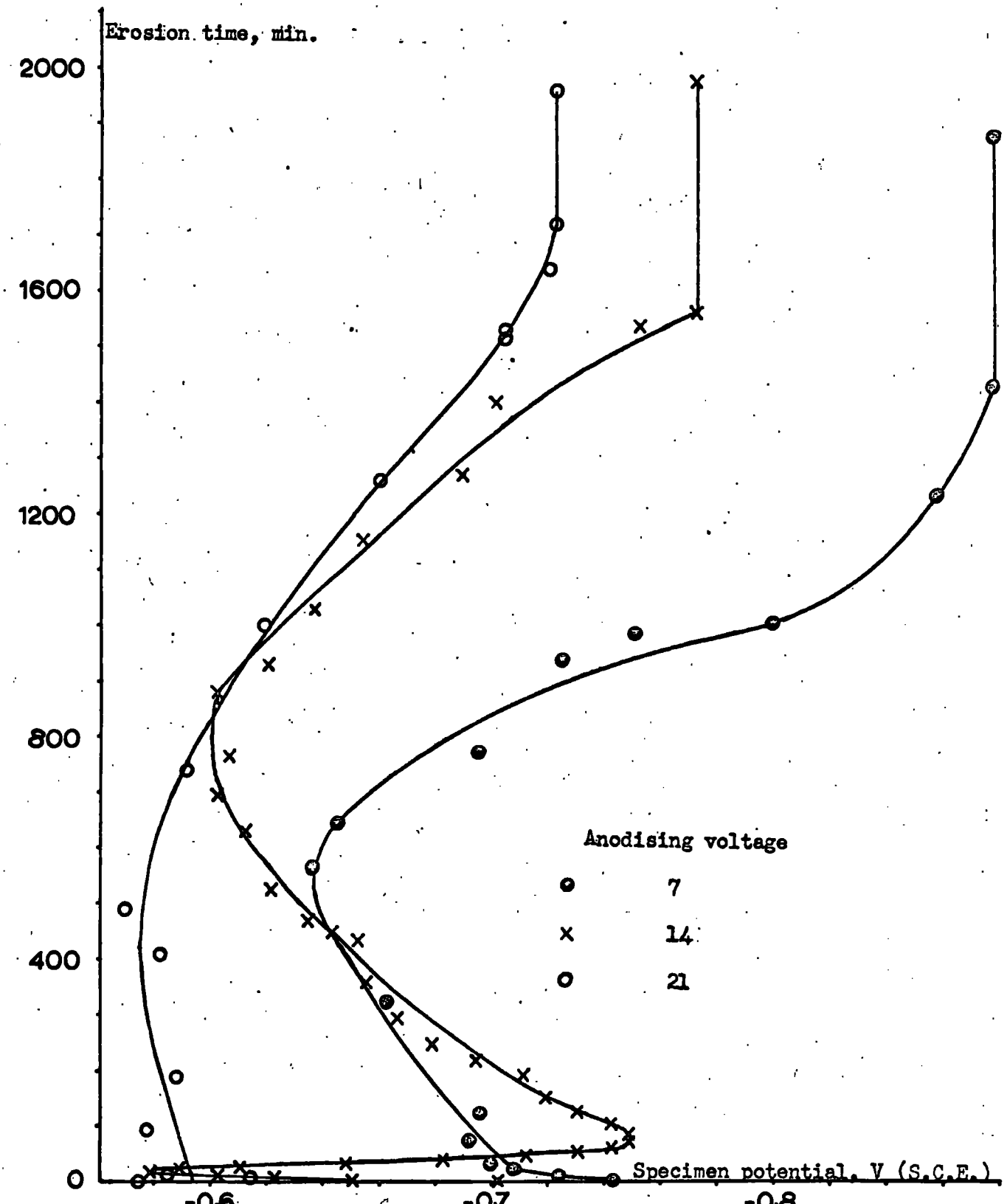

Fig.14.

The specimen potential - time study of the erosion of 14 volt anodised non-porous alumina films in sulphate solution, ionic strength 1.5 pH 1.0, aerated and deaerated.

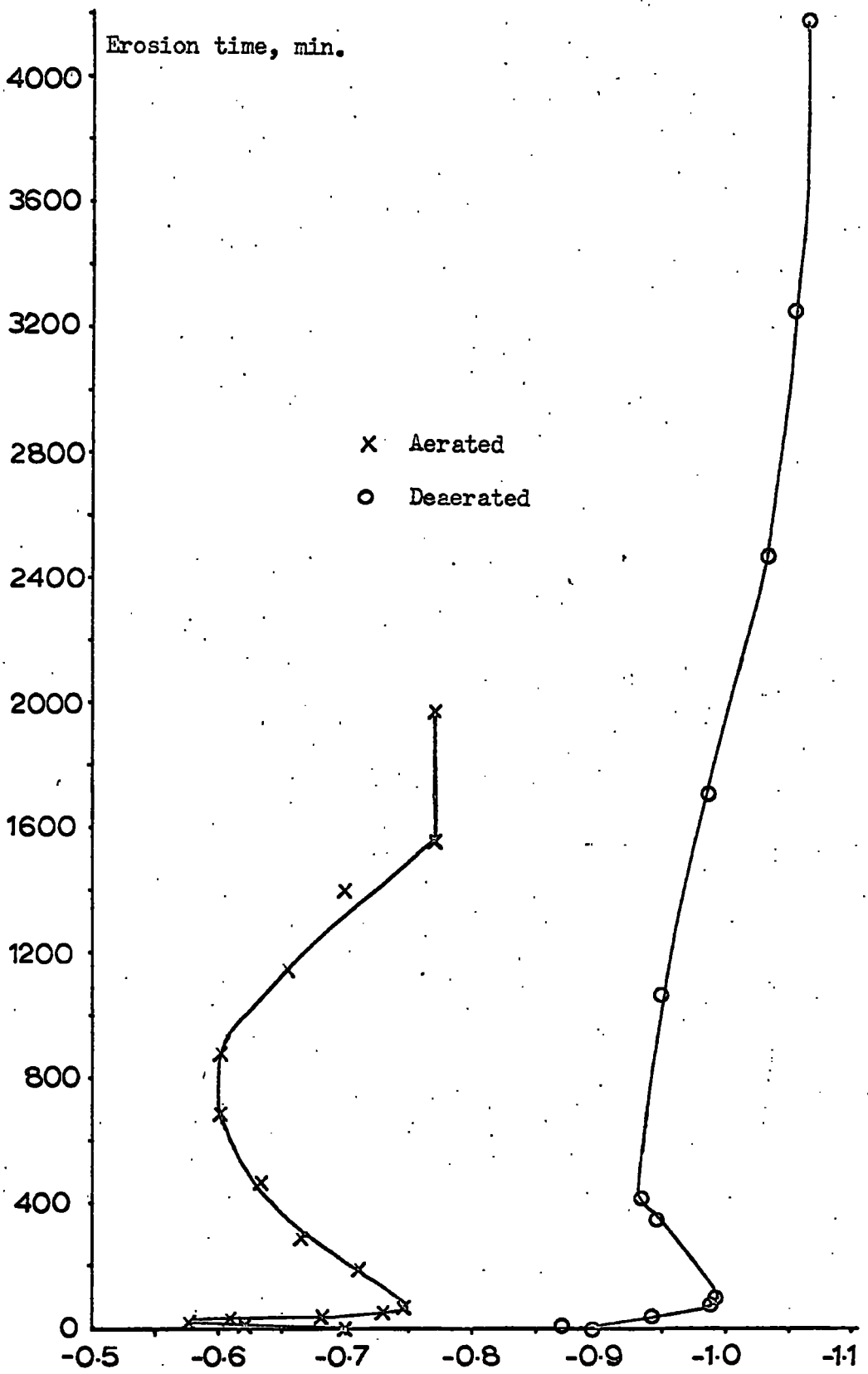

Fig. 15

latter case corresponded to the highest value of this ratio used throughout these studies, it would appear that dissolution was not limited, under the conditions used, by the solubility of alumina in the solution[9].

With values standardised as in Fig. 16, it is estimated, based on the calibration curve (Fig. 1), that the smallest total weight of aluminium ions detectable in 500 ml of solution was 0.38 mg and the smallest change detectable at this concentration was 0.05 mg. It would appear, therefore, that there was a considerable spread of values even at the earliest times but these values did not appear to follow any trend. It is interesting to note that even at these early times there was often a detectable concentration of aluminium ions in solution in excess of any present before specimen immersion.

In all cases where dissolution was continued for a sufficient length of time, the concentration of aluminium ions in solution was considerably in excess of that which would have arisen from dissolution of the original oxide film only, and when this concentration began to increase markedly, it appears that there was no reduction in the rate of increase up to the greatest time at which samples were taken.

5.5 Summary.

The most detailed results reported here refer to films formed anodically at 14 volts; rather less work was carried out using films formed at 7 and 21 volts. The results indicate that when 14 V films

Weight of aluminium ions in solution during dissolution of anodically-formed non-porous alumina films in ionic strength 1.5 pH 1.0 sulphate solution as a function of anodising voltage and initial aluminium surface area (apparent) / solution volume ratio, X.

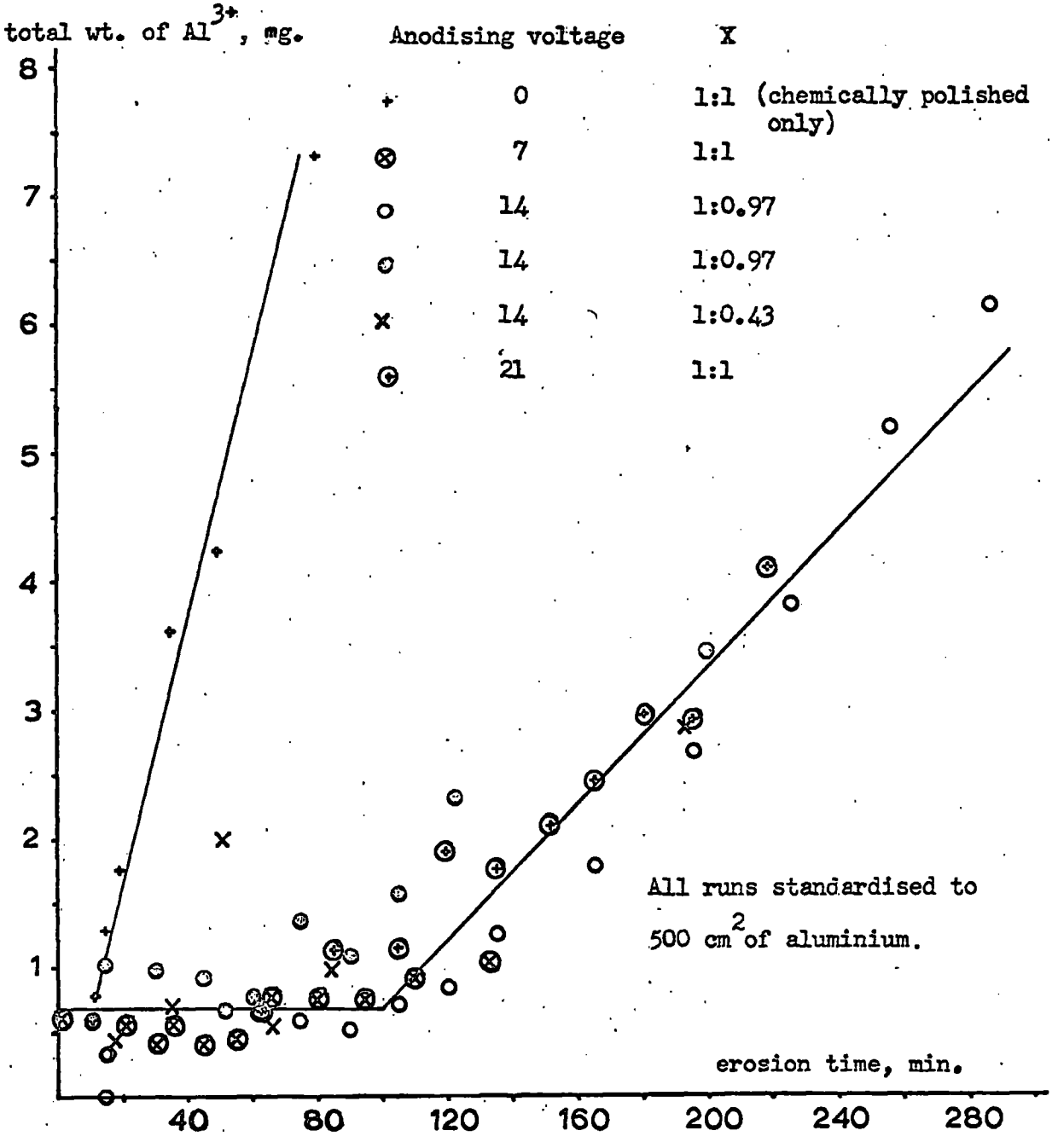

Fig. 16

were immersed in sulphate solutions of pH 0.3-3.5 and ionic strength 0.015-1.5, capacitance change always ceased after about 24 hours. This was also the approximate time required for capacitance change to cease when 7 V and 21 V films were immersed in sulphate solutions of pH 1.0, ionic strength 1.5. In most cases the final capacitance value was about 10 $\mu F\ cm^{-2}$. At a higher solution pH of 5 (I=1.5) a longer period of time, of about 10 days duration, was required for the capacitance to become steady.

A period of immersion of about 24 hours was also the time required for the specimen potential to become sensibly constant when films formed at all three voltages were immersed in a solution of pH 1.0, I=1.5.

In this solution, (pH=1.0, I=1.5), during the initial stages of immersion, 1/C appeared to vary in a linear manner with $(t)^{\frac{1}{2}}$. This was followed by a period of deviation from linearity, leading to a stage in which 1/C was sensibly constant. The slope $(d(1/C)/d(t)^{\frac{1}{2}})$ for the initial period of immersion, in these low pH solutions, increased with increasing film formation voltage; for films formed at 7, 14 and 21 volts respectively, the initial slopes were approximately in the ratio 1:2:3. Deviations from linear $1/C$-$(t)^{\frac{1}{2}}$ behaviour began after about the same immersion time in each case, namely 25 minutes. For 14 V films, this time corresponds closely to the time required for completion of the initial drift of specimen potential in the positive direction; no similar relationship was observed for

the 7 V and 21 V films.

Only 14 V films were studied in deaerated solution. In such solutions, the slope $(d(1/C)/d(t)^{\frac{1}{2}})$ was less than in aerated solutions, deviations from linearity occurred after 40 minutes immersion, and the initial positive drift of specimen potential which was observed in aerated solution was absent.

The period of virtual capacitance arrest observed during specimen immersion in low pH, high ionic strength solutions occurred at capacitance values approximately the same as those reported for the low impedance part of the corresponding full analogue (see Table VII). In all experiments, the time to reach the arrest was about 100 minutes. This corresponds closely to the time to reach the minimum negative value of potential for 14 V films in both aerated and deaerated sulphate solutions at pH 1.0, ionic strength 1.5. The time of 100 minutes also corresponds to the point at which the concentration of aluminium ions in solution began to increase (Fig. 16).

Studies on 14 $\bar{V}$ films in solutions of pH 2 indicate that the slopes of the $1/C-(t)^{\frac{1}{2}}$ graphs were reduced as the ionic strength of solution was reduced. A much greater reduction in slope was observed for a change in I from 1.1 to 1.0 than was the case for a reduction from 1.5 to 1.1 (Table XV). Also, deviations from linearity began later as the ionic strength was reduced. At about ionic strength 1.0, a transition from predominantly linear $1/C-(t)^{\frac{1}{2}}$ behaviour to

predominantly linear 1/C-t behaviour appeared to take place. There is some indication that at ionic strength 1.0, from about 350 to at least 650 minutes immersion, d(1/C)/dt was constant (see Fig. 11). Table XVI indicates that from ionic strength 0.015-0.5, d(1/C)/dt was independent of ionic strength at pH values close to 2 and its magnitude was about the same in all cases.

Under the same conditions as above, but at pH 3.5, the gradients of the linear parts of plots of 1/C versus t were apparently independent of ionic strength in the range 0.015-1.5, and the magnitudes of these slopes were about the same as indicated by Table XVII. In terms of a zeroth order process, which is consistent with the parts of plots where linear 1/C-t behaviour was observed, at pH 3.5, the rate of film thinning was 0.08 ± 0.02 Å min^{-1} and for pH values close to 2, for ionic strengths 0.015-0.5, this rate was 0.12 ± 0.02 Å min^{-1}, These may be compared with a value of 0.022 Å min^{-1} found for immersion of a 14 volt film in sulphate solution, pH 5.0, ionic strength 1.5. Also, in these cases, deviation from linear 1/C versus t behaviour occurred during approximately the first 40 minutes of specimen immersion, except at pH values close to 2, ionic strengths 0.075 and 0.015.

5.6 Significance of the Experimental Results.

5.6.1 Capacitance Studies.

5.6.1.1 Interpretation.

Capacitance increase which takes place during the immersion of alumina films on aluminium in sulphate solution has often been interpreted in terms of film thinning where the specimen potential becomes more negative. Lorking and Mayne[29] have suggested that a decrease in specimen potential indicates that either increased cathodic reaction or film thinning is occurring. Diggle, Downie and Goulding[36] found that the rate of capacitance increase of immersed porous-type films was virtually unaffected when the specimen was maintained at constant potentials by the application of small cathodic currents, and they concluded that thinning was probably taking place. If film thinning is occurring, aluminium ions should be present in the medium in which the specimen is immersed. Nagayama and Tamura[32] have determined spectrophotometrically the concentration of aluminium ions in the dissolution medium during the anodising and dissolution on open circuit of porous-type films immersed in 10% w./v. sulphuric acid. They found that on open circuit, the concentration of ions in solution increased with time and finally levelled off to a constant value. The manner in which the concentration of ions in solution increased with time was almost unaffected by the application of a small cathodic current, indicating that thinning only was involved.

5.6.1.2 Reproducibility.

In the present studies the reproducibility of derived slopes was, in general, $\pm$(15-20%), possibly since true specimen surface areas were unknown. However, the reproducibility was generally sufficiently good for the establishment of trends.

5.6.2 Potential-Time studies.

The specimen potential depends on the ratio of cathodic to anodic areas and on the relative tendencies of the anodic and cathodic reactions to polarise. In the case of alumina films on aluminium, the fall in potential may be understood in terms of corrosion of aluminium under anodic control with the area of the anodic parts of the metal increasing as a result of a reduction in the protective power of the overlying oxide film. This is consistent with film thinning. Similarly, for the same system, any intermediate increase in specimen potential may arise from increased protection of the metal by the deposition of insoluble material. The establishment of a final steady potential may arise from the equilibration of reactions which increase and decrease the protective power of the oxide film.

5.7 Dissolution of Porous-type Anodic Films in Sulphate Solutions.

It can be shown that for films anodised and then eroded on open circuit under similar conditions[32,36], in sulphate solution, the changes in capacitance with time calculated from weight loss values were similar in behaviour to those cases in which the

capacitance-time behaviour was actually determined.

The calculated capacitance-time behaviour is based on the aluminium weight loss measurements of Nagayama and Tamura[32], assuming that capacitance changes arose solely from thinning of the barrier layer at pore bases and from the exposure of fresh barrier layer as a result of simultaneous pore widening. The rate of penetration of a pore into the barrier layer is assumed to be equal to the rate of increase of the pore radius. Diggle, Downie and Goulding[23] have derived the following expression for the time dependence of the capacitance of the barrier layer under these conditions, assuming that the depressions at pore bases in the barrier layer are hemispherical.

$$C - C_o = 10^{-16}\, n\varepsilon k^2 t(r_o/k + t)^2 \,/\, 4L(L/ck^1 - t) \qquad (10)$$

C is the capacitance in e.m.u. at time t, C_o the capacitance at t=0, n the number of pores, each of initial radius r_o per cm^2 of true surface area, ε the dielectric constant of the barrier layer, k the rate of increase of the pore radius, k^1 the rate of pore penetration into the barrier layer, L the initial barrier layer thickness. c is the ratio of the mean depth of penetration of a pore into the barrier layer to the maximum penetration at time t, and may be shown[23] to have the value 0.6 - 0.7. Nagayama and Tamura[32] have determined for a film formed by anodising at 11.9 volts, current density 9.4 ma cm^{-2}, for 6 minutes in 10% w./v. sulphuric acid, pH value about 0.2, at 27°C, followed by dissolution under the same conditions but on open circuit,

the values of the following parameters based on the weights of aluminium ions found in solution after various times.

$$n = 1.2 \times 10^{11} \text{ cm}^{-2}$$

$$r_o = 62.2 \text{ Å}$$

$$k = 0.75 \text{ Å min}^{-1}$$

Assuming that the anodising ratio for the barrier layer of the porous film is 10 Å volt^{-1} [24] and that $\varepsilon = 10$, [70] the plot of 1/C versus t shown in Plate X was determined from the data of Nagayama and Tamura.

Diggle, Downie and Goulding[23] have examined the capacitance-time behaviour of porous films anodically-formed in 15% w./v. sulphuric acid at 10.0 volts, current density 13 ma cm^{-2} at 35°C, followed by dissolution on open circuit in N sulphuric acid, pH 0.3. Thus, after anodising, the barrier layer thickness in each case would be expected to be about the same as would also the oxide cell and pore wall dimensions. It should be borne in mind, however, that there is evidence[25,99,150] that the pore volume depends on the porous layer thickness, electrolyte concentration and anodising temperature. The open circuit dissolution was in solutions differing little in pH value. The results of Diggle[23] indicate that the rate of film thinning should be hardly affected by this change in pH value at constant ionic strength. The ionic strengths differed by about a factor of 2 but it has been reported[23] that the capacitance-time behaviour is unaffected by changes in solution ionic strength at constant pH. Capacitance-time

behaviour as observed[23] would therefore be expected to be about the same as that inferred from weight loss measurements[32]. Plate X also shows the capacitance-time data of Diggle[23]. It is assumed that the value of C_o in equation (10) is that expected for a barrier layer initially 119 Å thick, $\varepsilon = 10$ [70] and that the apparent surface area is the true surface area. The data[23] have been corrected in terms of similar considerations for a barrier layer initially 100 Å thick and the result of this is shown in Plate X. The zeroth order rate constant (the plot of reciprocal capacitance versus time was linear) of 0.495 Å min^{-1} reported[23] becomes 0.773 Å min^{-1} as a result of this correction, a value close to that of 0.75 Å min^{-1} reported for the rate of increase of the pore radius reported by Nagayama and Tamura[32] and assumed for the purposes of the present calculation to be the same as the rate of penetration of a pore into the barrier layer. This indicates that the rate of thinning of the barrier layer, expressed as a zeroth order rate constant, is about the same as the rate of penetration of pores into the barrier layer. The value of c implies that the former might be about 60-70% of the latter. However, in view of the several assumptions and approximations made, it may be said that equation (10) predicts reasonably well the capacitance-time behaviour of the barrier layer of porous alumina films on aluminium during film thinning in sulphate solutions.

It may be concluded that stirring of the solution did not greatly

Dissolution behaviour of porous alumina films of similar structure in sulphuric acid, pH about 0.3.

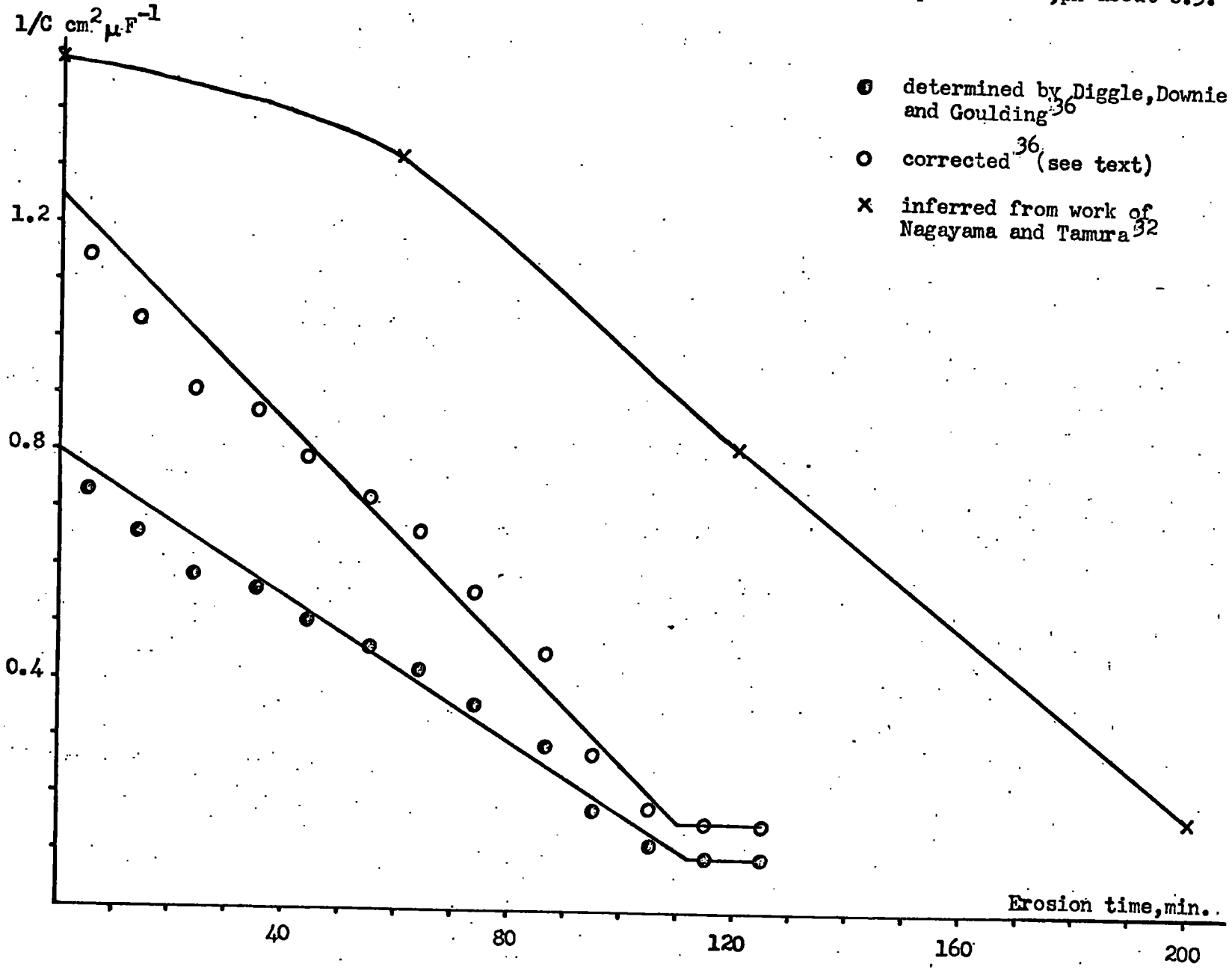

affect the dissolution behaviour since Nagayama and Tamura[32] stirred but Diggle[23] did not stir the solutions.

The specimen potential-time behaviour was also similar in each case. After an initial rapid decrease, the rate of reduction became zero for a short time so that a plateau occurred. After this, the potential rapidly became more negative and quickly achieved a final steady value. Diggle, Downie and Goulding[23, 155] have suggested, based on dye take-up experiments, that the final rapid fall in potential began when the porous layer had disappeared whilst Nagayama and Tamura[32] considered that it began when the pore diameter exceeded that of the inscribed circle of the hexagonal cell[100] resulting in a reduced film surface area.

Lorking and Mayne[9] have reported that the corrosion of oxide-covered aluminium was inhibited over a wide pH range in 0.1 N solutions of sulphate. The critical pH values found by Diggle, Downie and Goulding[36] correspond reasonably well with the lower limits reported by Lorking and Mayne[9]. Diggle, Downie and Goulding[36] have proposed the following reactions, considered to take place near the oxide surface, to account for the behaviour of porous films immersed in sulphate and chloride solutions from pH 0-9.

1) $Al_2O_3 + 3H_2O \rightleftharpoons 2Al(OH)_3$

2) $Al(OH)_3 + H^+ \rightleftharpoons Al(OH)_2^+ + H_2O$

3) $Al(OH)_2^+ \rightleftharpoons \underset{\text{boehmite}}{AlOOH} + H^+$

4) $Al(OH)_2^+ + OH^- \rightleftharpoons AlOOH + H_2O$

5) $2Al(OH)_2^+ + SO_4^{2-} \rightleftharpoons [Al(OH)_2]_2SO_4$

6) $Al(OH)_2^+ + Cl^- \rightleftharpoons Al(OH)_2Cl$

7) $Al(OH)_2^+ + 2H^+ \rightleftharpoons Al^{3+} + 2H_2O$

Restricting considerations to specimen immersion in sulphate solutions, the pH dependence observed below the critical pH was ascribed to reactions (2) and (7) (In both sulphate and chloride solutions, above a certain pH, Diggle, Downie and Goulding found that the capacitance of the barrier layer at first increased and then decreased with respect to time. The time required for the capacitance to pass through its initial value was termed the critical time by these workers, and the minimum pH at which this type of behaviour occurred was termed the critical pH). The virtual independence of the dissolution rate below the critical pH upon ionic strength at constant pH indicated[36] that the dissolution reactions were unimpeded by the adsorption of sulphate ions. Since reactions (1) and (2) must also occur above the critical pH, the initial increase in capacitance could have arisen from some initial film dissolution; the linear plots of $1/C$ versus $(t)^{\frac{1}{2}}$ may indicate that this dissolution was diffusion-controlled, although an increase in the film dielectric constant resulting from the diffusion of hydroxyl ions into the film[21,38,39] is another possibility since hydroxyl is the most polarisible ion present in sulphate solutions[20]. Since the critical time was found to be independent of pH, it was

proposed that reaction (5) was more important than (3) and (4). A white solid was isolated from specimens in high pH solutions and was identified as a hydrated aluminium sulphate. The decrease in critical time with decreasing ionic strength at constant pH was suggested[36] to arise from a decreasing competitive absorption between sulphate and hydroxyl ions, favouring reaction (4) and favouring reaction (3) by the possibility of easier diffusion of protons out of the film.

The complex structure of porous-type films makes an exact interpretation of the capacitance-time behaviour of thebarrier layer during dissolution difficult since one must account for barrier layer thinning at pore bases and the simultaneous exposure of fresh barrier layer as the pores widen. The rate: at which pores widen should not necessarily be assumed[70] to be the same as the rate at which they penetrate into the barrier layer. Diffusion of ions into and out of the barrier layer must also be considered.

The possibility of field-assisted dissolution of the barrier layer to form porous layer can be seen in terms of the current transient behaviour found during anodising, shown in Plate II (b). The point, A, of minimum current density has been interpreted in terms of pore initiation[24,41]. Hoar and Yahalom[41] found that point A occurred earlier the higher the applied voltage, which is evidence for field-assisted dissolution of the initially-formed barrier layer.

Diggle, Downie and Goulding[36] found that the capacitance-time

behaviour of porous-type films immersed in chloride and sulphate solutions was identical under aerated and deaerated conditions, indicating that the increased field resulting from oxygen ions present on the film surface had no effect on the dissolution rate.

5.8 Comparison of the Dissolution of Porous and Non-porous Anodic Films.

5.8.1 The Effect of Solution Deaeration.

In the present investigation on non-porous films, deaeration resulted in a reduced rate of capacitance increase as compared with the behaviour in aerated solutions during specimen immersion in solutions of low pH. The linear plots of $1/C$ versus $(t)^{\frac{1}{2}}$ obtained in the present studies for solutions having a low pH are consistent with a diffusion-controlled mechanism. It is proposed that the dissolution behaviour at low pH values was consistent with the diffusion of hydroxyl ions into the film. Under the conditions of reduced field on deaeration of the solution, this rate of diffusion would be less. The approximately linear plots of $1/C$ versus t reported for porous films[23,36], probably approximating to a zeroth order process, give no intimation of possible diffusion control and results were unaffected by deaeration.

5.8.2 Critical pH Values.

In the present studies, at up to solution pH 5, no critical solution pH value was observed above which the capacitance decreased with increasing immersion time[36]. However, at pH values close to 2.0, it

was observed that the dissolution kinetics depended on the ionic strength of the solution. As the ionic strength was reduced from a value slightly greater than 1.0 to a value slightly less than 1.0, the capacitance-time relationship changed from the predominantly linear $1/C-(t)^{\frac{1}{2}}$ type to the linear $1/C-t$ type. At pH 3.5 the behaviour was completely of the latter type for the range of ionic strengths from 0.015-1.5 It is possible that this change in behaviour took place at about pH 2.0 as a result of increased sulphate absorption by the oxide film with increased ionic strength of solution such that hydroxyl ion diffusion into the film became rate controlling at a sufficiently high level of sulphate ion absorption. The results reported here may indicate that the behaviour of porous films in high pH solutions is related to sealing processes in the porous layer.

5.8.3 Thinning of Porous and Non-porous Films.

For a sulphate solution at a pH of about 2.0, having an ionic strength less than about 1.0, the zeroth order rate constant for thinning of non-porous films about 200 $\overset{o}{A}$ thick was found to be about 0.12 $\overset{o}{A}\ min^{-1}$ compared with about 0.25 $\overset{o}{A}\ min^{-1}$ for porous films[36] formed at 10 volts for 30 minutes at a current density of 13 ma cm^{-2} and at 35°C. One would expect that if the only difference in the dissolution behaviour were caused by the barrier layer being exposed to dissolution only at pore bases, the rate would be smaller for porous films but would approach the value for non-porous films as pore-widening proceeded.

The apparent reversal of the expected values based on such considerations indicates that the state of the barrier layer may be different in each case. For example, it is well known that much sulphate ion is incorporated into porous-type films formed anodically in sulphuric acid[86,95].

5.9 Structure of Non-porous Anodic Films Formed in the Present Studies.

The discontinuity in the plots of 1/C versus $(t)^{\frac{1}{2}}$ during the immersion of films in sulphate solutions of low pH (Figs. 6 and 9) is consistent with the two layer structure indicated by the full electrical analogues and discussed in Section 1.1. The capacitance (about 0.8-2.5 $\mu F\ cm^{-2}$) of the low impedance layer was always about the same as the capacitance of films immersed in the sulphate solutions of low pH when the plateau region in Figs. 6 and 9 occurred, evidence that the low impedance part of the film was adjacent to the metal. The decreasing slopes shown in Figs. 6, 8 and 9 which occurred could have arisen from the diffuse nature of the hydrated outer region as reported by Heine and Pryor[21].

5.10 Controlling Factors in the Dissolution of Non-porous Films.

It is suggested that reactions (1), (2), (3), (4) and (7), proposed by Diggle, Downie and Goulding[36], are involved. Where linear plots of 1/C versus $(t)^{\frac{1}{2}}$ were obtained, consistent with a diffusion-controlled process, in the low pH solutions, ionic strengths 1.5 and above a

critical ionic strength at pH values close to 2, it is proposed that hydroxyl ion diffusion into the oxide films was rate-determining, resulting from reduced ratios of hydroxyl ion activity in solution to sulphate ion absorption at the oxide film surface.

That film dissolution took place is indicated by the increasing concentration of aluminium ions in solution during immersion, after about 100 minutes, for 7, 14 and 21 volt films in pH 1.0, ionic strength 1.5 sulphate solutions (Fig. 16). Further, for all three types of film preparation, the final steady capacitance value was about 10 $\mu F\ cm^{-2}$, corresponding to about 10 $\text{\AA}$ of oxide film and, where determined, the time required for the specimen potential to decrease to a steady value was about the same. The tendency for thefinal capacitance value to decrease with increasing solution pH may be understood in terms of increased hydroxyl ion activity in the solution, leading to increased field strengths across the oxide layer. Equilibration of the rates of film dissolution and repair would be expected to oxxur at increased film thicknesses, since aluminium ion conduction through the oxide film would occur at greater thicknesses due to the higher field strengths. Another factor might be an increase in the rates of reactions (3) and (4) leading to the formation of insoluble boehmite.

The general decrease in the slope with increasing solution pH for reciprocal capacitance plots of the same type, that is either

versus time or the square root of time may be viewed as arising from the increasing hydroxyl ion activity, resulting in increased rates of reactions (3) and (4) and reduced rates of (2) and (7). That boehmite formation was possible was indicated by the appearance of a white deposit after about 24 hours on a 14 volt anodised specimen immersed in a sulphate solution, pH about 9. A positive identification of this deposit is desirable.

Comparison of the specimen potential-time behaviour of 14 volt anodised non-porous films during dissolution in deaerated sulphate solutions, pH 1.0, ionic strength 1.5 (Fig. 15) shows that the first maximum in potential in aerated solution was absent in deaerated solution. If boehmite formation by reaction (4) took place, the reduced rate of hydroxyl ion diffusion into the film resulting from reduced fields produced by the absence of oxygen in the solution would be expected to lead to a reduced rate of boehmite formation and, by reaction (3), reduced boehmite formation resulting from a reduced rate of proton escape from the film. The difference in specimen potential-time behaviour could be understood in terms of a reduced initial increase in protection of the film by reduced boehmite deposition. The first minimum in potential corresponded in time with the loss of the outer layer, indicated by the beginning of the plateau region in the 1/C versus $(t)^{\frac{1}{2}}$ plot shown in Fig. 16. The second maximum in specimen potential may be associated with

increased protection resulting from the adsorption of sulphate ions by the exposed inner layer, together with greater boehmite deposition under aerated conditions since the effect was smaller under deaerated conditions.

5.11 Transition from Diffusion Control to Zeroth Order Thinning.

For 14 volt anodised specimens, at solution pH values close to 2.0, the slope of the plot of 1/C versus $(t)^{\frac{1}{2}}$ corresponding to dissolution of the outer layer of the film, decreased when the ionic strength of the solution was reduced from 1.5-1.1 and this reduction in slope was much greater on reducing the ionic strength from 1.1 to 1.0 (See Table XV). It is suggested that sulphate ion adsorption decreased with decreasing ionic strength, resulting in a greater accessibility of the oxide surface to hydroxyl ions and greater rates of removal of protons from the film surface, both leading to reduced slopes because of increased boehmite formation by reactions (3) and (4) respectively. The transition from the suggested predominantly diffusion-controlled to suggested predominantly zeroth order thinning which occurred at a solution pH value close to 2.0, ionic strength close to 1.0 (Fig. 11), indicates that the level of sulphate ion adsorption was low enough for the rates of transfer of ions between oxide and solution to be sufficient for the rates of reactions (1), (2), (3), (4) and (7) to be controlled by equilibrium levels of protons, hydroxyl ions and water at relevant reaction sites so that

predominantly diffusion-controlled thinning, where the rate of arrival from the solution at reaction sites of reacting species was possibly controlled by the rate of diffusion of hydroxyl ions into the film, gave way to zeroth order thinning. There was a little indication of a short period of initial diffusion control, absent at the lowest ionic strengths at pH values close to 2.0 (see Figs. [illegible], 11 and 12), for those cases where mainly zeroth order thinning was indicated and this initial period might be associated with the establishing of the equilibrium levels of reacting species at reaction sites.

The independence of slopes of ionic strengths at constant pH where zeroth order thinning was indicated is further evidence that the level of sulphate ion adsorption had no effect on the rate of dissolution.

5.12 Physical Mechanism of Dissolution.

Evidence has been presented in Chapter III (3.8.1) for the existence of discrete pores in formally non-porous films formed anodically under conditions similar to those adopted in the present study. It is likely that their contribution to the overall impedance was small since a pore contribution to the full analogue led to no improvement in matching of the charging curves with that of the films.

The initial slopes of the plot of $1/C$ versus $(t)^{\frac{1}{2}}$ for 7, 14 and 21 volt films during dissolution in pH 1.0, ionic strength 1.5 sulphate solution were found to be almost in the ratio 1:2:3 (see

Table XIII) and the time of the first virtual capacitance arrest, after about 100 minutes in each case, was close to the times required for the rapid increase in the concentration of aluminium ions in the solution (Fig. 16). After this time, the capacitance values were in all cases close to those of the respective inner layers as indicated by the full analogues.

This indicates that the time of loss of the outer layer was independent of the anodising voltage and therefore of the thickness of the outer layer. Similar findings have been reported[23] for porous films anodised at constant voltage but for different lengths of time and it would appear that for both cases, a pore widening mechanism[23] may control the rate of loss of the outer layer. The comparatively low concentrations of aluminium ions in solution (see Fig. 16) up to about 100 minutes for 7, 14, and 21 volt films immersed in pH 1.0, ionic strength 1.5 sulphate solutions were considerably lower than that which could have arisen from the total outer layer. If a pore widening mechanism were controlling the removal of the outer layer, there would be a reduction in the film surface area as the last traces of the outer layer was removed which could result in the rapid release into solution of aluminium ions previously adsorbed. The rapid increase from the earliest times of the concentration of aluminium ions in solution where the specimen was chemically polished only (see Fig.16) is in keeping with this interpretation. Both for specimens chemically

polished only, and for those anodised, the eventual attainment of considerably larger concentrations of aluminium ions in solution than could have arisen from the initially-present oxide alone, indicates that self-corrosion of the underlying metal was taking place. Nagayama and Tamura[32] have reported that for porous films anodically-formed in sulphuric acid, the total amount of ions dissolved on open circuit agreed well with the amount of aluminium initially present in the oxide film, indicating that there was little self-corrosion of the underlying metal[32]. Also, confirming this, amounts of hydrogen evolved during dissolution were found to be negligible[32]. It would appear, then, that the film remaining after thinning was highly protective[32], unlike that of specimens chemically polished only and of non-porous anodically-formed films prepared in the present investigation even when only the outer layer had been removed. Since Nagayama and Tamura initially electropolished their specimens, this difference in behaviour could arise from the different initial surface preparations used. That sulphate ion incorporation into each type might have been to a different extent is another possible factor. Nagayama and Tamura found that the amount of aluminium ions in solution increased from the earliest times, indicating that the extent of adsorption of these ions by the oxide film was probably small and this might arise from the initial high level of sulphate ion incorporation of the porous film.

Table XVIII (a)

Frequency Response of Balancing Series Resistance, R_s, and Capacitance, C_s, for 2 Alumina Films Formed in Dry Oxygen at 500°C.

Film No	1		2	
Frequency Hz	R_s ohm cm^2	C_s μF cm^{-2}	R_s ohm cm^2	C_s μF cm^{-2}
10	0.0	1.38	0.0	0.94
83	0.0	1.30	0.0	0.90
500	5.3	1.32	0.0	0.92
5 000	11.7	1.25	9.9	0.88
50 000	11.3	0.96	11.4	0.71

Table XVIII (b)

Frequency Response of Balancing Series Resistance, R_s, and Capacitance, C_s, for 3 Alumina Films Formed in an Atmosphere of Oxygen and Water (p_{H_2O} = 43.1 mm) at 500°C

(i)

Film	1		2	
Frequency Hz	R_s ohm cm^2	C_s μF cm^{-2}	R_s ohm cm^2	C_s μF cm^{-2}
10	1.620	1.37	0.0	1.10
83	0.0	1.20	0.0	1.03
500	0.0	1.22	0.0	1.03
5 000	6.5	1.14	8.7	1.02
50 000	7.6	0.56	10.1	0.64
100 000	7.0	0.30	10.1	0.45

Table XVIII (b) continued

(ii)

Film	3	
Frequency Hz	R_s ohm cm^2	C_s μF cm^{-2}
10	3 000	1.04
83	0.0	0.91
500	0.0	0.96
5 000	7.9	0.94
50 000	9.1	0.66

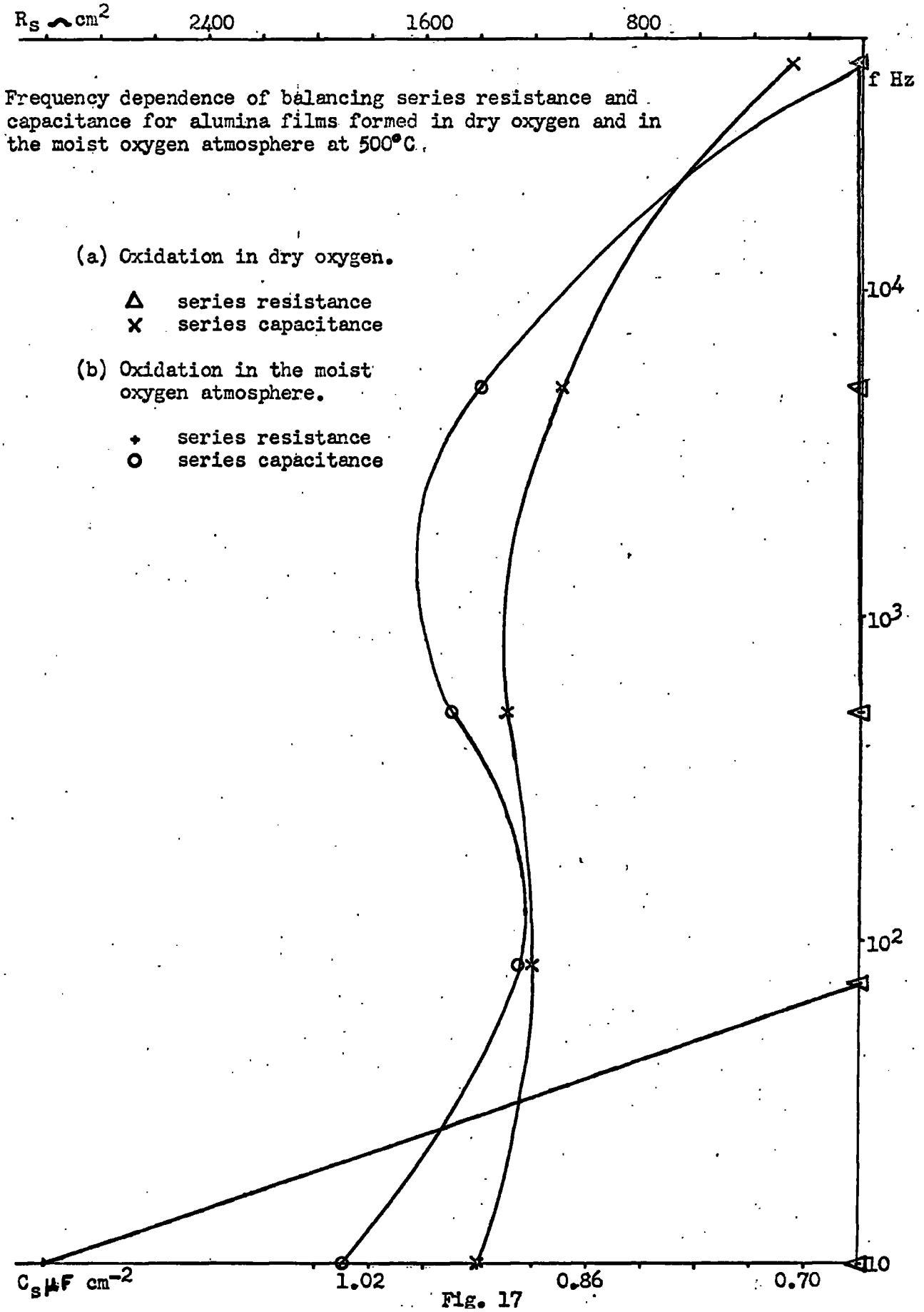

Frequency dependence of balancing series resistance and capacitance for alumina films formed in dry oxygen and in the moist oxygen atmosphere at 500°C.

(a) Oxidation in dry oxygen.

△ series resistance
× series capacitance

(b) Oxidation in the moist oxygen atmosphere.

+ series resistance
○ series capacitance

Fig. 17

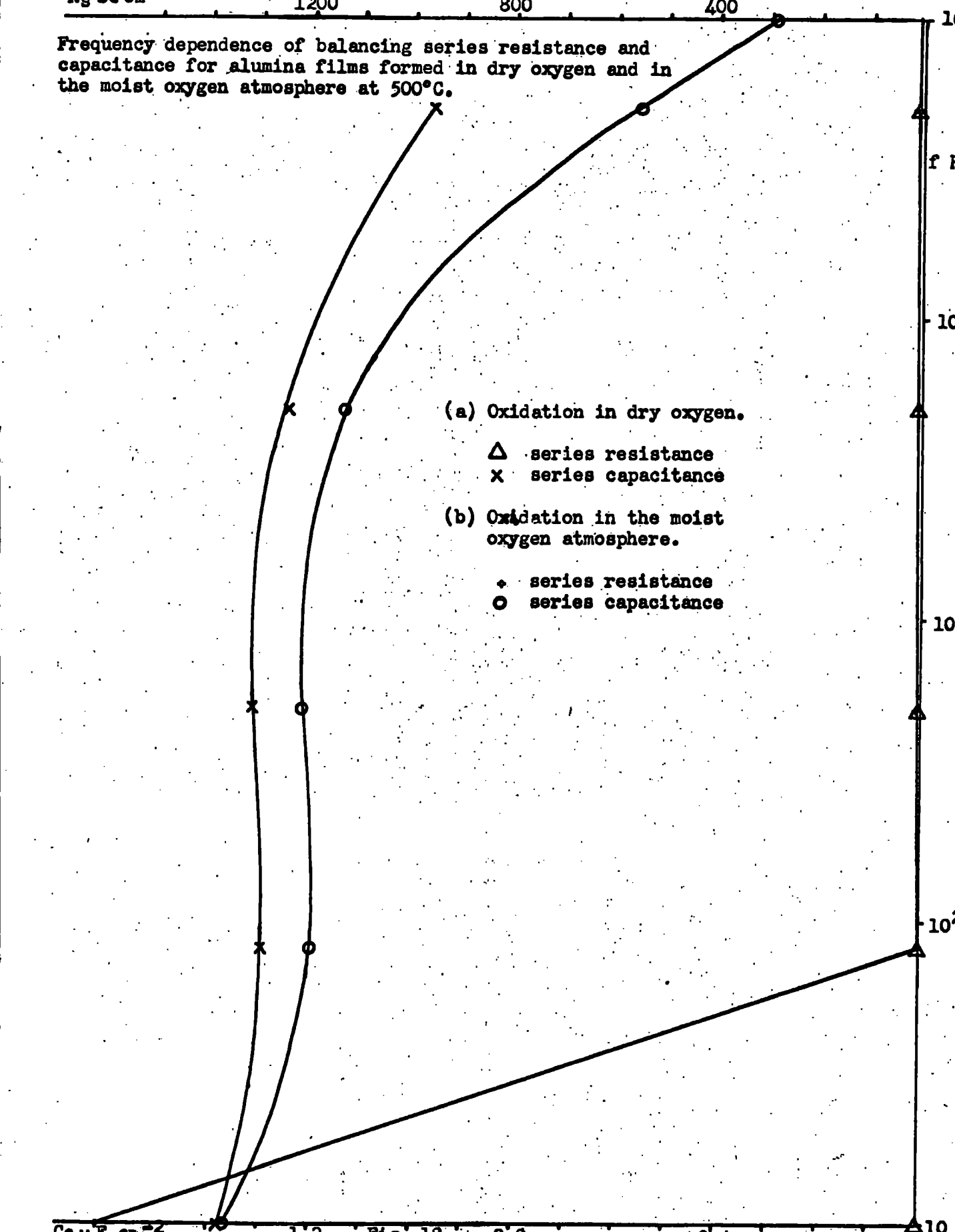

Frequency dependence of balancing series resistance and capacitance for alumina films formed in dry oxygen and in the moist oxygen atmosphere at 500°C.

CHAPTER VI

Experimental Results for Alumina Films Formed in Dry and Moist Oxygen.

6.1 Construction of full electrical analogue.

The best matching of response curves that could be obtained was with the simple analogue shown in Fig. 2 (b). A small phase discrepancy was present, however, which was sensibly frequency-independent. This type of behaviour was also found for anodically-formed films and again may be due to film hydration producing a diffuse region, although no improvement in matching was obtained by modifying the analogue to account for an additional layer in the film structure.

Values of R_1 (see Fig. 2(b)) were identified with the measured ohmic drop of about 40 ohm cm^{-2} across the ammonium tartrate solution.

The frequency responses of the components of the simple series resistance-capacitance analogue for films produced by oxidation in dry oxygen and oxygen containing gaseous water, p_{H_2O} = 43.1 m.m., at 500°C are shown in Figs. 17 and 18 and are summarised in Table XVIII.

The following tables summarise the results obtained and illustrate the reproducibility which was not too satisfactory.

Table XIX

Electrical Characteristics of Films Formed in Dry Oxygen, 1 Atmosphere Pressure.

	C_2 μF cm^{-2}	R_2 ohm cm^2
(1)	1.23	210 000
(2)	0.88	260 000

Table XX

Electrical Characteristics of Films Formed in Oxygen containing Gaseous Water, p_{H_2O} = 43.1 m.m. Atmosphere Total Pressure.

	C_2 μF cm^{-2}	R_2 ohm cm^2
(1)	1.17	35 000
(2)	1.02	87 000
(3)	0.87	42 000

At 83 Hz, in general, the value of the capacitative component of the simple series analogue increased by up to 15% during a frequency run and the impedance of this component was much greater than the resistive component at this frequency. This increase in capacitance

might be associated with film dissolution and/or changes in the film dielectric constant resulting from film hydration. Good matching of the charging curves would not therefore be expected.

The poor reproducibility of series resistance at low frequencies for films formed in moist oxygen might arise from the small contribution made by this component to the overall impedance.

Values of C_2 for the two types of film preparation were about the same but R_2 was considerably smaller for films formed in the moist oxygen atmosphere.

6.2 Impedance Measurements During Specimen Immersion.

The reproducibility of the capacitance-time behaviour was very poor for films formed in moist oxygen during specimen immersion in aerated sulphate solution, pH 1.0, ionic strength 1.5 but was better in the same medium when deaerated. Typical 1/C versus $(t)^{\frac{1}{2}}$ behaviour in deaerated solution is shown in Fig. 19 where the behaviour of films formed in dry oxygen during specimen immersion in aerated and deaerated sulphate solution, pH 1.0, ionic strength 1.5 is also shown.

Fig. 20 shows typical plots of 1/C versus t for immersion of films formed in dry oxygen in sulphate solutions having pH values close to 2, ionic strengths 0.015-1.5. Fig. 21 represents the results obtained in solutions of pH 3.5, ionic strengths 0.015-1.5.

Fig. 22 shows 1/C versus $(t)^{\frac{1}{2}}$ behaviour for films formed in dry oxygen during immersion in sulphate solutions, ionic strength 1.5,

pH values 1.0 and 2.0 and Fig. 23 shows 1/C versus t behaviour for the same system but at pH values of 3.5 and 5.0.

Where predominantly linear plots of 1/C versus $(t)^{\frac{1}{2}}$ were found, the values of the oxide film resistance Rp, when first measured, were always low and fell quite quickly. The initial values of Rp were considerably greater for films formed in moist than in dry oxygen under the same conditions. The initial values of Rp increased as the pH of the solution increased from 1.0 to 3.5. The value observed in a solution of pH 5.0 was, however, less than that at pH 3.5. The rate at which Rp decreased with time generally fell with increasing solution pH except at pH 5.0 when the behaviour was intermediate between pH 2 and pH 3.5. Throughout these studies, where consideration of the linear plot is restricted to the same type, that is 1/C versus either t or $(t)^{\frac{1}{2}}$, the rate at which Rp fell was reduced as the rate of change of 1/C was reduced.

The following tables summarise the results obtained. The slopes are corrected in terms of the mean values for capacitance from the full analogues.

Capacitance behaviour of alumina films formed in dry or moist oxygen, immersed in ionic strength 1.5, pH 1, sulphate solutions, aerated and deaerated.

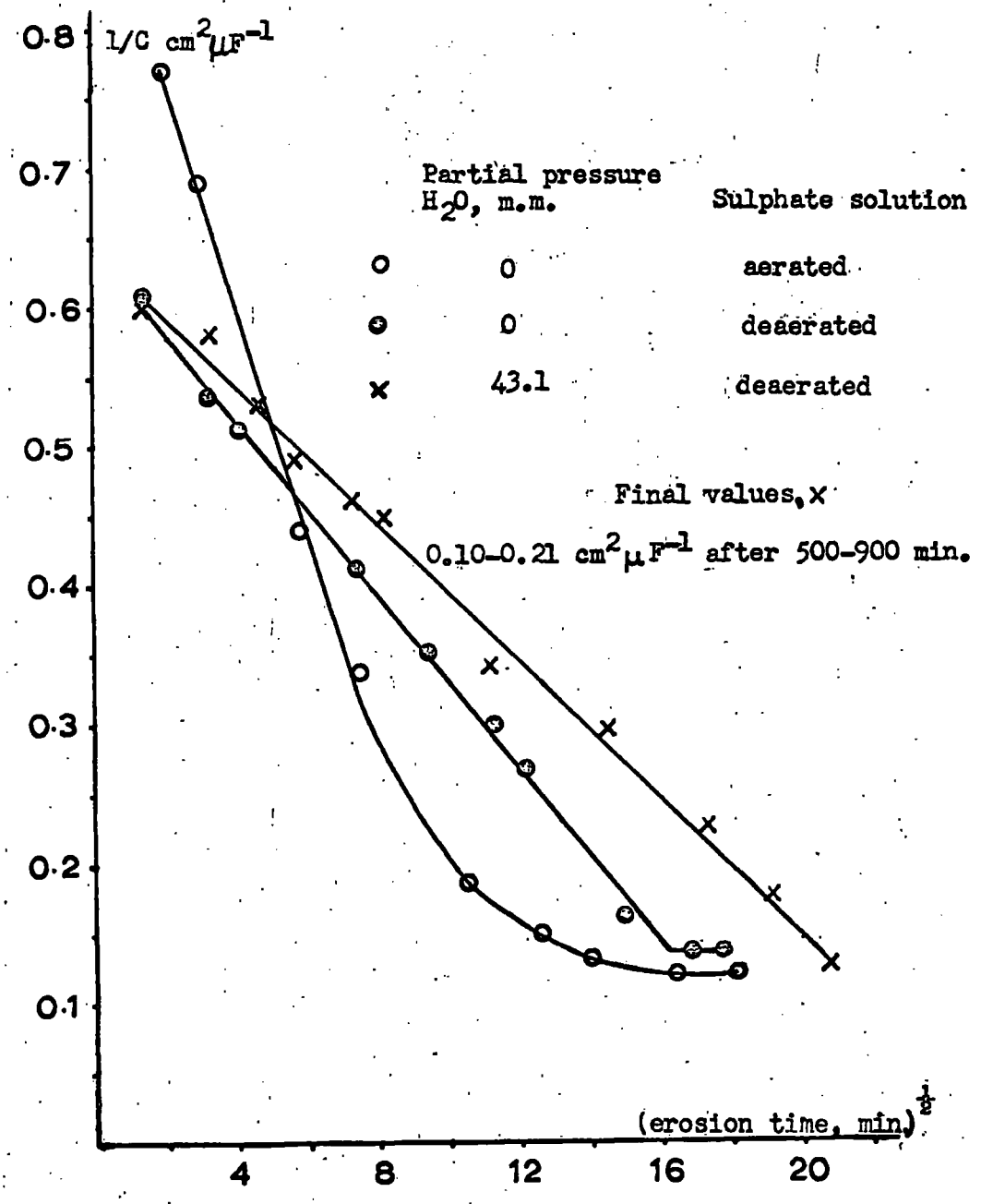

Fig. 19

Capacitance behaviour of alumina films formed in dry oxygen at 500°C, immersed in pH 2 sulphate solutions as a function of ionic strength.

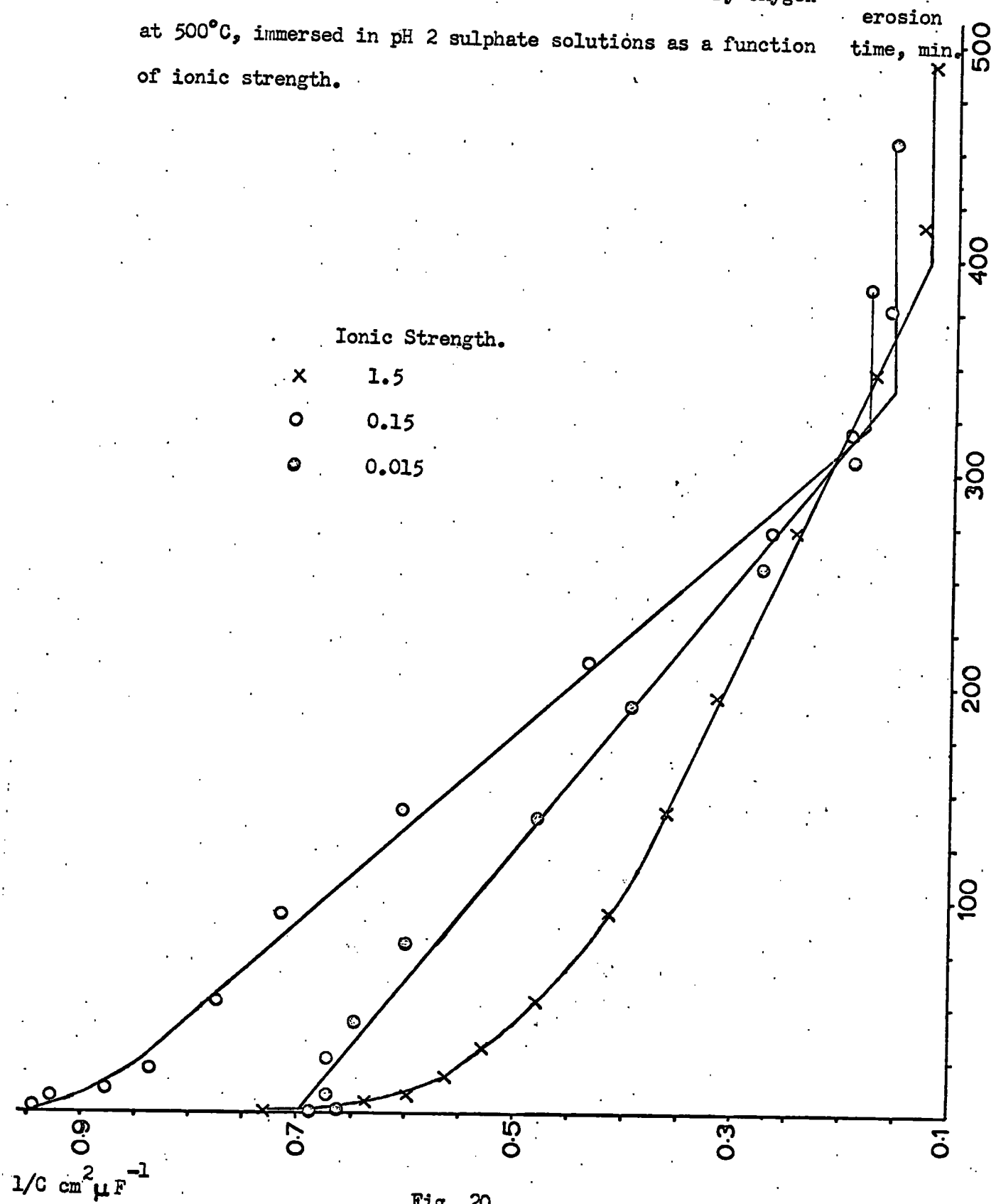

Fig. 20.

Capacitance behaviour of alumina films formed in dry oxygen at 500°C, immersed in pH 3.5 sulphate solutions as a function of ionic strength.

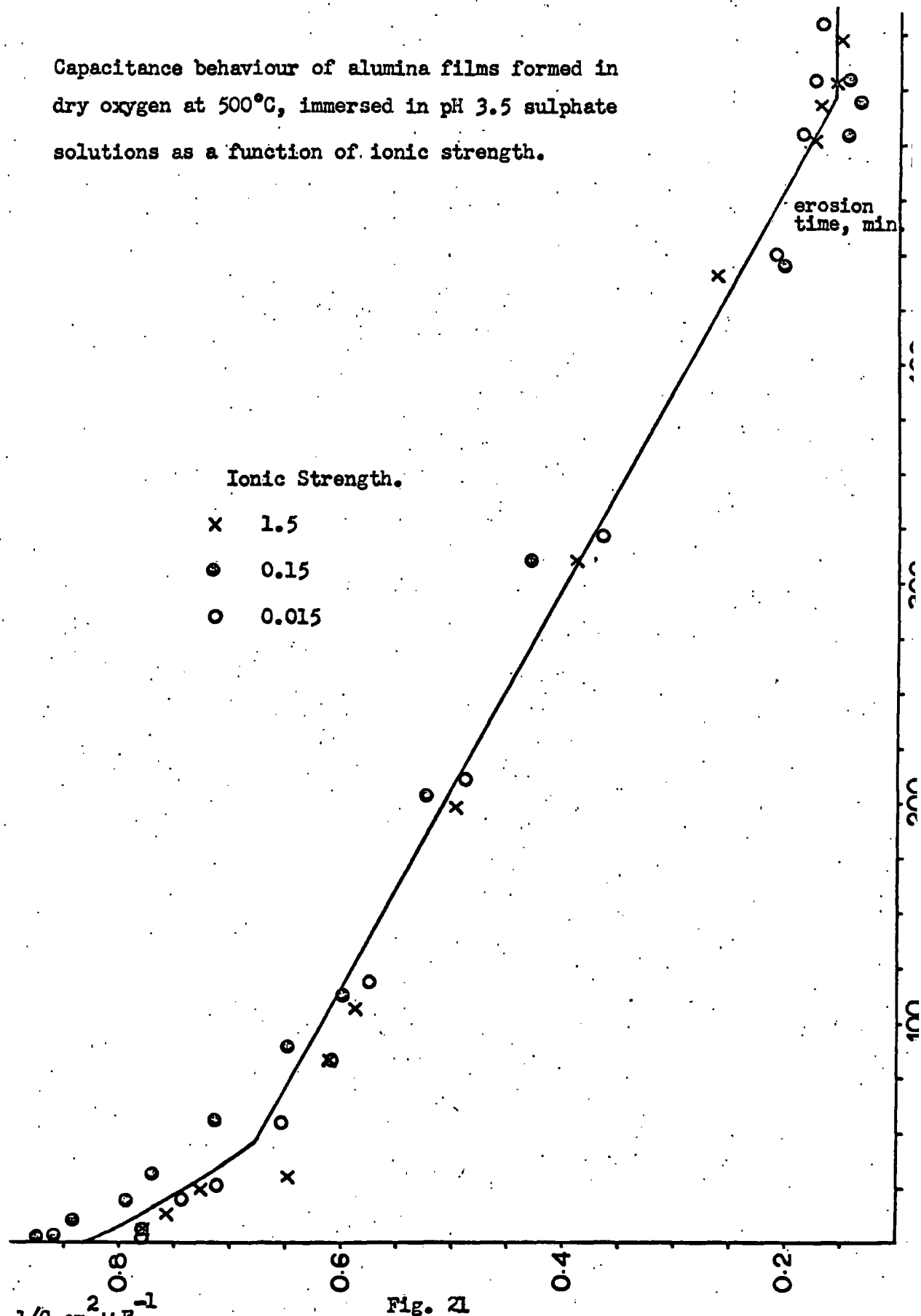

Fig. 21

Capacitance behaviour of alumina films formed in dry oxygen at 500°C, immersed in ionic strength 1.5 sulphate solutions as a function of pH.

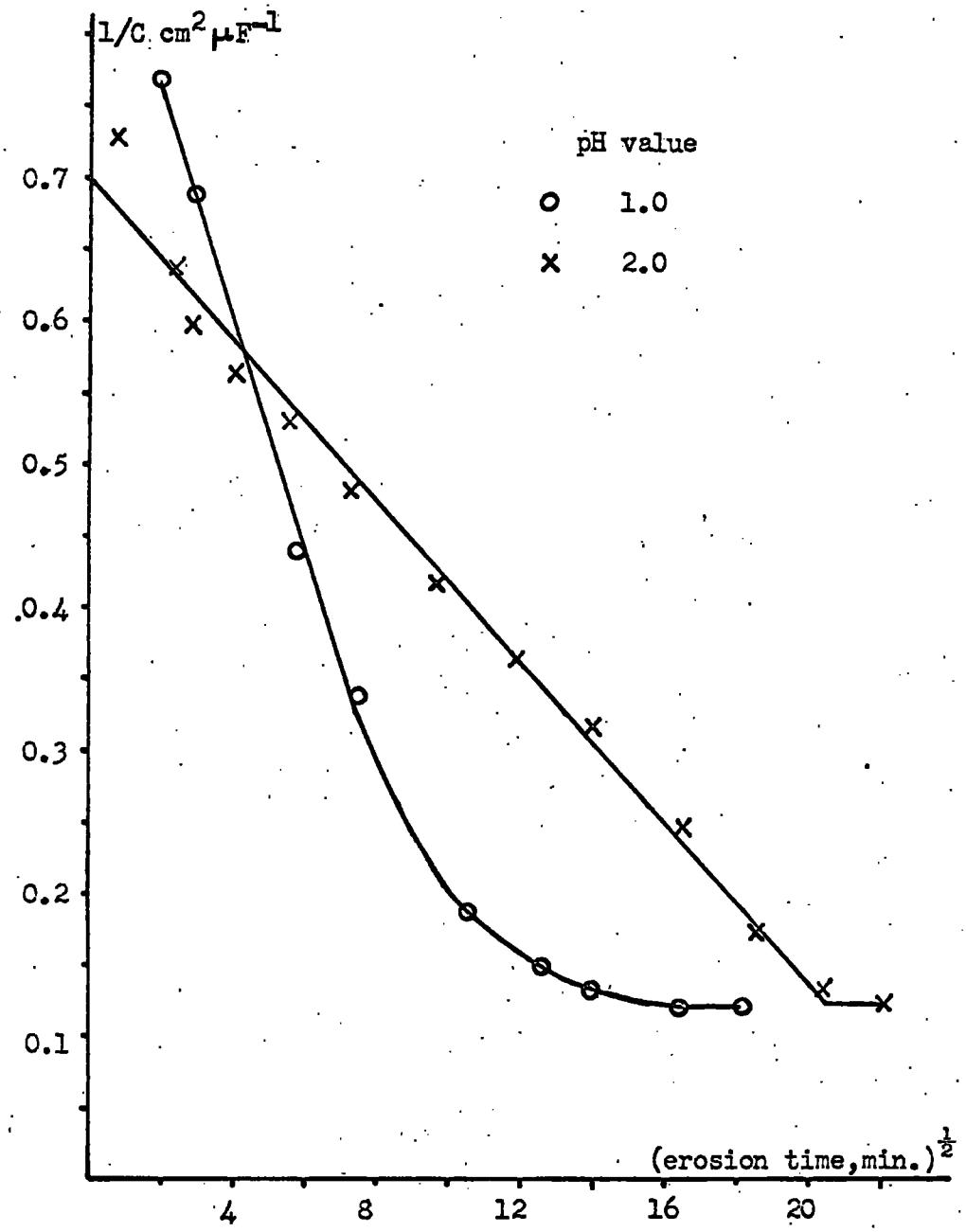

Fig. 22

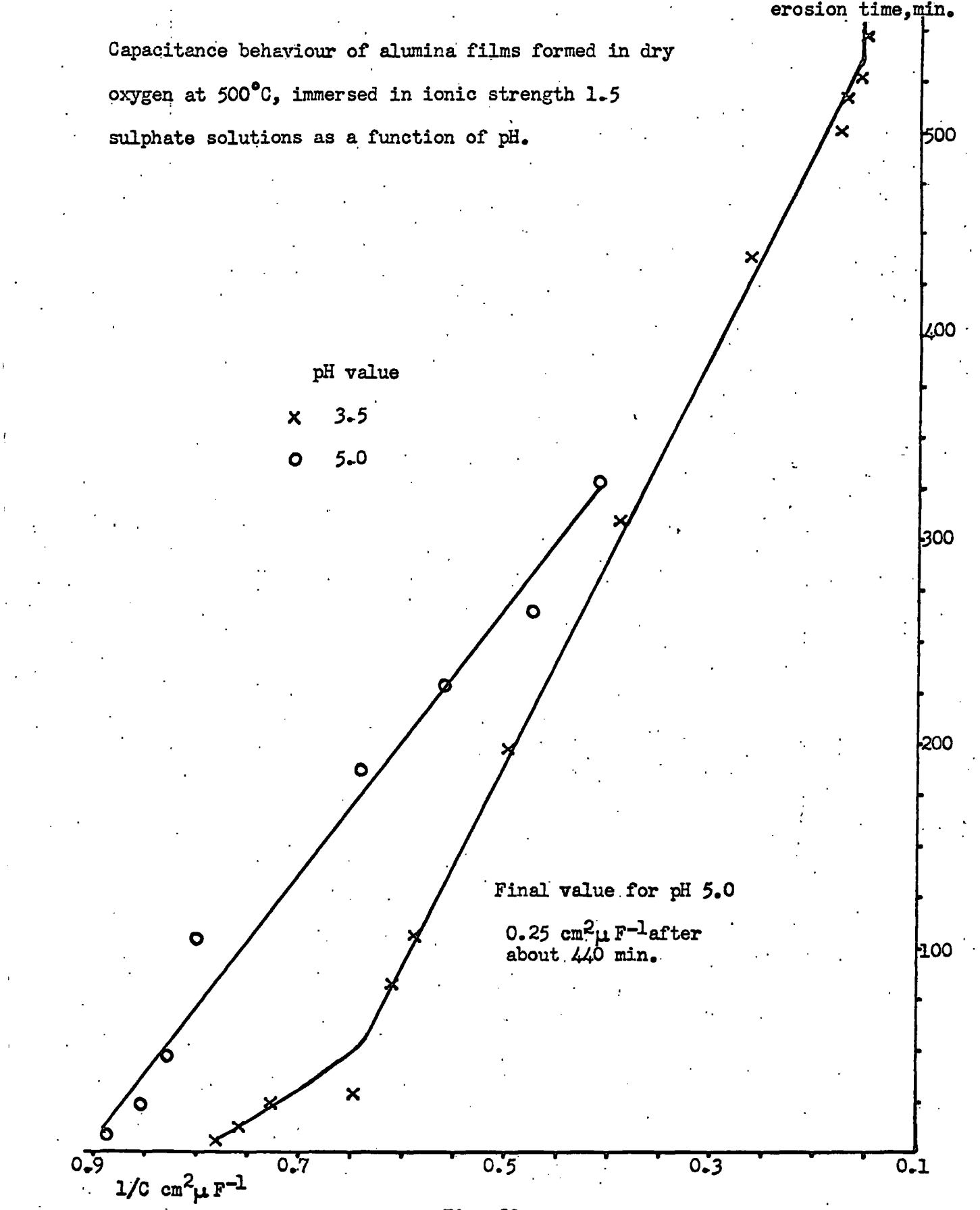
Capacitance behaviour of alumina films formed in dry oxygen at 500°C, immersed in ionic strength 1.5 sulphate solutions as a function of pH.
erosion time, min.
pH value
× 3.5
o 5.0
Final value for pH 5.0
0.25 cm²μF⁻¹ after about 440 min.
0.9
0.7
0.5
0.3
0.1
1/C cm²μF⁻¹
100
200
300
400
500

Fig. 23

Table XXI

Kinetic Data for Dissolution of Oxide Films Formed in Oxygen at 500°C in Sulphate solutions, Ionic Strength 1.5.

Film preparation	pH value	Slope as per graphs	Reciprocal of interpolated initial capacitance	Corrected slope	Comments
		k_1 $cm^2 \mu F^{-1}$	$1/C_o$ $cm^2 \mu F^{-1}$	k_2 $cm^2 \mu F^{-1}$ $min^{-\frac{1}{2}}$	
Dry oxygen	1.0	- 0.081 - 0.066	0.93 0.74	- 0.082 - 0.084	Deviation from linearity after about 60 mins
Dry oxygen	2.0	- 0.034 - 0.028	0.90 0.70	- 0.036 - 0.038	Some evidence for zeroth order after about 170 mins.
Dry oxygen	1.0	- 0.032 - 0.018	0.64 0.44	- 0.047 - 0.038	Deaerated solution
Oxygen with gaseous water content, P_{H_2O} = 43.1mm	1.0	- 0.0247 - 0.0244	0.64 0.96	- 0.035 - 0.023	Deaerated solution

Table XXII

Kinetic Data for Dissolution of Oxide Films Formed in Dry Oxygen at 500°C in Sulphate Solutions, Ionic Strength 1.5.

pH value	Slope as per graph	Reciprocal of interpolated initial capacitance	Corrected Slope converted to Å min^{-1} assuming $\varepsilon = 10$	Comments
	k_1 $cm^2 \mu F^{-1} min^{-1}$	$1/C_o$ $cm^2 \mu F^{-1}$		
3.5	- 0.0010 (- 0.0011)	0.83 (0.83)	- 0.088 (- 0.097)	some evidence for diffusion control during first 40 min.
5.0	- 0.0015	0.875	- 0.126	

In parentheses - based on all data for ionic strengths 0.015-1.5.

Table XXIII

Kinetic Data for Dissolution of Oxide Films Formed in Dry Oxygen at 500°C in Sulphate Solutions, pH Values Close to 2.0.

Ionic strength	Slope as per graph	Reciprocal of interpolated initial capacitance	Corrected slope converted to Å min^{-1} assuming $\varepsilon = 10$	Comments
	k_1 $cm^2 \mu F^{-1} min^{-1}$	$1/C_o$ $cm^2 \mu F^{-1}$		
0.15	- 0.0022 - 0.0014	1.00 0.80	- 0.16 - 0.13	some evidence for diffusion control during first 25 min.
0.015	- 0.0016 - 0.0021	0.70 0.94	- 0.17 - 0.16	

6.3. Potential-Time Studies.

Typical potential-time curves obtained using films formed in dry oxygen when immersed in aerated and de-aerated sulphate solutions, pH 1.0, ionic strength 1.5, are shown in Fig. 24.

Results for films formed in oxygen containing gaseous water (p_{H_2O} = 43.1 m.m.) during specimen immersion under identical conditions are shown in Fig. 25. Fig. 24 shows that the initial rate of fall of specimen potential was greater under deaerated than aerated conditions for films formed in dry oxygen, and the minimum in potential occurred after about the same time for each. Fig. 25 shows that for films formed in the moist oxygen atmosphere, deaeration led to the absence of the first and second maxima in the specimen potential, features present under aerated conditions. Under both sets of conditions, a final minimum in potential was observed after about the same time.

6.4 Barrier Voltage Studies.

Typical current-time behaviour is shown in Fig. 26 using the methods of Hunter and Fowle[24] and of Hart[45]. The identification of the minimum voltage to support ionic conduction is also indicated in Fig. 26 and was known since the rate of voltage increase and the chart speed were known.

6.4.1 Films Formed in Dry Oxygen.

The barrier voltage was found to be sensibly independent of the

The specimen potential - time study of the erosion of alumina films, formed in dry oxygen at500°C, in sulphate solution,pH1.0,I=1.5,aerated and deaerated.

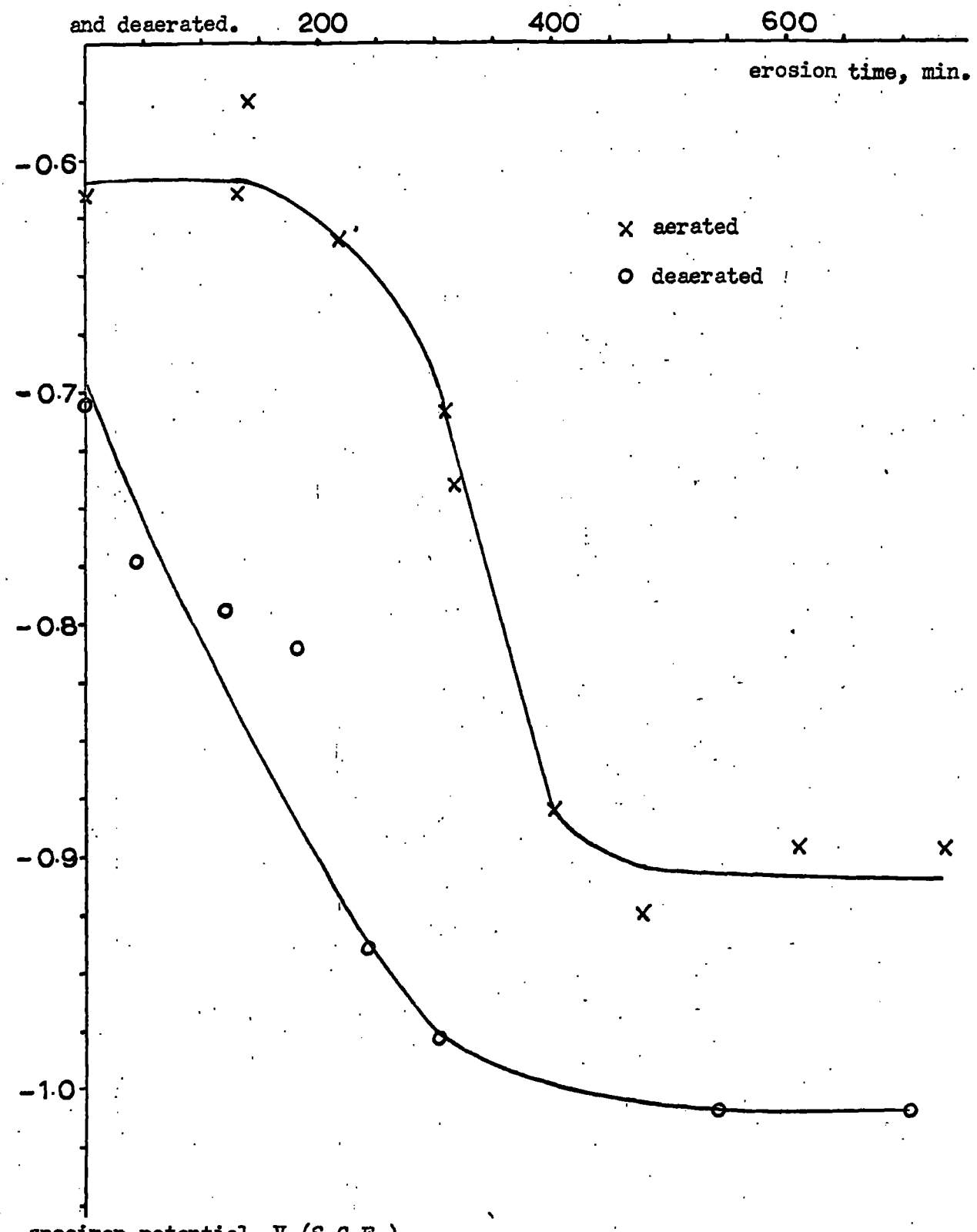

Fig. 24

Potential behaviour of aluminium specimens oxidised in the moist oxygen atmosphere at 500°C, in sulphate solution, pH 1.0, ionic strength 1.5, aerated and deaerated.

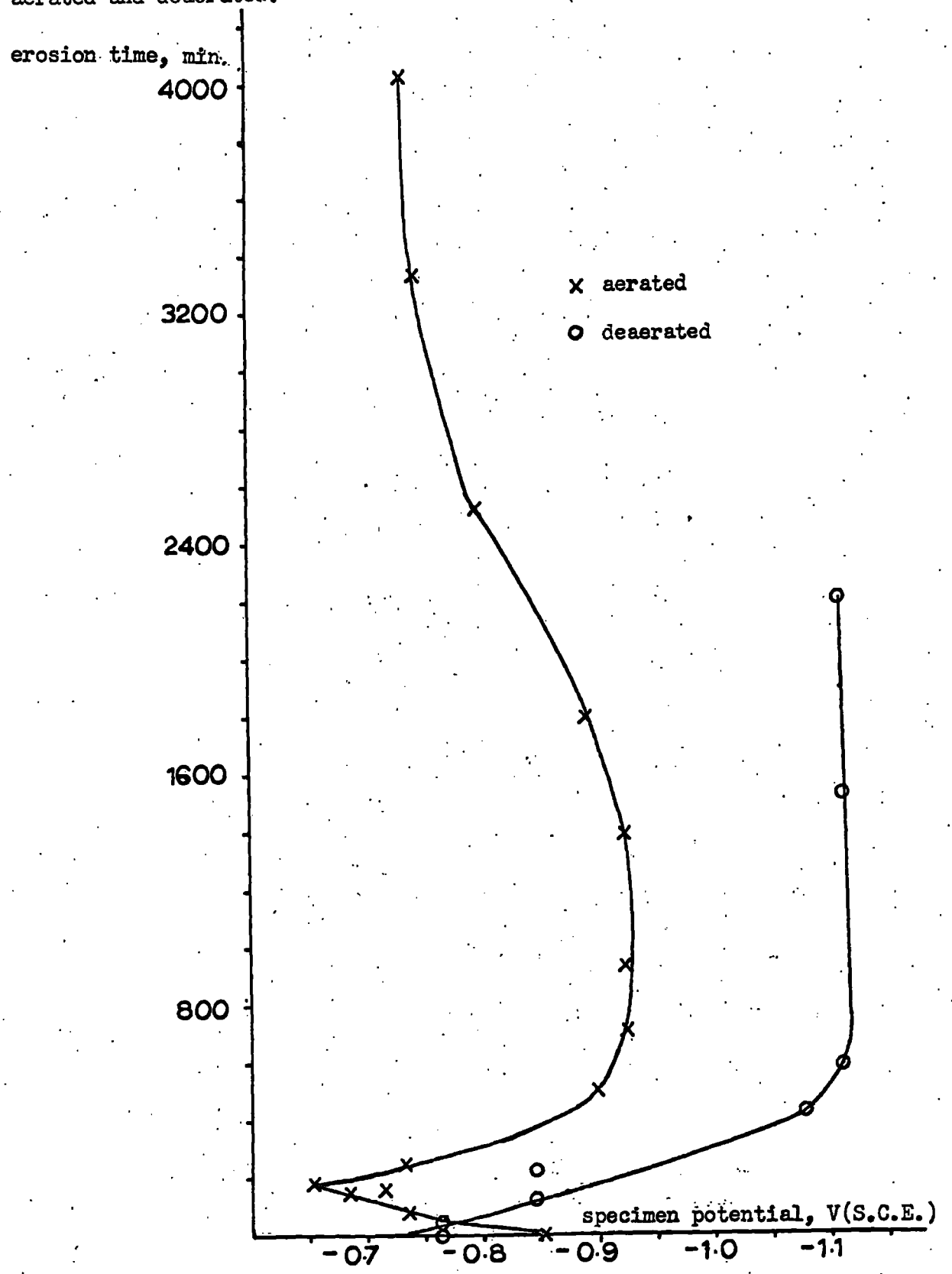

Fig. 25

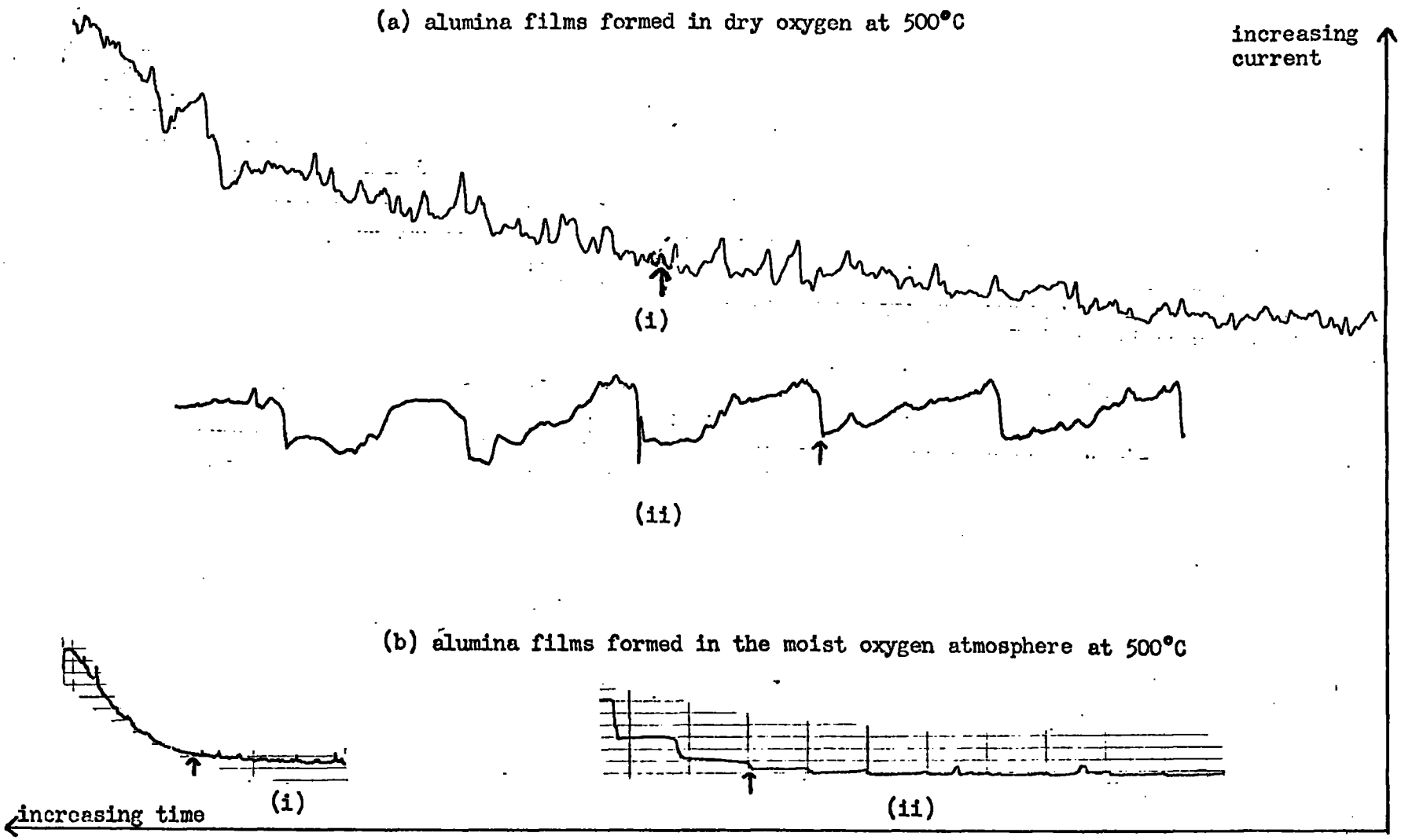

arrows indicate time and, therefore, voltage at which ionic conduction appeared to occur

Typical behaviour observed for alumina films immersed in 3% w/v ammonium tartrate solution during the application of, (i) a steadily increasing voltage [24] and, (ii) step-wise voltage increase [45].

Fig. 26

rate of voltage increase and was found to be 9.3 volts using the method of Hunter and Fowle, and 8.8 volts using the method of Hart.

6.4.2 Films formed in Oxygen Containing Gaseous Water.

The following tables summarise the results obtained.

Table XXIV

Barrier Voltages Using the Method of Hunter and Fowle.[24]

Rate of voltage increase, $\bar{V}$ min^{-1}	Barrier voltage	Specimen type	Electronic leakage current $\mu a\ cm^{-2}$
0.83 0.42 0.17	4.7 4.5 no break	cylindrical	about 4
0.83 0.42	4.6 no break	wire	20-40

Table XXV

Barrier Voltages Using the Method of Hart.[45]

Rate of voltage increase, $\bar{V}$ min^{-1}	Barrier voltage	Specimen type
2.4 0.6 0.2	5.2 5.0 4.8	cylindrical
2.4 0.6	5.0 4.8	cylindrical
2.4 0.6 0.2	4.8 4.6 4.4	wire

The mean barrier voltage, based on both methods, was 4.8 ± 0.3 volts.

It would appear that reduced rates of voltage increase led to reduced barrier voltages. The method of Hunter and Fowle gave somewhat lower values than the method of Hart, a reversal of the behaviour observed for films formed in dry oxygen.

6.5 Summary.

For films formed in dry oxygen, capacitance measurements indicate that the time required for capacitance increase to cease increased, except for pH 5.0, with increasing solution pH. These times were about 260 minutes at pH 1.0, about 400 minutes at pH 2.0, about 520 minutes at pH 3.5 and about 450 minutes at pH 5.0. In deaerated solution, pH 1.0, this time was about 350 minutes and appeared to be independent of ionic strength at pH values close to 2.0 and at pH 3.5. The final capacitance values decreased with increasing pH from about 10 $\mu F\ cm^{-2}$ at pH 1.0 to about 4 $\mu F\ cm^{-2}$ at pH 5.0. In those cases where the specimen potential was measured during specimen immersion, the time required to achieve the final maximum negative potential appeared to correspond with the time required to achieve the maximum capacitance.

Where linear plots of $1/C$ versus $(t)^{\frac{1}{2}}$ were obtained, the slope decreased with increased pH and for a given pH was lower under deaerated than aerated conditions. Films formed in the moist oxygen atmosphere gave smaller slopes than those formed in dry oxygen during specimen immersion in pH 1.0, ionic strength 1.5 deaerated solution.

Linear behaviour of 1/C versus $(t)^{\frac{1}{2}}$ was found for these last two systems throughout the period of capacitance increase, but in the other cases, deviations from linearity took place, occurring later at pH 2.0 than at pH 1.0. At pH 2.0, ionic strength 1.5 (Figs. 20 and 22), there was some evidence for linear 1/C versus t behaviour after the first stage of linear 1/C versus $(t)^{\frac{1}{2}}$ behaviour. For films formed in dry oxygen, during specimen immersion in pH 1.0, ionic strength 1.5, sulphate solution under both aerated and deaerated conditions, the rate of drift of specimen potential in the negative direction increased after about 200 minutes but before this time, this rate was greater under deaerated conditions. For films formed in the moist oxygen atmosphere, during specimen immersion in pH 1.0, ionic strength 1.5, sulphate solution under deaerated conditions, the drift of specimen potential in the negative direction was at approximately a constant rate, whereas in aerated solution, during the first 200 minutes, the potential became more positive before drifting to a more negative value. The final drift in the positive direction was not observed for any other system examined.

For films formed in dry oxygen, a change from predominantly linear 1/C versus $(t)^{\frac{1}{2}}$ to predominantly linear 1/C versus t was indicated at solution pH value 2.0 between ionic strengths 1.5 and 0.15, probably rather close to ionic strength 1.5, since at this ionic strength, there was some evidence for linear 1/C versus t behaviour

after about 170 minutes. For 14 volt anodically-formed oxide films during immersion in sulphate solution, pH 2.0, a similar transition was indicated at an ionic strength rather less than 1.0 and at this ionic strength there was some evidence for linear 1/C versus t behaviour after about 350 minutes.

Where linear plots of 1/C versus t were obtained, the slopes appear to be independent of ionic strength and were for pH 2.0 > pH 5.0 > pH 3.5. A run in pH 7.4, ionic strength 1.5 sulphate solution indicated that the slope was about half that in pH 5.0, ionic strength 1.5 solution. For 14 volt anodically-formed films, the relationship was, pH values close to 2.0 > pH 3.5 > pH 5.0. For films formed in dry oxygen, initial deviations from linearity, which could be indicative of diffusion processes, were found during about the first forty minutes except for pH 2.1, ionic strength 0.015 and for pH 5.0, ionic strength 1.5. This type of behaviour was also found for 14 volt anodically-formed films except that at pH 5.0, ionic strength 1.5, possibly initial diffusion control during about the first forty minutes was indicated.

Whereas the full electrical analogue indicates that the capacitances of the two types of film formed in oxygen were about the same, the barrier voltage for films formed in dry oxygen was found to be about twice that for films formed in the moist oxygen atmosphere.

6.6 Significance of Barrier Voltage Determinations for Alumina Films Formed in Oxygen.

Hunter and Fowle[44] have determined barrier voltages as a function of oxidising time at constant temperature for aluminium oxidised in dry oxygen at temperatures sufficiently high for the formation of crystalline γ - alumina. The type of surface pre-preparation was not mentioned. At lower temperatures, at which only amorphous oxide formed, the barrier voltages were found to be low, about 4 volts. At the higher temperatures, from the time of onset of crystallite formation, a rapid rise in barrier voltage was observed, increasing from about 4 volts and levelling off quickly to about 12 volts. This increase was interpreted[44] in terms of an increase in the minimum field for ionic conduction for the crystalline oxide, although it may be that the total film thickened rapidly as a result of crystal formation[47,48].

6.7 Structures of Alumina Films Formed in Moist and Dry Oxygen.

No discontinuities were observed in the $1/C$-$(t)^{\frac{1}{2}}$ behaviour for the immersion of these films in sulphate solutions of low pH, supporting the evidence of the simple type of analogues, reported in Section 6.1, found for both oxidation in dry oxygen and in the most oxygen atmosphere, that only one type of material was present.

Barrier voltages determined in the present investigation were about 9 volts for oxide formed in dry oxygen and about 5 volts for

oxide formed in the moist oxygen atmosphere at 500°C. These values may indicate, according to the interpretation of Hunter and Fowle[44], which was discussed in Section 6.6, that the former oxide film type was crystalline and the latter type amorphous. In this connection, in Chapter II (2.2.3) it was concluded that oxidation of aluminium in moist air or oxygen might lead to boehmite formation from about 175° - 500°C and at temperatures greater than about 500°C, some crystalline γ-alumina might be present with a little water adsorbed. Plate IV shows that the current-voltage behaviour observed[23,24] in an almost non-solvent electrolyte during the application of a steadily increasing voltage to aluminium specimens bearing porous oxide film is smooth. A trial experiment indicated that the current behaviour was also smooth for an anodic barrier-type film. Fig. 26 shows that in the present barrier voltage studies on films formed in oxygen using both the method of Hunter and Fowle[24] and of Hart[45], the current stability was poor for films formed in dry oxygen but was better for films formed in the moist oxygen atmosphere. It is suggested that in the present studies both porous and non-porous anodic films were less faulted than films formed in oxygen and that the "filling in" of faults by the anodic formation of oxide in the course of the barrier voltage determination was responsible for the unsteady current behaviour. It is further suggested that the possibility of the entry of water into an oxide film formed in oxygen may result in a less

faulted film. In this connection Chistyakov and his co-workers[54,64] have reported that at temperatures sufficiently high for the formation of crystalline oxide, during the oxidation of aluminium in both wet and dry oxygen or air, epitaxial growth of the crystalline oxide led to fractures of crystalline film located on metal of different crystal orientations because of small differences in the dimensions of the aluminium and crystalline oxide lattices.

The capacitance values of the full electrical analogues (Tables XIX and XX) indicate, assuming that the film dielectric constant was, in both cases 10 [70], the value for non-porous anodically-formed films which are generally regarded as amorphous, a film thickness of about 80 Å for both types formed in moist and dry oxygen at 500°C. The lower resistive component of the full analogue for films formed in the moist oxygen atmosphere might be associated with the presence of water in the films[21,39]. It would appear that these films did not consist predominantly of boehmite since this compound is highly insoluble and the films were apparently thinned in deaerated sulphate solution, pH 1.0, ionic strength 1.5, from about 80 Å to about 10 Å in 500 - 900 minutes (see Fig. 19). It is suggested, tentatively, that they consisted of amorphous alumina.

The higher weight gains observed in the formation of crystalline γ-alumina compared with values involved in the formation of amorphous oxide only[47,51,55,62] indicate that in the present work, the capacitance

values of the full analogue for films formed in dry oxygen were abnormally high. Beck and his co-workers[48] have reported that γ-alumina films showed abnormally high capacitance values at high crystal coverages. Electron micrographs revealed[48] that the crystalline oxide was highly faulted and the high capacitance values could have arisen from easy aluminium ion conduction via these faults[48]. Indeed, these workers found that the ionic resistivity of the crystalline oxide was low and the observation that the rate of growth of the amorphous oxide was unaffected by the appearance and growth of crystallites was interpreted in terms of this low ionic resistivity.

Surface pre-preparation appears to be an important factor in relation to film structure. The simple analogue found for films formed in dry oxygen at 500°C may indicate that nearly all of the oxide film was crystalline, in agreement with the findings of Dignam and Fawcett[47], but not with those of Beck and co-workers[48]. The surface properties of specimens initially chemically polished, the procedure adopted in the present studies, may resemble more closely those of specimens electropolished, the procedure followed by Dignam and Fawcett[47], than those of specimens etched in sodium hydroxide solution, the procedure adopted by Beck and his co-workers. Although Beck and his co-workers avoided methods such as electropolishing and chemical polishing because of the reduced[48] ionic resistance of films so produced, one might expect that if the appearance and completion of the crystalline

phase had no effect on the rate of growth of the amorphous oxide, this type of behaviour would also have obtained in the studies of Dignam and Fawcett[47]. However, Dignam and Fawcett found limiting weight gain behaviour. It may well be that the highly faulted nature of the crystalline oxide reported by Beck and his co-workers was strongly influenced by the nature of the original surface produced by etching with sodium hydroxide solution and that faulting was not so extensive in the crystalline film produced by Dignam and Fawcett and in the probably crystalline film produced in dry oxygen at 500°C in the present studies. The possibility remains that the ionic resistivity of films formed in dry oxygen at 500°C in the present studies was somewhat less than that of those films formed in the moist oxygen atmosphere to account for the abnormally high capacitance of the former. Barrier voltage determinations in the present studies, as has been pointed out previously, indicate that films formed in dry oxygen may be more faulted than those formed in the moist atmosphere.

The following table lists the frequency dependence of the measured impedance of:-

(i), a 14 volt anodic barrier-type film when the lowest current density during anodising was maintained for about 5 minutes,

(ii), a film formed in the moist oxygen atmosphere at 500°C, and

(iii), a film formed in dry oxygen at 500°C . The values given

include the contribution from the solution and the external circuitry but this contribution was negligible at frequencies of 500 Hz and below and only a few percent at 5.000 Hz. At the highest frequencies, the measured impedance tended to that of the solution plus external circuitry.

Table XXVI

Frequency Dependence of Impedance for Non-porous Alumina Films

Oxide type	(i)	(ii)	(iii)
f Hz	z ohm cm^2	z ohm cm^2	z ohm cm^2
10	2.84×10^4	1.16×10^4	1.15×10^4
83	3.71×10^3	1.60×10^3	1.48×10^3
500	694	261	244
5×10^3	76	28.6	25.8
50×10^3	13.6	9.5	11.7
100×10^3	12.0	8.8	

Films of type (i) were about 200 Å thick and, assuming a value for the dielectric of 10 [70], films of type (ii) were about 80 Å thick. If the outer layer, apparently much thicker than the inner layer, of type (i) consisted of material similar to that of films of type (ii),

the ratio of impedances at a given frequency up to 5 000 Hz of about 2.5:1 can be understood in terms of the different thicknesses.

It has already been suggested that films of type (iii) are considerably thicker than 80 Å. However, the impedance at a given frequency was found to be about the same as that of a film of type (ii) at frequencies up to 5 000 Hz. It is suggested that this behaviour could be associated with a more faulted structure of the films formed in dry oxygen at 500°C which could lead to a greater ionic conductivity in films of this type. In this connection, Beck and his co-workers[48] reported that crystalline γ-alumina appeared to have a greater ionic conductivity than the amorphous oxide and this difference in behaviour was suggested[48] to be due to the highly faulted structure[48] of the crystalline modification.

Assuming, as do Dignam and Fawcett[47], that the densities of crystalline and amorphous γ-alumina are not much different and taking the value to be 3.17 g cm^{-3} as reported by Bernard and Cook[115] for barrier-type films formed anodically on aluminium in ethylene glycol/ammonium pentaborate solution, an estimate of the limiting weight gain achieved after about 40 hours at 500°C, for electropolished aluminium oxidised in dry oxygen, based on data for other temperatures (see Plate VII), assuming a surface roughness factor of 1.0 [47], indicates a limiting film thickness of about 190 Å. The same treatment applied to the weight gain after 49 hours (the period of oxidation chosen in

the present investigation) at 500°C, of aluminium, initially etched in sodium hydroxide solution, oxidised in dry oxygen[48], assuming a surface roughness factor of 1.2[48], indicates a total film thickness of about 370 Å. The results of Beck and his co-workers[48] indicate, that under these conditions, the inner crystalline phase was 217 Å thick and the overlying amorphous layer was 120 Å thick (about 90 Å for a period of oxidation of 40 hours). The density of crystalline γ-alumina was reported[48], based on measured crystallographic parameters, to be 3.69 g cm^{-3}, indicating that a total film thickness of 370 Å was rather high. Adopting a density of 3.69 g cm^{-3}, rather than the value of 3.17 g cm^{-3} adopted by Dignam and Fawcett[47], the total film thickness inferred from the data of these workers was about 165 Å, so that if, in the present work, the thickness of the supposedly crystalline oxide formed in dry oxygen at 500°C were about the same, its capacitance would appear to be abnormally high as suggested before.

6.8 Controlling Factors in the Dissolution of Alumina Films Formed in Moist and Dry Oxygen.

It is suggested that the dissolution behaviour of oxide films formed in dry oxygen at 500°C can be explained in terms of the factors suggested to influence the dissolution in sulphate solutions of anodic non-porous oxide films. The increase in slope of the plot of 1/C versus t for films formed in dry oxygen on increasing the sulphate

solution pH from 3.5 to 5.0, both at ionic strength 1.5 (see Table XXII) can be explained as follows. The possibility of initial diffusion control, present at pH3.5 was absent at pH5.0, possibly because of the increased hydroxyl ion activity, resulting in a greater equilibrium proton activity more rapidly achieved at reaction sites, in spite of the reduced proton activity in solution. The lower initially observed oxide resistance found for a solution pH of 5.0, compared with pH 3.5, could have arisen from enhanced proton entry into the film .

It would appear that sulphate ion absorption may be less, under the same conditions, for films formed in dry oxygen than for non-porous anodic oxide films, indicating a difference in surface properties for the two types. This is in keeping with the transition from suggested predominantly diffusion-controlled to suggested predominantly zeroth order thinning appearing to take place at a rather higher ionic strength at solution pH values of about 2.0 for films formed in dry oxygen. Also, although there could have been, initially, diffusion controlled thinning of an anodic film in pH 5.0, ionic strength 1.5 sulphate solution, this did not apparently take place for dissolution of a film formed in dry oxygen under the same conditions.

The possibility of reduced boehmite formation by reactions (4) and (3) with reduced accessibility of the film surface to hydroxyl ions from the solution and a diminished rate of removal of protons respectively may explain why the rate of capacitance increase was

greater where diffusion control was indicated. This type of behaviour was found for both so-called non-porous anodic films and for films formed in dry oxygen at 500°C. Since the earliest measured oxide resistance values were always found to be much greater where zeroth order thinning was indicated, boehmite deposition may be initially in pores or faults.

For films formed in dry oxygen, the more rapid initial decrease in specimen potential found under deaerated conditions, compared with aerated, in pH 1.0, ionic strength 1.5 sulphate solution (see Fig. 24) could arise from a reduced rate of boehmite formation. Increased boehmite formation in aerated solution could account for the initial and final maximum in potential found for films formed in the moist oxygen atmosphere (Fig. 25).

6.9 Electrical Resistance of Oxide During Dissolution.

For both types of film examined extensively in the present studies, much larger rates of reduction of oxide film resistance were observed for those cases where zeroth order thinning was indicated. This is consistent with the idea of an enhanced rate of proton entry into the film during the period of measurement as suggested earlier (page 96), resulting from reduced sulphate ion absorption. In general, for reciprocal capacitance plots of the same type, an increased rate of reduction of film resistance was consistent with an increased rate of proton entry, that is with reduced solution pH at constant ionic strength.

As mentioned in Section 6.8, the values of the oxide resistance when first measured were always much greater in those cases in which zeroth order thinning was indicated. This might have arisen from a greater rate of boehmite deposition under these conditions, possibly in pores or faults.

6.10 Comparison of the Rates of Thinning of Films Formed by Anodic and Dry Gaseous Oxidation.

In cases in which diffusion control of dissolution was indicated, the time required to remove the outer layer of anodic films was much less than that required for removal of the thinner inner layer. For a given ionic strength of solution the time for removal of the outer layer increased slightly as the pH of the solution increased.

If, initially, there were considerable incorporation of hydroxyl ions into the outer layer of anodically-formed films, as suggested by Heine and Pryor[21], this could contribute to enhanced thinning by providing easy diffusion paths for protons. The presence of pores may also facilitate rapid removal of the outer layer. Films formed in dry oxygen thinned at intermediate rates under the same conditions. At higher solution pH values, the rate of thinning of films formed in dry oxygen approached and at pH 5.0 exceeded that for anodic films and this behaviour might be associated with the smaller sulphate ion absorption suggested earlier for films formed in dry oxygen.

CHAPTER VII

Conclusions.

7.1 Conclusions.

Differences between the dissolution behaviour of anodic barrier-type films and oxide films formed in dry oxygen, when immersed in sulphate solutions of the concentrations and pH values used in the present work, appear to be related to the extent of sulphate ion adsorption on the films. It is suggested that, in a given type of solution, the extent of sulphate ion adsorption was greater for the anodic films, which are generally regarded as amorphous, than for the films formed by gaseous oxidation, which were probably composed of crystalline γ-alumina. A reaction scheme proposed by Diggle, Downie and Goulding[36] to account for the effects of solution pH and ionic strength on the dissolution behaviour in sulphate solutions of the barrier layer of porous films formed anodically in sulphuric acid appears to satisfactorily account for the behaviour found in the present studies.

For the dissolution behaviour of the barrier layer of porous films, a critical solution pH was reported to occur[23,36] below which suggested approximately zeroth order thinning took place. This type of behaviour did not occur in the present investigation. Rather, a critical ionic strength was observed at solution pH values close to 2.0, below which suggested predominantly diffusion-controlled thinning

gave way to suggested zeroth order thinning. Deaeration of the solution resulted in reduced rates of thinning where diffusion control was indicated but this had no effect on the suggested zeroth order rate of thinning of porous films below the critical pH [23,36]. In the present studies, deaeration is suggested to result in reduced diffusion of hydroxyl ions and, therefore, of protons into the films, under reduced fields arising from the absence of oxygen at the film surface, leading to reduced rates of film thinning. It would not be surprising to find, therefore, that where zeroth order thinning was indicated, deaeration had no effect. The large amount of sulphate ion incorporation in porous films during anodising [91-93] might be an important factor in the different type of behaviour observed, even after the effect of the porous layer on the rate of thinning of the barrier layer had been accounted for [23,36]. Initial preparation of the specimen surface cannot account for this difference since it was the same for all.

It is tentatively suggested that films formed in a moist oxygen atmosphere, total pressure 1 atmosphere, $\bar{p}_{H_2O}$ = 43.1 m.m., at 500°C, consisted of amorphous alumina with some water adsorbed and were less faulted than the probably crystalline γ-alumina films formed in dry oxygen at 500°C.

Anodic barrier-type films studied in the present investigation appear to consist of two regions, an inner less soluble and an outer

more soluble region into which, it is suggested, hydroxyl ions were incorporated. It is suggested that the slightly different structure reported by Heine and Pryor[21] arises from the different initial preparation of surfaces adopted by these workers. It appears possible that the outer region of this type of film, studied in the present work, contained pores, as suggested by other workers,[39,81-83,118], and that in low pH solutions, the removal of the outer layer was controlled by a pore widening mechanism, the mechanism suggested to control the removal of the porous layer of formally porous films[23].

In the present studies, self corrosion apparently occurred for anodised specimens when the outer oxide layer had been removed, and also for a specimen chemically polished only. This did not occur for specimens initially electropolished and then anodised in sulphuric acid[32]. This indicates that the film remaining after thinning was more protective in the latter case than for even thicker films remaining on the metal after the removal of the outer layer of barrier-type films. This might be related to the different initial surface preparations used and/or a different extent to which sulphate ion was absorbed.

Whereas the films formed in dry oxygen at 500°C were apparently crystalline and contained little amorphous oxide, in agreement with the findings of Dignam and Fawcett[47], who first electropolished their specimens, Beck and his co-workers[48] found that amorphous oxide was

an important constituent for specimens initially etched in sodium hydroxide solution and the difference is suggested to arise from different surface properties produced by this initial preparation compared with those of specimens electropolished or chemically polished. The consequence of these different surface properties may well be the extensive faulting observed by Beck and his co-workers[48], resulting in easy aluminium ion conduction through the crystalline layer leading to the continued growth of amorphous oxide after the underlying crystalline layer was completed. For specimens initially electropolished[47] or chemically polished, it is suggested that faulting was considerably less.

There is, then, considerable evidence that the structure and dissolution behaviour of several types of oxide film on aluminium may be strongly influenced by the initial preparation of the specimen surface.

7.2 Proposed Future Work.

Confirmation of the type of material present in oxide films formed in this investigation in dry and moist oxygen at 500°C is desirable, together with the extent of faulting in each type.

The effect of different initial preparation techniques of the specimen surface on the extent of faulting of crystalline films formed in dry oxygen and on the relative amounts of crystalline and amorphous oxide should be investigated. It might be possible to relate the

dissolution behaviour of the three types of film studied to this initial surface preparation.

If a pore widening mechanism controls the dissolution behaviour of anodic barrier-type films in low pH sulphate solutions, electron microscopy might confirm this.

Appendix I

Apparatus Specifications.

(a) Anodising.

Shandon water thermostat.

Heathkit valve voltmeter, model V-7AU.

Solartron Dual constant voltage supply unit, model P.S.U. AS 1416.

(b) Oxidation in oxygen.

Constant voltage transformer - Advance Components Ltd., Type M.T. 262 XA.

Heating tape powered from Powerstat mains transformer - Superior Electrical Co. Ltd.

Furnace powered from Rotary Berco Regavolt mains transformer, Type 72 C.

Cenco Lab Jack.

Shandon water thermostat.

(c) Impedance measurements.

Decade boxes-resistance and capacitance-Educational Measurements Ltd.

Farnell, Type LF sine/square oscillator.

Solartron C.D. 1400 oscilloscope, maximum sensitivity 10 mV cm^{-1}.

Specimen potential monitoring by Philips GM 6001 volt-ohmeter.

Switches - Radiospares.

Sunvic, Type TS 3 (bimetallic strip type) thermostat in conjunction with Sunvic, Type R 10313 relay.

(d) Specimen potential/time measurements.

E.I.L. Vibron electrometer, model 33 B.

Sefram (Paris) Graphispot recorder, Type GRVAT.

Servoscribe recorder, Type RE S11-Kelvin Electronics Co. Ltd.

(e) Determination of concentrations of aluminium ions in solution.

Unicam, Type SP 600 spectrophotometer.

(f) Barrier voltage determinations.

Solartron Dual constant voltage supply unit, model P.S.U. AS 1416.

Motorpotentiometer, Type MP 165 - Erwin Halstrup.

Sefram (Paris) Graphispot recorder, Type GRVAT.

Servoscribe recorder, Type RE S11-Kelvin Electronics Co. Ltd.

(g) Determination of solution pH values.

Vibron Laboratory pH Meter, Model 39A - E.I.L.

APPENDIX II

Establishment of the Calibration Curve for the Optical Densities of Solutions Containing Aluminium Ions.

The experimental procedure used to determine the concentration of aluminium in solution (Chapter IV (4.3.5)) depended on the establishment of a suitable calibration curve for the optical densities of solutions. The procedure used is described here.

Standard aluminium solutions (as sulphate) were prepared in sodium sulphate - sulphuric acid solution used in the dissolution experiments; this solution was of ionic strength 1.5, and pH 1.0. 2 ml portions were buffered with 2M sodium acetate solution to pH 4.5-6.5, and extracted with 10 ml 1% w/v 8-hydroxy quinoline in spectroscopic grade chloroform by shaking for three minutes. Extracts were dried over anhydrous sodium sulphate. Except at very low concentrations, complete extraction of aluminium should be achieved under these conditions[154]. Using as a blank an extract made by using a solution (pH1.0, I = 1.5) which contained no added aluminium, an absorption-concentration plot was constructed spectrophotometrically at 3 900 Å.

References

1. Sasaki Y., J. Phys. Chem. Solids, 13,177(1960).

2. Guntherschultze A. and Betz H., Electrolytkondensatoran, Herbert Cran, Berlin, 1932.

3. Anderson. S., J. App. Phys., 14,601(1943).

4. Alwitt R.S. and Hills R.G., J. Electrochem. Soc., 112,974(1965).

5. Lorking K.F., J. App. Chem., 10,449(1960).

6. Charlesby A., Proc. Phys. Soc., B66,317(1953).

7. Keller F., Hunter M.S. and Robinson D.L., J. Electrochem. Soc., 100,411(1953).

8. Wood G.C., O'Sullivan J.P. and Vaszko B., J. Electrochem. Soc., 115,618(1968).

9. Lorking K.F. and Mayne J.E.O., J. App. Chem., 11,170(1961).

10. Piontelli R., Proc. C.I.T.C.E., Milan, p. 185, Butterworth's Press, London, 1950.

11. Hart R.K., Trans. Farad. Soc., 53,1020(1957).

12. Anderson P.J. and Hocking M.E., J. App. Chem., 8,352(1958).

13. Downie T.C. and Goulding C.W., Metallurgia, 68,193(1963).

14. Downie T.C. and Goulding C.W., ibid, 73,45(1966).

15. Downie T.C. and Goulding C.W., ibid, 73,93(1966).

16. Stern M., J. Electrochem. Soc., 102,609(1955).

17. Greenblatt J.H. and Levy, J. App. Chem., 9,269(1959).

18. Bockris J.O'M. and Potter E.C., J. Electrochem. Soc., 99,169(1952).

19. Stern M. and Makrides A.C., ibid, 107,782(1960).

20. Pryor M.J. and Keir D.S., ibid, 102,605(1955).

21. Heine M.A. and Pryor M.P., ibid, 110,1205(1963).

22. Heine M.A., Keir, D.S. and Pryor M.P., ibid, 112,24(1965).

23. Diggle J.W., Thesis for Res. Dip. R.I.C., December, 1966.

24. Hunter M.S. and Fowle P.E., J. Electrochem. Soc., 101,481(1954).

25. Paolini G., Masaero M., Sacchi F. and Paganelli M., ibid, 112,32(1965).

26. Tosterud M. and Mason R.B., ibid, 90,221(1946).

27. Wood G.C., Marron V.J.J. and Lambert B.W., Nature, 199,239(1963).

28. Diggle J.W., Downie T.C. and Goulding C.W., J. Electroanalyt. Chem., 18,192(1968).

29. Katoh M., J. Electrochem. Soc., Jap., 35,42(1967).

30. Katoh M., Corros. Sci., 8,423(1968).

31. Beck A.F., Heine M.A., Keir D.S., Van Rooyen D. and Pryor M.J., ibid, 2,133(1962).

32. Nagayama M. and Tamura K., Electrochim. Acta, 12,1097(1967).

33. Conway B.E. and Bourgault P.E., Canad. J. Chem., 37,292(1959).

34. Uhlig H.H. and King P.F., J. Electrochem. Soc., 106,1(1959).

35. Diggle J.W., Downie T.C. and Goulding C.W., Corros. Sci., 8,907(1968).

36. Diggle J.W., Downie T.C. and Goulding C.W., Electrochim. Acta,(in Press).

37. Hoar T.P. and Wood G.C., Conf. on Anodising Aluminium, Nottingham, p.186, 1961, Aluminium Dev. Association.

38. Brock A.J. and Wood G.C., Electrochim. Acta, 4,395(1967).

39. Brock A.J. and Wood G.C., Nature, 209(5025), 773(1966).

40. Dekker A.J. and Urquhart H.M.A., Canad. J. Res., 28,1541(1950).

41. Hoar T.P. and Yahalom J., J. Electrochem. Soc., 110,614(1963).

42. Hoar T.P. and Wood G.C., Electrochim. Acta, 7,333(1962).

43. Hunter M.S. and Fowle P.E., J. Electrochem. Soc., 101,514(1954).

44. Hunter M.S. and Fowle P.E., ibid, 103,482(1956).

45. Hart R.K., Proc. Roy. Soc., A236,68(1956).

46. Dignam M.J., J. Electrochem. Soc., 109,192(1962).

47. Dignam M.J. and Fawcett W.R., ibid, 113,663(1966).

48. Beck A.F., Heine M.A., Caule E.J. and Pryor M.J., Corros. Sci., 7(1), 1(1967).

49. Ervin J.R. Guy, Acta Cryst., 5,103(1952).

50. Wilsdorf H.G.F., Nature, 168,600(1951).

51. de Broukere L., J.I.M., 71,131(1945).

52. Randall J. and Bernard W.J., J. App. Phys., 35,1317(1964).

53. Hass G., Optik, 1,134(1946).

54. Chistyakov Yu.D., Pankatov V.V. and Kruglova L.S., Izv. Akad. Nauk. S.S.S.R. Neorg. Mater,3(3),506(1967).

55. Thomas K. and Roberts M.W., J. App. Phys., 32,70(1961).

56. Cabrera N. and Mott N.F., Rep. Prog. Phys., 12,163(1948-49).

57. Cabrera N. and Hamon J., Compt. Rend., 224,1713(1947).

58. Smeltzer W.W., J. Electrochem. Soc., 103,209(1956).

59. Gulbransen E.A. and Wysong W.S., J. Phys. Colloid Chem., 57,1087(1947).

60. Heine M.A. and Sperry P.R., J. Electrochem. Soc., 112,359(1965).

61. Dignam M.J., Fawcett W.R. and Bohni H., ibid, 113,656(1966).

62. Aylmore D.W., Gregg S.J. and Jepson W.B., J.I.M., 88,205(1960).

63. Cochran C.N. and Sleppy W.C., J. Electrochem. Soc., 108,322(1961).

64. Chistyakov Yu. D. and Mendelevich A.Yu., Izv. Vysshikh Uchebn Zavedenii, Tsvetn. Met., 8(3),127(1965).

65. Spannheimer H. and Knoezinger H., Ber. Bunsenges. Physik. Chem., 70(5), 570(1966).

66. Lippens B.C. and de Boer J.H., Acta Cryst., 17,1312(1964).

67. Litvintzev A.I. and Arbuzova L.A., Porosh. Met., 7(1),1(1967).

68. Hass G., J. Opt. Soc. Amer., 39,532(1949).

69. Barrett M.A. and Winterbottom A.B., 1st Inter. Cong. Met. Corrosion (1961), p.657, Butterworth's Press, London, 1962.

70. Diggle J.W., Downie T.C. and Goulding C.W., Chem. Rev., (in Press).

71. Verwey E.J.W., Electroplating and Met. Finish, 7,274(1954).

72. Verwey E.J.W., J. Chem. Phys.,3,592(1935).

73. Verwey E.J.W., Z. Krist., 91,65(1935).

74. Verwey E.J.W., ibid, 91,317(1935).

75. Harrington R.A. and Nelson H.R., Trans. Amer. Inst. Met. Eng., 137,128(1940).

76. Taylor C.S., Tucker C.M. and Edwards J.D., Trans. Electrochem. Soc., 88,325(1945).

77. Stirland D.J. and Bicknell R.W., J. Electrochem. Soc., 106,481(1959).

78. Altenpohl D., Conv. Record of I.R.E., 3,35(1954).

79. Franklin R.W., Conf. on Anodising Aluminium, Nottingham, p.96, 1961. Aluminium Dev. Association.

80. Trillat J.J. and Tertain R., Rev. Aluminium, 26,315(1949).

81. Dorsey Jr. G.A., J. Electrochem. Soc., 113,169(1966).

82. Dorsey Jr. G.A., ibid, 113,172(1966).

83. Dorsey Jr. G.A., ibid, 113,284(1966).

84. Kormany I.T., Tavkozlesi Kut. Int. Kozlemen, 9,113(1964).

85. Lichtenberger E., Zhur. Priklad. Khim.,34,1268(1961).

86. Thach Lan Tran, Naudin F. and Robbe Bourget P., J. Phys.(Paris), 25,11(1964).

87. Pavelkina V.P. and Bogoyavlenskii A.F., Zhur. Priklad. Khim., 37,819(1964).

88. Burgers W.G., Classen A. and Zernicke J., Z. Physik, 74,593(1932).

89. Lichtenberger E., Metalloberfläche, 15,38(1961).

90. Bernard W.J. and Randall Jr. J.J., J. Electrochem. Soc., 108,822(1961).

91. Pullen N.D., J. Electrodepos. Tech. Soc., 15,69(1939).

92. Phillips H.W., Symposium on Props. of Metallic Surfaces, Inst. Metals, Monograph 13(1952).

93. Mason R.B., J. Electrochem. Soc., 102,671(1955).

94. Hoar T.P., Modern Aspects of Electrochemistry, No. 2, p. 309, Butterworth's Press, London, 1959.

95. Ginsberg H. and Wefers K., Metall., 17,202(1963).

96. Liechti F. and Treadwell W.D., Helv. Chem. Acta, 30,1204(1947).

97. Brace A.W. and Baker H., Trans. Inst. Metal Finishings, 40,31(1963).

98. Bogoyavlenskii A.F. and Vedernikov A.P., Zhur. Priklad. Khim., 31,310 (1958).

99. Tomashov N.D. and Byalobzheskii A.V., Trudy. Inst. Fiz. Khim., Akad. Nauk. S.S.S.R., No. 5, Issledovan Korrozii Metal, 4,114(1955).

100. Edwards J.D. and Keller F., Trans. Electrochem. Soc., 79,135(1941).

101. Guntherschultze A. and Betz H., Z. Physik., 68,145(1931).

102. Guntherschultze A. and Betz.H., ibid, 71,106(1931).

103. Guntherschultze A. and Betz H., ibid, 73,508(1932).

104. Guntherschultze A. and Betz H., ibid, 91,70(1934).

105. Guntherschultze A. and Betz H., ibid, 92,367(1934).

106. Mott N.F., Trans. Farad. Soc., 43,429(1947).

107. Verwey E.J.W., Physica, 2,1059(1935).

108. Dewald J.F., Acta Met., 2,340(1954).

109. Dewald J.F., J. Electrochem. Soc., 102,1(1955).

110. Dignam M.J., ibid, 112,722(1965).

111. Dignam M.J., ibid, 112,729(1965).

112. Dignam M.J., Extended Abstracts, Dielectrics and Insulation Division, p. 33, Vol. 1-2, Electrochemical Society Meeting, Dallas, Spring 1967.

113. Jepson W.B., J. Sci. Instr., 36,319(1959).

114. Bray A.R., Jacobs P.W.M. and Young L., Proc. Phys. Soc., 71,405(1958).

115. Bernard W.J. and Cook J.W., J. Electrochem. Soc., 106,643(1959).

116. Willis Jr. G.C., Adams G.B. and Van Rysselberghe P., Electrochem. Acta, 9,93(1964).

117. Vermilyea D.A., Acta Met., 1,282(1953).

118. Hunter M.S. and Towner P.F., J. Electrochem. Soc., 108(2),139(1961).

119. Wilkins N.J.M., Corros. Sci., 4,17(1964).

120. Khan I.H., Leach J.S.L. and Wilkins N.J.M., ibid, 6(11-12),483(1966).

121. Barrett M.A., IV Scandinavian Corrosion Congress, Helsinki, p. 41, 1964. (Current Corrosion Research in Scand.).

122. Barrett M.A., Ellipsometry Sym. Washington, N.B.S. Publ. 256, p. 213, 1963.

123. Ord J.L., Extended Abstracts, Dielectrics and Insulation Division, p. 50, Vol. 1-2, Electrochemical Society Meeting, Dallas, Spring 1967.

124. McMullen J.J. and Hackerman N., J. Electrochem. Soc., 106,345(1959).

125. Bowden F.P. and Rideal E.K., Proc. Roy. Soc., A120,59(1928).

126. Wagner C., J. Electrochem. Soc., 97,71(1950).

127. Brodd R. and Hackerman N., ibid, 106,345(1959).

128. Grahame D.C., Chem. Rev., 41,44(1947).

129. Wood G.C., Cole M. and Hoar T.P., Electrochim. Acta. 3,179(1960).

130. Leach J.S.Ll., Nature, 182,1085(1958).

131. Leach J.S.Ll., J.I.M., 88,24(1959).

132. Leach J.S.Ll. and Isaacs H.S., ibid,91,80(1962).

133. Isaacs H.S. and Leach J.S.Ll., J. Electrochem. Soc., 110,680(1963).

134. Mason R.B. and Slunder C.J., Ind. Eng. Chem., 39,1602(1947).

135. McMullen J.J. and Pryor M.J., 1st Intern. Conve. Metallic Corrosion, p. 52, Butterworth's Press, London, 1961.

136. Vermilyea D.A., J. Electrochem. Soc., 101,389(1954).

137. Latimer W.M., Oxidation Potentials, Prentice-Hall Inc., 2nd Ed.,1959.

138. Peisach N., Poole D.O. and Rohm H.F., Talanta, 14(2),187(1967).

139. Hoar T.P. and Mott N.F., J. Phys. and Chem. Solids, 9,97(1959).

140. House J.R., Personal Communication to Diggle J.W. (1967).

141. Murphy J.F., Plating, 54,1241(1967).

142. Videm K., Paper presented at the 17th Meeting C.I.T.C.E., Tokyo, 1966.

143. Dunn C.G., Extended Abstracts, Dielectrics and Insulation Division, p. 44, Electrochemical Society Meeting, Dallas, Spring 1967.

144. Dunn C.J., J. Electrochem. Soc., 115(2),219(1968).

145. Barber J., ibid, 112,1143(1965).

146. Mason R.B. and Fowle P.E., ibid, 101,53(1954).

147. Grubitsch H., Geymeyer W. and Buvik E., Aluminium, 37,569(1961).

148. Paganelli M., Alumino, 27,3(1958).

149. Burwell R.L., Smudski P.A. and May T.P., J. Amer. Chem. Soc., 69,1525(1947).

150. Mason R.B., Metal Finishing, 8,55(1957).

151. Sacchi F., Galvanotechnica, 13,1(1962).

152. Golubev A.I. and Ignatov N.N., Protection of Metals, 4,396(1965). Translated from Zashchita Metal., 4,445(1965).

153. Jason A.C. and Wood J.L., Proc. Phys. Soc., 68B,1105(1955).

154. Gentry C.H.R. and Sherrington L.G., Analyst, 71,432(1946).

155. Diggle J.W., Downie T.C. and Goulding C.W., To be published.